# Fragmentation Behaviour of Plastic Litter in the Marine Environment

**Dissertation**

by

**M. Sc. Ann-Katrin Reuwer**

In Partial Fulfillment of the Requirements for the Degree of

Doctor rerum naturalium
(Dr.rer.nat.)

Institute of Environmental Systems Research
Institute of Mathematics
School of Mathematics/Computer Science
Osnabrück University

November 2021

Supervisor:

**Dr. Jörg Klasmeier**
Institute of Environmental Systems Research
Institute of Mathematics
School of Mathematics/Computer Science
Osnabrück University, Germany

Second examiner:

**Prof. Dr. Peter Fiener**
Institute of Geography
Faculty of Applied Computer Sciences
University of Augsburg, Germany

Third examiner:

**PD Dr. Marcus Schulz**
AquaEcology GmbH & Co. KG
Oldenburg, Germany

Date of disputation: 06.04.2022

# Abstract

The marine environment is polluted by plastics of all forms and sizes. To reduce this serious pollution, it is important to identify its sources. This work focuses on the mechanically induced breakdown of plastic into smaller fragments as a source of secondary microplastic, the time scale in which these microplastics are formed as well as the influence of different environmental conditions like matrix conditions, collision potential or UV irradiation on the abrasion and fragmentation behaviour of plastic debris.

Since a systematic investigation of parameter influence is not possible in the environment, laboratory experiments were developed to simulate natural conditions such as drift on the beach or wave action in the (low tide) surf and swash zone. For this purpose, selected plastic objects (PET bottles, HDPE caps, PS cups and LDPE bags) were exposed to collision and/or friction forces under different conditions. Besides visual inspection of the destruction procedure, a number of different methods was used to characterize the process, e.g., counting of visible fragments (larger than 350 µm), microscopic analysis of the surface structure (binocular, SEM) and highly resolved analysis of particle numbers in the size range below 350 µm. In order to extract microplastic particles (<5 mm) from the matrix, extraction methods were developed that were adapted to the given sample properties (matrix volume). Furthermore, based on the particle numbers, the power law model was applied to analyse the fragmentation process in the context of the observed particle size distributions.

Plastic samples exhibited various signs of mechanical impairment in form of surface abrasion, cracks, tears, perforation, crumpling and finally fragmentation. The formation of fragments in different sizes (macro-, meso- and microplastics) was observed. The plastic objects were classified according to their degree of destruction to elucidate the effect of the different experimental conditions.

Results show that fragmentation and abrasion depend on individual properties of the plastic objects such as thickness or shape and on the potential of weakening the plastic structure by mechanical forces (collisions) or chemical degradation (UV irradiation). Environmental conditions also influence the plastic damage; surface abrasion plays a major role on the beach; fragmentation will most likely happen in the surf- and in the swash zone. However, both processes occur simultaneously and interact with each other. Formation of secondary microplastics was shown to be likely in the marine environment; it must therefore be considered as an important process in the light of microplastic contamination.

**Keywords:** marine environment, plastic litter, fragmentation, abrasion, secondary microplastic

# Kurzfassung

Die Meeresumwelt wird durch Plastikmüll aller Formen und Größen verschmutzt. Um diese Verschmutzung zu verringern, ist es wichtig, deren Quellen zu ermitteln. Diese Arbeit konzentriert sich auf den mechanisch induzierten Zerfall von Kunststoff in kleinere Fragmente als Quelle von sekundärem Mikroplastik, die Zeitskala, in der diese Art von Mikroplastik gebildet wird, sowie den Einfluss verschiedener Umweltparameter wie Matrixbedingungen, Kollusionspotenzial oder UV-Bestrahlung auf das Fragmentierungsverhalten von Plastikmüll.

Da in der Umwelt eine systematische Untersuchung des Parametereinflusses nicht möglich ist, werden Laborexperimente entwickelt, die natürliche Bedingungen wie Windverwehungen am Strand oder die Wellenbewegung in der Brandungszone simulieren. Dazu werden ausgewählte Kunststoffobjekte (PET-Flaschen, HDPE-Verschlüsse, PS-Becher und LDPE-Tüten) unter verschiedenen Bedingungen Kollisions- und Reibungskräften ausgesetzt. Neben der visuellen Inspektion des Zerstörungsprozesses werden verschiedene Methoden zu dessen Charakterisierung eingesetzt, wie z. B. das Zählen der sichtbaren Fragmente (>350 µm), die mikroskopische Analyse der Oberflächenstruktur (Binokular, REM) und eine hochauflösende Analyse der Partikelanzahl im Größenbereich unter 350 µm. Um Mikroplastikpartikel (<5 mm) aus der Sandmatrix zu extrahieren, wurden Extraktionsmethoden entwickelt, die an die gegebenen Probeneigenschaften (Matrixvolumen) angepasst sind. Darüber hinaus wurde auf der Grundlage der Partikelzahlen das Potenzgesetzmodell angewandt, um den Fragmentierungsprozess im Zusammenhang mit den entstandenen Partikelgrößenverteilungen zu analysieren.

Die Kunststoffproben wiesen verschiedene Anzeichen von mechanischer Beeinträchtigung in Form von Oberflächenabrieb, Rissen, Perforation, Zerknittern und schließlich Fragmentierung auf. Fragmente in verschiedenen Größen (Makro-, Meso- und Mikroplastik) entstanden in Abhängigkeit der Versuchsbedingungen. Der Grad der der Beschädigung der unterschiedlichen Plastikobjekte wurde zur Aufdeckung des Einflusses der äußeren Bedingungen in Kategorien eingeteilt.

Die Ergebnisse zeigen, dass Fragmentierung und Abrieb von individuellen Eigenschaften der Plastikobjekte wie Dicke oder Form und vom Potenzial der Schwächung der Struktur durch mechanische Kräfte (Kollisionen) oder chemische Degradation (UV-Bestrahlung) abhängen. Auch die Umweltbedingungen haben Einfluss auf die Schädigung der Kunststoffe; der Oberflächenabrieb spielt am Strand eine große Rolle, die Fragmentierung in der Schwemmzone. Beide Prozesse treten jedoch gleichzeitig auf und beeinflussen sich gegenseitig. Es hat sich gezeigt, dass die Bildung von sekundärem Mikroplastik in der Meeresumwelt wahrscheinlich ist; sie muss daher als ein wichtiger Prozess im Hinblick auf die Verunreinigung durch Mikroplastik betrachtet werden.

**Schlagwörter**: Marine Umwelt, Plastik Verschmutzung, Fragmentation, Abrasion, sekundäre Mikroplastik Partikel

# Table of Content

# List of Figures

# List of Tables

# List of Boxes

# List of Abbreviations

| | |
|---|---|
| AIO | Air Induced Overflow |
| ATR | Attenuated Total Reflectance |
| BE | Bottle Experiment |
| CSF | Corey Shape Factor |
| EINP | Experiments to Investigate the influence of Natural Parameters on plastic debris |
| EFP | Experiments to investigate the Fragmentation Pattern over the time |
| EPS | Expanded Polystyrene |
| FTIR | Fourier Transform Infrared |
| GES | Good Environmental Status |
| GESAMP | Joint Group of Experts on the Scientific Aspects of Marine Environmental Protection |
| HDPE | High Density Polyethylene |
| KOH | Potassium Hydroxide |
| LDPE | Low Density Polyethylene |
| MP | Microplastic |
| MPP | Microplastic Particle |
| MSFD | Marine Strategy Framework Directive |
| NaOH | Sodium Hydroxide |
| NOOA | National Oceanic and Atmospheric Administration |
| NSE | Nash–Sutcliffe model Efficiency coefficient |
| PA | Polyamide |
| PE | Polyethylene |
| PET | Polyethylene Terephthalate |
| PMMA | Poly (Methyl Methacrylate) |
| POP | Persistent Organic Pollutant |
| PP | Polypropylene |
| PS | Polystyrene |
| PSD | Particle Size Distribution |
| PTFE | Polytetrafluoroethylene |
| PUR | Polyurethane |
| PVC | Polyvinyl Chloride |
| Pyr/GC-MS | Pyrolysis/Gas Chromatography-Mass Spectrometry |

| | |
|---|---|
| Rpm | Revolution Per Minute |
| SEM | Scanning Electron Microscope |
| TDS | Thermal Desorption Spectroscopy |
| TRWP | Tyre and Road Wear Particles |
| UV | Ultraviolet |
| WTE | Wave Tub Experiment |

# 1 Introduction

A widely discussed problem of our century is the pollution of the environment with plastic. Due to their functional characteristics like durability, carrying capacity and little weight as well as cost-effective production, plastic materials are used in almost every aspect of our daily life. The world's plastic production increased over the last decades with a peak of primary plastic production in 2017 of 64.4 million tons and a slightly decreasing trend since then (57.9 million tons in 2019) (PlascticEurope, 2020; PlasticEurope, 2019).

Consequently, plastic objects of all sizes are almost ubiquitously found in the environment. This can lead to serious hazards for marine life caused by entanglement or ingestion, both with the potential of leading to death. The advantageous characteristic of long durability unfortunately causes problems when plastic items end up in the environment after use, since this results in exceptionally long resistance times. This leads to the necessity of intervention by humankind to solve the problems we have caused.

Over the last years, a lot of research has been undertaken to determine the extent of contamination, identify the main sources as well as to clean up aquatic ecosystems (Barnes et al., 2009; Bergmann et al., 2015; Kershaw et al., 2011; W. C. Li et al., 2016; R. C. Thompson et al., 2009). Potential contamination sources are littering, discarded fishing gear (Naji et al., 2017), illegal dumping of waste (Kershaw et al., 2011), tourism and discharges from rivers including input from storm water events or sewage outfalls (Bergmann et al., 2015; Naji et al., 2017). Plastic may then accumulate on the coastlines and in beach sediments because of transport in the aquatic environment. It is assumed, that plastic materials with similar densities as water float on the sea surface, while denser materials can even accumulate on the sea floor (Woodall et al., 2014). Even microscopic small plastic particles were found in the world's oceans in distant untouched areas like the deep-sea sediment (Bergmann et al., 2017; van Cauwenberghe et al., 2013).

Many studies have proven the presence of plastic debris including all material types and size ranges in the aquatic environment (Barnes et al., 2009; Gewert et al., 2017). It is important to get a meaningful assessment over the plastic pollution so long-term and large-scale monitoring of the environment is necessary. Therefore, plastic debris is classified in size classes (macro-, meso-, micro- and even nanoplastic) but no unique, official definition has been established so far. Unfortunately, this leads to a lack of comparability of data from different studies. Besides particle size, another classification is often made according to the origin of microplastic particles (MPP). Primary microplastics were already manufactured in a micro size range. This category includes industrial pellets and microbeads for cosmetic products. Secondary microplastics are formed from larger particles as a result of mechanical stress and weathering governed by environmental factors.

Synthetic fibres released from textiles are also considered secondary microplastics but should preferably be treated separately due to their different sources and environmental fate (de Falco et al., 2018; Shaikh & Agrawal, 2014). Tyre and road wear particles (TRWP) constitute a large fraction of microplastics as well, originating from driving processes and accumulate in soils and aquatic compartments. Like microplastics, TRWP are suspected to be hazardous to health for living creatures, but further research is needed (Baensch-Baltruschat et al., 2020).

Caused by weathering processes plastic garbage can become brittle and break into smaller fragments, which is assumed a significant source of so-called secondary microplastic particles (Duis & Coors, 2016). Chemical and microbiological degradation processes lead to weakening of the polymer structure by oxidation (Singh & Sharma, 2008), which then facilitates breakdown into fragments. At the same time, friction stress due to environmental forces can cause abrasion of very small particles from the plastic's surface (Song et al., 2017).

Different environmental factors can affect the respective processes involved. To date, only little data exist on the extent and time scale of plastics fragmentation and abrasion under environmental conditions. Since observations of single objects in the aquatic environment over time are practically impossible and boundary conditions are not controllable, laboratory experiments are mandatory to get insight into the processes forming secondary microplastics.

In this work, the focus is on the systematic investigation of the formation of secondary microplastics under typical environmental conditions such as UV irradiation, matrix conditions and sediment grain size in the (low tide) surf- or swash zone or the beach. For this, a set of experiments representing such conditions was performed on an orbital shaker with a horizontal amplitude with different typical plastic litter items.

# 2 Aim of the Study

To date, there is still a large knowledge gap regarding the main sources of microplastics in the aquatic environment, and especially the origin of microplastic contamination of the marine environment is disputed. To minimize environmental pollution with microplastic particles (MPP), effective strategies to reduce plastic emission need to be developed. A major source of MPP is probably abrasion of and fragmentation from larger plastic objects (secondary microplastic) discarded into the environment by intentional littering.

This research focusses on the question to what extent and on which time scale secondary MPP can be generated by mechanically induced breakdown under the influence of environmental forces. In order to get an idea of the contribution of secondary MP to the overall plastic contamination it is fundamental to explore the potential of larger plastic objects for fragmentation and abrasion under different environmental conditions. This would allow a first overview over the expected numbers and particle size distributions (PSDs) of secondary microplastics and a first assessment which marine areas have the highest potential for their formation.

The aim of this study is to get deeper insight into the fragmentation and abrasion behaviour of different daily used plastic objects under simulated marine environmental conditions such as they are present in the swash- and low tide surf zone and on beaches. The focus of the investigations lies on the identification of environmental conditions (sunlight, wave action, collisions and friction) and properties of the objects (material, density, shape) that induce or favour fragmentation and abrasion processes (mechanical degradation).

# 3 Scientific State of the Art

## 3.1 Definitions and categorization of plastic particles

The history of microplastics began in the 1970s with first findings of microscopic-small plastic particles in the North Sea (Buchanan, 1971) and in 1974 in the North Atlantic and Caribbean on the sea surface (Colton et al., 1974). The term "microplastic" (MP) was first introduced by Richard C. Thompson, who described small plastic particles in the size region of 20 µm on beaches and estuarine and subtidal sediments in Great Britain (Richard C. Thompson et al., 2004). An early definition used by different international working groups was based on the size of industrial plastic pellets specifying microplastics as particles smaller than 5 mm in diameter. It was introduced by the National Oceanic and Atmospheric Administration (NOAA) (Arthur et al., 2009). Several other size classifications have been suggested since then (Andrady, 2015; Browne et al., 2007), but until today no general classification scheme has become accepted. However, due to pragmatic reasons many analytical data are still reported in size classes given by the sampling equipment (e.g., 335 µm manta trawl). Not at least this lack of standardized size definitions makes comparison of microplastic numbers reported by different researchers very difficult.

Another important issue is the lower boundary delimiting microplastics from nanoplastics, which most likely have other physical characteristics. By now, this lower boundary is not generally defined, but is often defined by practical and technical limitations of the analytical equipment during the individual studies. A logical boundary often suggested is 1 µm.

Table 1 demonstrates the dilemma of different size class categorization in the literature. For example, the intermediate fraction of mesoplastics is defined differently in the various classification schemes.

**Table 1:** Examples for size categories for plastic debris in scientific literature.

| Author | Year of publication | Nanoplastics | Microplastics | Mesoplastics | Macroplastics |
|---|---|---|---|---|---|
| (Browne et al., 2007) | 2007 | <1 µm | 1-1000 µm | - | >5 mm |
| (Moore, 2008) | 2008 | - | <5000 µm | - | >5 mm |
| **NOAA** (Arthur et al., 2009) | 2009 | - | <5000 µm | - | - |
| **EU MSFD GES** (Joint Research Centre, 2014) | 2013 | - | 20-5000 µm | 5-25 mm | >2.5 cm |
| (GESAMP Joint Group of Experts on the Scientific Aspects of Ma- | 2015 | <1 µm | 1-1000 µm | 1- 25 mm | 2.5-100 cm |

| Author | Year of publication | Nanoplastics | Microplastics | Mesoplastics | Macroplastics |
|---|---|---|---|---|---|
| rine Environmental Protection, 2015) | | | | | |
| (Wagner et al., 2014) | 2014 | <20 µm | 20-5000 µm | 5-25 mm | >2.5 cm |
| (Andrady, 2015) | 2015 | <1 µm | 1-1000 µm | 1-25 mm | 2.5-100 cm |
| (Koelmans et al., 2017) | 2017 | <335 µm | 335-5000 µm | - | >5 mm |
| (Hartmann et al., 2019) | 2019 | <1 µm | 1-1000 µm | 1-10 mm | >1 cm |
| (PlastikNet, 2020) | 2020 | <1 µm | 1-5000 µm | - | - |

Hartmann et al. (2019) recently proposed a framework for plastic debris categorization in general is proposed. Seven criteria are discussed, which consider different characteristics for plastic particle definition. These criteria define plastics firstly along chemical composition, solid state and solubility (criteria I−III) and secondly according to their physical properties size, shape and structure, colour and origin (criteria IV−VII). This framework with the combination of important plastic characteristics seems to be a promising proposal for future.

In this thesis, the classification of the MSFD GES Technical Subgroup on marine litter for the Marine Strategy Framework Directive (Joint Research Centre, 2014) is used. Due to the potential for particles with different sizes to differ in their behaviour, a distinction is made between large MP (5mm-1 mm) and small MP (<1 mm).

## 3.2 Sources of microplastic particles

The development of effective countermeasures to reduce MP pollution requires identification of the emission sources and pathways into the environment. Known sources for MPP in the marine environment are first divided in ocean- or land-based. Discarded or lost fishing equipment and ship and boat traffic (by littering of waste and sewage or cargo loss) are the major ocean-based sources (Andrady, 2011; Cole et al., 2011; Hammer et al., 2012). Land-based sources are littering at beaches by coastal tourism, landfills on the coasts or illegal dumping from industrial facilities supporting microplastic pollution (Hammer et al., 2012). Due to transport of microplastics along waterway systems (limnic system) followed by entering the ocean, MP contamination sources for rivers should also be included. (Sighicelli et al., 2018) even discussed whether the freshwater system is the major source of the marine environment. A widely discussed MP source is treated effluent from wastewater treatment plants (WWTP), which is potentially polluted due to microbeads from use of cosmetic products, fragments from household articles or textile fibres. However, multiple studies show that most of it is removed from the wastewater stream (Gatidou et al., 2019; Sun et al., 2019) and is enriched in sewage sludge (Edo et al., 2020). This sludge is partly used for fertilizing agricultural fields where the MPP can accumulate. The use of plastic foil on agriculture fields in interac-

tion with weathering and wind action is also supposed to enhance the MP contamination of soils. During heavy rainfall, surface runoff and erosion may lead to MP-transport into the aquatic system from soil (Hammer et al., 2012).

Furthermore, the formation of secondary microplastics through the breakoff of larger plastic objects due to weathering and mechanical stress is undeniable as an MPP source both on land and at sea (W. C. Li et al., 2016; Yang et al., 2021). However, the analysis of the main formation processes and the general contribution to pollution have not yet been studied in detail.

## 3.3 Analysis of microplastics

A huge number of investigations on the occurrence of plastic materials in marine and freshwater systems have been performed to date. However, most of the sampling results are not comparable with each other because of the non-uniform sampling and extraction procedures as well as the large uncertainties still associated with MP quantification. There are three basic steps involved in the MP analysis (J. Li et al., 2018):

1. Sampling
2. Extraction and purification
3. Identification and quantification

### 3.3.1 Sampling and extraction methods

Efficient separation of MPP from the matrix is one of the limiting factors in the analysis of microplastics from environmental samples. Since this is a crucial step, several extraction procedures have been suggested so far. In the following, the most commonly used sampling and extraction methods are briefly described.

#### 3.3.1.1 Water samples

The extraction of water samples is often partly integrated into sampling by filtering the water phase. Surface water samples are taken mainly with neuston or plankton nets with a mesh size between 50 to 3000 µm. The most common mesh size is 300 µm, since smaller mesh sizes lead to fast clogging of the nets by natural debris (Löder & Gerdts, 2015; Mai et al., 2018). Another frequently used tool is a filter cascade, which filters the water samples over subsequently arranged filters with different pore widths. Thus, this method already includes separation of the MPP into different size classes (Löder & Gerdts, 2015). In addition, the sample volume can be increased due to the distribution on several filters dependent on the contamination of organic particles in the water. These cascade systems have the advantage to allow an easy sampling of the water column supported by submersible water pump, which increase the sample flow rate (Klein et al., 2018).

#### 3.3.1.2 Sediment samples

For sediment samples, there is no commonly accepted sampling strategy developed by now (Klein et al., 2018). Mostly non-plastic tweezers or spoons are used to transfer between 500 g up to 10 kg sediment (Hidalgo-Ruz et al., 2012) in storing containers or bottles (Löder & Gerdts, 2015). The sampling location (beach zone and sampling depth) depends on the underlying assumption of the studies. However, without a standardized sampling method comparable data on plastic particle distribution is limited (Löder & Gerdts, 2015).

For the inevitable extraction of plastics from the sediment sample matrix, various methods have been suggested in the literature. For macroplastics, on-site picking of large objects and sieving (down to 2 mm) is a practical method to separate plastic items directly from the sediment matrix. Depending on the grain size distribution of the sediment, the extraction of smaller particles is more complicated.

The most common methods to extract MP from sediment samples are based on density separation using the principle of flotation or fluidization. Here, the sample is added to a solution that has a higher density than plastic particles and a lower density than sediment. After a certain operating time, the supernatant containing MPP is collected and subsequently filtered. The most frequently used separating fluid is saturated sodium chloride (NaCl) solution (Claessens et al., 2011; Richard C. Thompson et al., 2004). However, with a density of 1.2 g/cm³, the extraction of plastics such as PVC (1.2-1.4 g/cm³) or PET (1.38 g/cm³) is hardly possible. For extraction of these MP with higher densities, higher density solutions of zinc chloride (Imhof et al., 2012), sodium tungstate or sodium iodide (Nuelle et al., 2014) are used. A major disadvantage of these salts is that they are very expensive and ecologically harmful or even toxic. Thus, re-use of the solutions after appropriate clean-up is imperative.

Besides using the same general principle of flotation, the practical setup can be quite different. Sediment samples are added to the separating fluid in flasks, columns or other appropriate vessels. A commercially available extraction setup is the Munich Plastic Sediment Separator (MPSS), which can separate MPP in samples of up to 6L (Imhof et al., 2012). Some methods additionally make use of fluidization introducing turbulent flow by gentle air or water flow, which is meant to support the buoyant lift of the particles (Claessens et al., 2013; Naji et al., 2017; Nuelle et al., 2014; Zhou et al., 2018). Another widely used method is the use of a closed flow system with an elutriation column where the MPP are collected in a directly installed mesh (Claessens et al., 2013; Hengstmann et al., 2018; Kedzierski et al., 2016; Wessel et al., 2016).

Other less common extraction methods are based on the electrostatic behaviour of MPP (Felsing et al., 2018), their hydrophobic properties using oil separation (Crichton et al., 2017), their solubility performing solvent extraction (Ceccarini et al., 2018) or the use

of a pressurized fluid extractor (Fuller & Gautam, 2016). All these methods require a specialized equipment, whose acquisition is only profitable for routine analysis.

The development of a feasible method for the extraction of microplastic particles from sediment samples is inevitable for the study of abrasion and fragmentation behaviour, since a high sample throughput is to be expected.

#### 3.3.1.3 Purification

A purification step for separating MP from natural debris is often necessary to reduce false positive or false negative MP detects. Additionally, signals from organic debris may interfere with the applied analytical detection techniques. Purification most often makes use of either chemical or enzymatic procedures. The most common method is the oxidation of organic constituents with hydrogen peroxide, Fenton reactant or sulfuric acid. It is important to consider that some polymer materials are also oxidizable (e.g., polycarbonates, see Klein et al., 2018) or have a low pH tolerance like PA or PS (Cole et al., 2014). Alternatively, an alkaline treatment (NaOH, KOH) could be used, but again some polymers are not completely persistent against high pH values (e.g., Nylon, PE or PVC). Another published method is the use of an ultrasonic bath in combination with organic solvents like sodium dodecylsulfate (Enders et al., 2015) but this method is suspected to lead to an emergence of small plastic particles especially from weathered plastics (Löder & Gerdts, 2015).

A gentler method for removal of biological material is the enzymatic digestion using the enzyme proteinase K, or a mixture of different enzymes including cellulase. However, these treatments are very time consuming (up to 15 days per sample) and expensive in comparison with chemical treatments (Cole et al., 2014; Klein et al., 2018).

### 3.3.2 Identification and quantification

The most common and simple method to identify plastic and determination of particle numbers in the samples is the optical analysis under a stereomicroscope (Frias et al., 2018; Hidalgo-Ruz et al., 2012; Zhao et al., 2017). Optical analysis is, however, no reliable method, not at least because it strongly depends on the expertise of the individual person. Natural particles of different origin can easily be mistaken for plastics due to their physical appearance (colour, surface structure etc.). Reported error rates range from 20% (Eriksen et al., 2013) up to 70% (Hidalgo-Ruz et al., 2012). Thus, optical analysis should always be combined with a more specific identification method, if possible.

Pyrolysis (Pyr) in combination with gas chromatography (GC) coupled with mass spectrometry (MS) for MP mass determination or spectroscopic identification methods like Fourier transform infrared (FTIR) or Raman for particle number determination are the methods of choice. These methods allow for unequivocal identification of most of the polymer types according to their chemical composition.

Pyr/GC-MS includes thermal destruction and analysis of the gaseous pyrolysis products (Fries et al., 2013). In the GC-MS, each polymer produces a specific chromatogram (pyrogram) with characteristic fragments that can be used as markers in a fingerprinting-like procedure (Fischer & Scholz-Böttcher, 2017).

Identification with FTIR spectroscopy is based on the absorption of infrared light by molecular functional groups. Each material produces a characteristic spectrum. Attenuated total reflectance (ATR) FT-IR (Fok et al., 2017), and focal plane array detector-based μFT-IR imaging (Löder & Gerdts, 2015) make it possible to detect particles down to 20 μm and scan even large areas of filters for MPPs directly.

For a Raman spectrum, the samples are irradiated by a monochromatic laser source resulting in interaction of the laser light with the molecules and atoms. The so-called Raman shift, the difference in the frequency of the backscattered light as compared to the irradiating laser frequency (Löder & Gerdts, 2015), leads to a material-specific Raman spectrum. Using the μ-Raman technique allows for scanning whole filters for MPP. A main advantage is the possibility to detect particles down to 1 μm (Klein et al., 2018).

For analysing additives of polymers a thermal desorption spectroscopy (TDS) is used. By increasing the surface temperature, thermal energy is transferred to absorbed molecules inducing them to desorb by breaking bonds resulting in characteristic TDS spectra.

For the identification methods, good purification of the samples is necessary to prevent misidentification. In addition, the degree of weathering/degradation of a sample might lead to erroneous results if the molecular structure of the sample had changed or a biofilm on the sample surface had grown (Fernández-González et al., 2021).

## 3.4 Weathering and plastic degradation

A change in the polymer material induced by environmental impact is called weathering. Exposure to natural parameters like sunlight, heat, oxygen and physical stress (so called weathering factors) can induce degradation of plastic materials. In material sciences, degradation of plastics is defined as breakdown of the polymer material resulting in changes of its properties inducing the weakening of the material. Due to their different molecular structures, degradation pathways of polymer materials vary widely (Gewert et al., 2015). Weathering of plastics plays an important role for plastic abrasion and fragmentation behaviour since the degradation leads to a decrease of stability of the plastic (Figure 1).

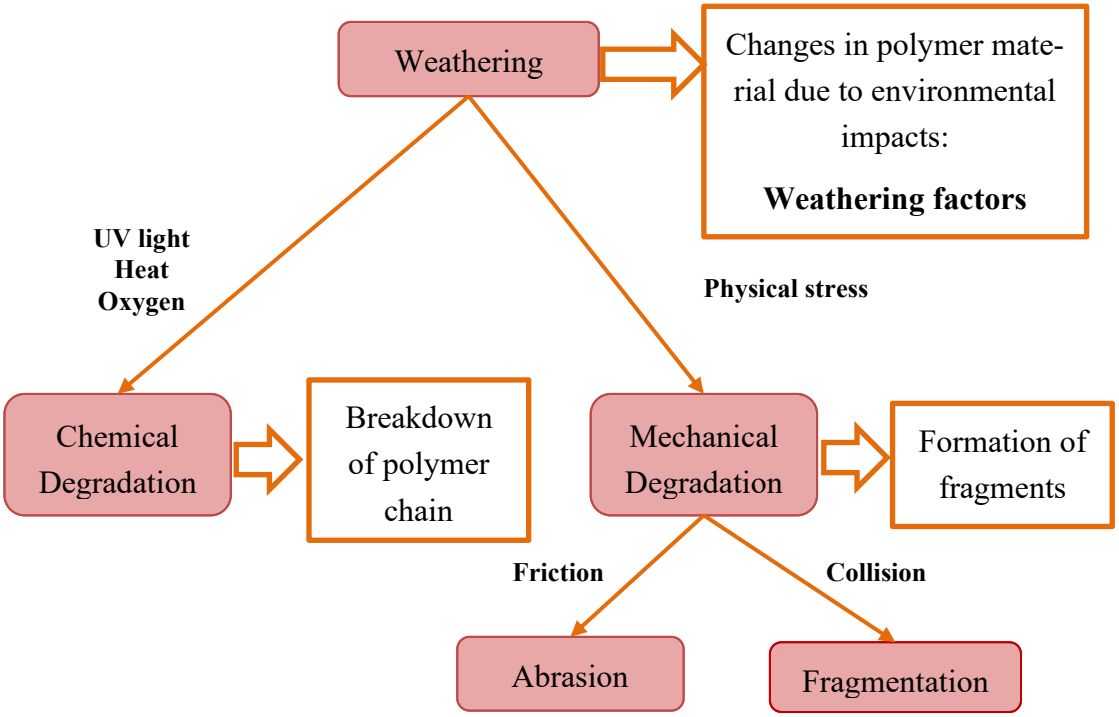


**Figure 1**: Connection between different processes which are important in the marine environment for plastic abrasion and fragmentation behaviour.

### 3.4.1 Chemical degradation

The weathering factors UV light and/or heat induce the decomposition of the molecular structure in the presence of oxygen (photo-oxidative, thermo-oxidative degradation). This process is called chemical degradation. Due to light absorption of chromophores included in the molecular structure of the polymers (as impurities or as structural parts), the molecular chains break und the molecular weight decreases leading to chain scission and/or cross-linking. These changes of the molecular structure may lead to increased brittleness and cracking/crazing of the material. Common effects are discoloration, tackiness and loss of surface gloss. UV irradiation results in the weakening of the material structure. Oxygen is an important factor, since it builds free radicals (hydroperoxides) and increases the degradation rates (Feldman, 2002). It is assumed that degradation induced by light is orders of magnitude higher compared to other degradation processes (Wang et al., 2016). To protect polymer materials against chemical degradation additives like heat and/or light stabilizers or UV absorbers are added. They absorb or block UV radiation to reach the chromophores in the material matrix or hinder reactive free radicals or excited species generated by UV light to react with the molecular structure by converting them into stable forms (Zweifel, 1998).

Biological degradation is the breakdown of the molecular structure by living microorganism like bacteria, algae or fungi by biochemical processes (Zhang et al., 2021). This process can potentially lead to the complete mineralisation of the original material (Shah et al., 2008) which depends on different factors like the molecular structure of the

plastic material, the environmental conditions (pH-value, temperature etc.) as well as the microorganism themselves (concentration, specific degradation mechanism etc.) (Ali et al., 2021). However, conventional plastics shows minimal biological degradation rates under environmental conditions (Zhang et al., 2021). Nevertheless, colonisation of microbes especially on rough plastic surfaces leading to a formation of a biofilm (bio-fouling) has been observed (Yuan et al., 2020). This biological formed shield protects plastics from UV irradiation and decreases the photo-oxidative degradation. It may also affect their sinking behaviour in the aquatic environment.

### 3.4.2 Mechanical degradation

As opposed to chemical alterations of the molecular structure by biological or chemical degradation, physical/mechanical degradation does not necessarily cause changes of the molecular structure but damage or even destruction of plastic debris leading in the emergence of smaller fragments often caused by physical forces to which plastics may be exposed in the environment. There are two important mechanical degradation processes identified by now (see Figure 2) which are described in the following.

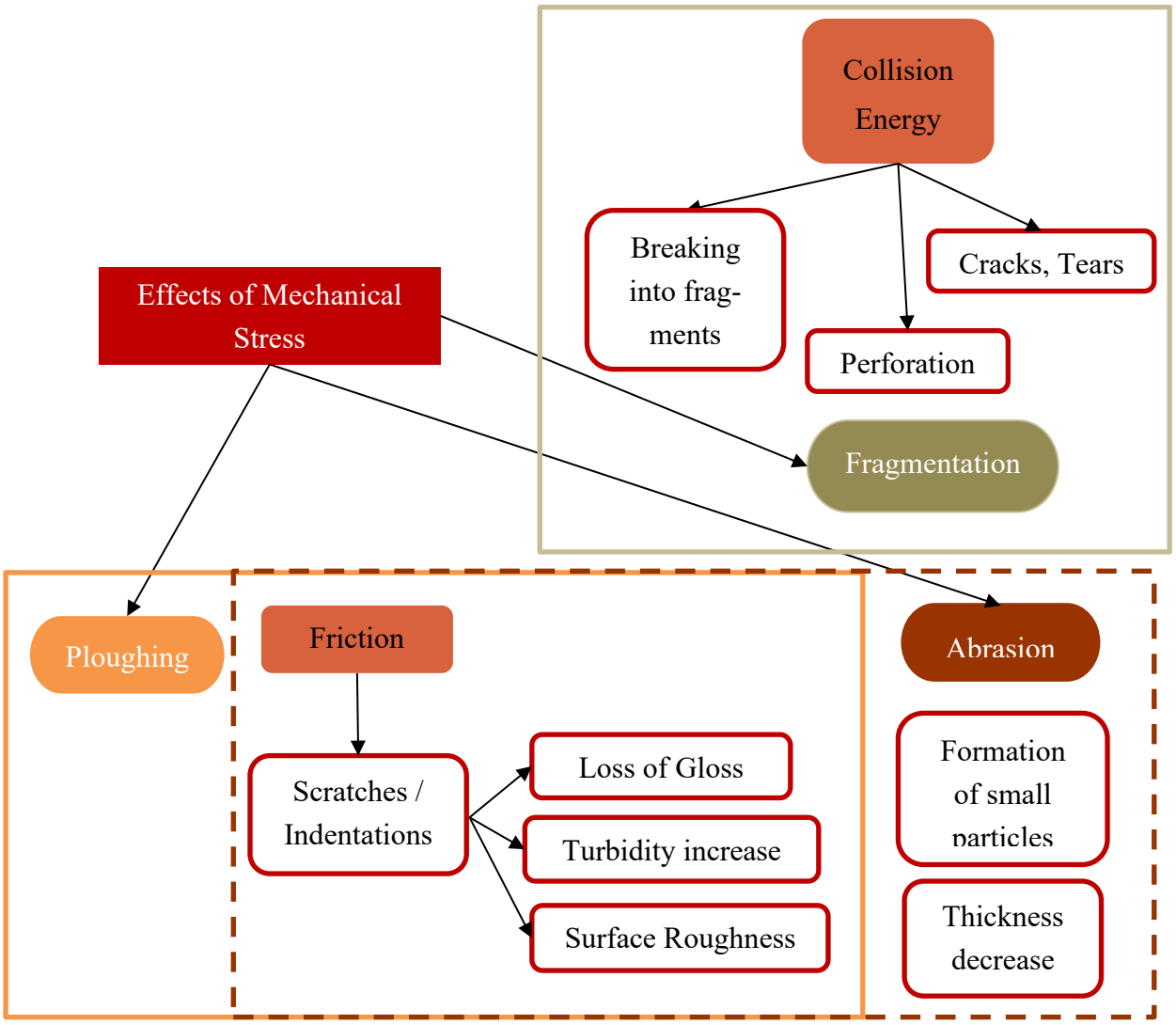


**Figure 2:** Effects of mechanical stress.

The first process is called abrasion, which is the process of loss of very small particles from the material's surface due to friction. In the environment, the mechanism of ploughing (plowing) seems to be important as well. It leads to the formation of surface asperities (plastic deformation), which is caused by the friction forces when the plastic surface rubs against harder material such as sand or stones whilst no direct material removal is included (Barge et al., 2007; Lancaster, 1969). Ploughing and abrasion lead to the change of material`s mechanical properties and thus to material fatigue, shear stress and tensile tearing. Surface roughness is increased, which changes the optical properties of the material. This leads to an increasing fraction of scattered light making its visible appearance less shiny and dull. These changes in surface texture are most likely induced by hard particles dragged along the surface resulting in small scratches and/or indentations (so-called grooves; Cooper, 2012). The cavities in the surface open up the possibility for wedging of fine sediment particles or the emergence of small microplastic particles and at the same time reduces the thickness of the material. Finally, the objects become perforated or break into pieces, which happens when the thickness falls below a critical value depending on the sample type.

The second process is the fragmentation, which is defined as the breakdown of larger particles into two or more smaller particles (fragments) induced by collision forces when plastic objects collide with harder materials like sand grains, rocks or stones. A classical fragmentation process leads to the stepwise formation of two or more fragments of similar size starting from the original object (Figure 3). Such stepwise fragmentation could not be observed in the fragmentation experiments since it would have required multiple observations over time.

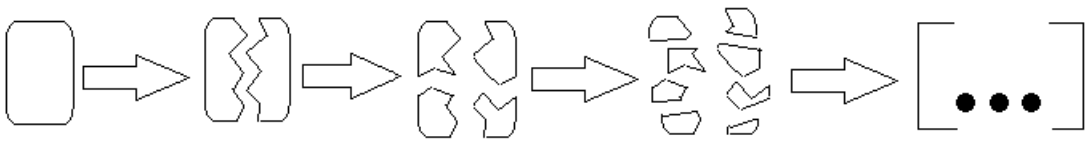

**Figure 3:** Classical fragmentation pattern.

Mechanical stress can lead to several different states of destruction depending on experimental conditions, exposure time and sample type. Abrasion will preferably lead to the emergence of small microplastics (<1 mm), while fragmentation initially results in the formation of fragments in the size range of large microplastics and mesoplastics (1 mm-25 mm). Material breaking and the formation of small fragments subsequently leads to holes in the polymer structure. Cracking of samples without formation of fragments can also be observed in the first step. Under the influence of collision energy, these cracks are intensified finally leading to the emergence of long shaped fragments.

Fragmentation and abrasion are assumed to have different influence on plastic debris in diverse environmental compartments. On the beach, friction between plastic particles and sand induced by wind and water movement probably plays a major role. In the surf

zone, plastics are affected by turbulent wave action making collisions more probable. Especially at beaches with high tidal dynamics, large areas on the beach, in the mud-flats, or in the free water phase plastics can be affected by the movement of water (low and high tide). In the open ocean, fragmentation and abrasion are less likely to occur. Instead, biofouling and colonisation of the surface by microbes will most likely happen. Nevertheless, weathering during long exposure times may enhance the susceptibility of plastic litter for mechanical degradation even in open waters.

## 3.5 Fate of plastics in the marine environment

Plastic debris can accumulate in different marine zones (open water, surge or beach). Depending on the boundary conditions, it is exposed to different environmental factors (UV-light, heat, microorganisms and movements). It is assumed that the degradation induced by UV-light and/or heat preferentially takes place on the beach. In the open water (for floating debris) and in the surf zone, plastics are more protected from light, oxygen and direct heat so that chemical degradation rates are higher on beaches (Andrady, 2011; Corcoran et al., 2009; Ryan et al., 2009). Consequently, beaches are considered as the reservoir of highly fragmented particles (Rezania et al., 2018).

As already described, weathering of plastic debris can facilitate the generation of MPP. MPP are able to migrate easily between environmental compartments by water or wind action because of their low weight and buoyancy. Due to tidal action, MPP generated on beaches can migrate into coastal water and finally into the open ocean (Fok et al., 2017). Since many MPP have a low density, they are likely to accumulate in the top water layer. However, it is discussed that colonisation of microorganisms on MPP may increase the density of the particles and thus reduce their buoyancy (Rummel et al., 2017). This would allow for sinking of materials with densities similar to water and thus to slow sedimentation (Wang et al., 2016). Once having entered the water body, water currents even open up the possibility of migration to remote areas introducing the accumulation to the global ocean circulation (Yang et al., 2021).

## 3.6 Laboratory fragmentation studies

Chemical degradation of plastic material, especially the UV-mediated oxidation, is the process best investigated so far. Several studies under natural as well as under artificial conditions have been reported (Bertoldo et al., 2003; Cai et al., 2018; Gulmine et al., 2003; Valadez-Gonzalez et al., 1999). Systematic investigation of fragmentation and abrasion under natural conditions is much more difficult since shear stress factors can hardly be controlled aggravating generalization of experimental observations. To date, only very few laboratory experiments, which investigate the fragmentation of plastics through mechanical stress under simulated environmental conditions have been published.

Cooper (2012) exposed plastic debris to mechanical impacts and identified six different specific surface textures, which he subsequently compared to surfaces from plastic samples taken out of the coastal zones of Hawaii and Newfoundland. He concluded that "beaches are the most optimal sites for the degradation of synthetic polymers in natural environments" (Cooper, 2012). Song (2017) investigated mechanical abrasion of PE, PP and EPS after UV irradiation in beach sediment on a roll mixer (37 rpm) in a two-month experiment. His results show that UV-oxidative degradation enhance the fragmentation of plastic materials. Secondly, the rate of degradation of different plastic materials proved to be different. EPS, for example, reacts fast to mechanical stress even without UV irradiation. (Kalogerakis et al., 2017) found mild abrasion of PE bags in experiments for estimating the onset of a fragmentation process conducted in roller bottles (13 rpm) filled with beach sediment for 24h. This very short duration time and slow movement conditions resulted in low fragmentation only of irradiated samples. The results confirm that UV irradiation in combination with material characteristics (thickness, additives) have an influence on the mechanical degradation in the environment. As a hypothesis, weakening of the material by weathering needs to be above a certain threshold before fragmentation starts. Consequently, it is assumed that plastics fragment faster onshore (on the beach) than offshore (in the open water).

Efimova (2018) developed an experiment simulating the swash zone in the marine environment using an adopted concrete mixer where LDPE, PP and PS samples were mixed with pebbles and water for 24 hours. Visual inspection of traces of mechanical stress was performed every three hours. The results show an increase in mass and number of MPs over time for all investigated materials. Statistically significant linear dependencies were derived for the relation between the fraction of mass and total number of generated MP particles (after the fragmentation of 1 kg of plastic). A conclusion they draw from their results is that the swash zone seems to be a high fragmentation area with a fragmentation rate higher than in the open water. Furthermore, it was observed that emerged MPP from different polymer samples were different in fragment shapes. Chubarenko et al. (2020) replicated the Efimova experiment to investigate the influence of sediment size on the fragmentation process with four different sediment sizes (sand, granules, small and large pebbles). The results show that larger sediment particles lead to formation of more MPPs when treating polymers. The texture of the natural coast potentially plays an important role for the fragmentation rate of plastic debris.

Chen and his team (2021) analysed the influence of mechanical action of water flow with a constant temperature shaker (200 rpm) in interaction with sunlight UV irradiation with an ultraviolet lamp (average UV intensity was approximately 1.52±0.02 $wm^2$) on thin PE and PP films (<10 µm). Results show, even without sediment particles, the formation of MPP in water setups after 23 weeks (freshwater, seawater with different salinities) while samples exposed under land-conditions were unaffected (Chen et al., 2021).

The results of the different studies indicate that the fragmentation of MPP from larger plastic debris is a main source for MPP in the ocean. Weathering and chemical degradation and the resulting weakness of plastic structure increase the fragmentation probability of plastic debris. Especially on beaches and in the swash zone, mechanical degradation of plastics will lead to the formation of smaller particles.

## 3.7 Own preliminary work

Experimental investigation of the abrasion and fragmentation behaviour of plastic debris in the marine environment is difficult, since simulating natural conditions in laboratory experiments is not trivial. For the development of the experimental setup in this study, experiences and results from earlier fragmentation studies with different plastic materials were used (Reuwer, 2015). In the following, the main conclusions from this preliminary work are described shortly.

Cut offs from plastic items (PE foils, PP caps, PS cups and PET bottles) were shaken for different durations (30d/ 17d) on an overhead shaker in different setups. To simulate beach, seawater and surf zone conditions, the plastic objects were shaken in 1L bottles with sand, artificial seawater or a mixture of sand and seawater, respectively.

Experiments showed that in the pure seawater setup no visible signs of mechanical stress on the material's surface occurred and no microplastic particles could be detected. This led to the conclusion, that plastic floating on the seawater surface will not fragment at all before it has been weakened by weathering.

Under beach and surf conditions, all tested plastic objects showed clearly visible signs of mechanical stress after 30 days of treatment. Surface roughness was increased and discoloration of the materials was observed. The visible increase of surface roughness was attributed to abrasion of small particles. Thicker filmstrips and bottle caps (polypropylene) did not fragment, but visual inspection revealed abrasion of material from the surface of the PP bottle caps, e.g., the white imprint on top of the cups was obviously abraded. This process was more effective in the surf experiment compared to the beach experiment (Figure 4).


**Figure 4:** Polypropylene bottle caps before (left) and after 30 days shaking under beach conditions (middle) and breakwater conditions (right).

Other investigated items were fragmented into more or less smaller particles during the experiments. Thin foil sheets (15x80 mm) from polyethylene bags bore clearly visible signs of physical impact. The foils were partly perforated and showed cracks and kinks. They were also crumpled with wrinkles and curled up at the edges. Fragments with elongated shapes were detected originating from the edges of the foils. Plastic cups and similar items broke into smaller fragments most likely supported by the tension originating from their hollow shape. Figure 5 exemplary depicts the result of the fragmentation process of a polystyrene cup. After 30 days of shaking with sand, the cup was fragmented into five large parts (Figure 5, middle) and 71 smaller particles (Figure 5, right).

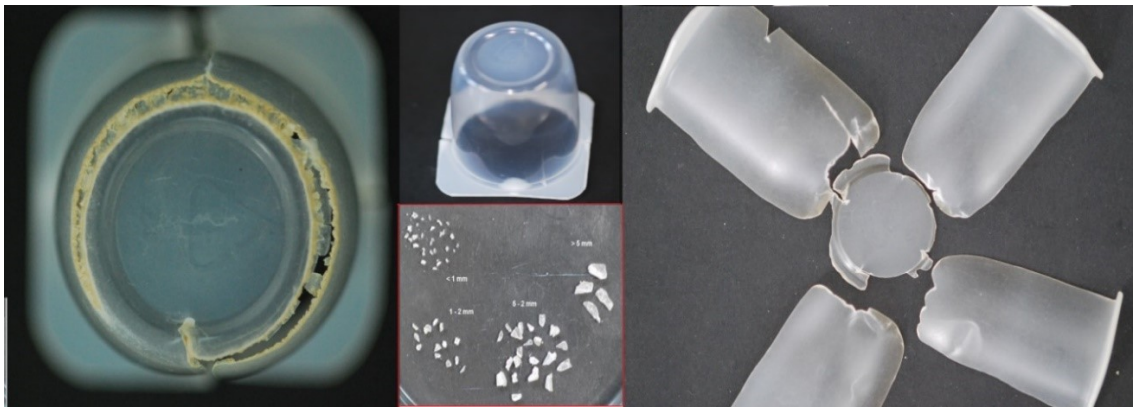

**Figure 5**: Polystyrene cup before (middle, above) and after 30 days of shaking under surf (left) and beach conditions (right) along with extracted fragments (middle, bottom).

The experiments showed that fragmentation of plastic material as result of friction stress in the marine environment will most likely produce large numbers of plastic fragments of all size classes including meso- and microplastics (and potentially nanoplastics). Total numbers, form and size class distribution of fragments were different between the different forms of investigated plastic items, but similar for different polymers of the same form. These results led to the assumption that fragmentation behaviour of plastic debris is dependent on the objects' characteristics, e.g., shape and thickness.

Plastic bags and packaging materials fragmented within 30 days of exposure, while thicker sheets persisted in their original form. Hollow objects formed for specific use like bottles or cups obviously fragment easier due to inner tensions. The observed time scale of the fragmentation process in the experiments gave reason to define 30 days of exposure to mechanical stress as adequate to cause visible damage to plastic samples in shaker experiments.

Therefore, it can be concluded that disposed plastic items indeed constitute a large source for formation of secondary microplastics in the medium-term.

# 4 Hypotheses

The mechanisms of mechanical degradation and its effects on plastic litter in the marine environment are still not well known. Especially the processes of surface abrasion and fragmentation in interaction with natural compartment conditions are insufficiently explored. Based on the existing data and literature information, a number of hypotheses regarding the abrasion and fragmentation behaviour of plastic objects in the environment was set up. The experiments allow the first systematic analysis of the influences on the mechanical degradation pattern of the plastic samples and the emergence of secondary microplastic particles.

The following hypothesis were selected for further investigation:

I. Particle size distributions from fragmentation can be described by a power law relationship, especially in closed experimental systems.
II. Fragmentation of plastic material in the environment occurs under mechanical stress and produces plastic fragments of all size classes including meso- and microplastics.
III. Object form (shape, compactness, stiffness) of plastic litter has an influence on the fragmentation behaviour leading to individual destruction patterns.
IV. Fragmentation of plastic objects is triggered by collisions with environmental structures (stones, rocks, weirs).
V. UV exposure leads to material weakening and subsequently an increasing of the fragmentation probability. UV irradiated plastic samples show higher levels of fragmentation under identical conditions than virgin items.
VI. In the swash zone, friction stress may also cause abrasion. In the low tide surf zone, shear stress by wave action will cause fragmentation of plastic objects into pieces.
VII. On the beach, friction stress from wind-induced movement along the sand surface will mainly induce abrasion. Abrasion will lead to an increasing number of small microplastics, while the plastic object is not necessarily fragmented.
VIII. Grain size distribution of the sediment (sand) affects the size distribution of abraded particles. Fragmentation probability is affected by grain size.

To describe the fragmentation process, the power law model was considered, which describes particle size distributions of a classical fragmentation pattern for a plastic object (I). Mechanical degradation (stress) leads to the destruction of plastic litter, to perforation and cracking with the emergence of fragments in all sizes. The experimental data was subsequently analysed by the power law, to examine the application potential for fragmentation process in the marine environment (II). Plastic characteristics such as polymer type, thickness or object form may have an influence on the destructive effects of abrasion and fragmentation on the plastic objects. A significant influence of the pol-

ymer type on mechanical degradation processes had not been observed in the preliminary experiments, where standard sheets of different polymer types had been exposed in an overhead shaker. Therefore, in this work the focus lays on the influence of object form (III).

The environmental conditions to which plastic waste is exposed determine its fragmentation and abrasion behaviour. In this study, fragmentation and abrasion processes on the beach (wind induced) and in the (low tide) surf zone or rather in the swash zone (wave induced) on plastics was investigated. Since pre-experiments show no significant effect on plastics in open water experiments, they were not further considered. In particular, the effect of collusions with hard materials such as stones (IV), the wave run-up on the beach (VI) and friction stress with sediment particles (VII) were taken into account. But also the influence of UV irradiation on the breaking behaviour (V), which plays especially on beaches a main role, and the sediment grain size distribution were considered (VIII).

# 5 Materials and Methods

## 5.1 Fragmentation experiments

Simulating natural conditions in the surf/swash zone or on ocean beaches in laboratory experiments is a challenging task. One aim of this study was to conduct experiments simulating the abrasion and fragmentation behaviour under beach and surf/swash conditions as realistic as possible.

In preliminary experiments in an overhead shaker turbulent movement with high friction stress in the surf zone had been simulated. In this thesis, the focus was set on horizontal movements of plastic litter induced by wind on beaches (beach conditions) and waves in flat water of the low tide surf zone and the swash zone (breakwater conditions). To represent such less turbulent conditions an orbital shaker with a horizontal amplitude was applied.

Since the objectives of this work were to analyse the natural parameters that influence the fragmentation of plastic debris in MPP, as well as to get a first insight into the time horizon that plastic litter needs for fragmentation, two experimental approaches were investigated:

- EINP: Experiments to investigate the influence of natural parameters on plastic debris
- EFP: Experiments to investigate the fragmentation pattern over the time

### 5.1.1 Investigated plastic items

The aim of the experiments was to get more insight into the abrasion and fragmentation behaviour of commercial plastics in the marine environment. Besides nets and ropes from the fishing industry (Schulz et al., 2017) bottles, carrier bags and food packaging dominate among litter objects found (Veiga et al., 2016). These items are mainly made of PET, PE and PS, which are all thermoplastic polymers. They can be elastically deformed within a certain temperature range depending on the type of material in a reversible process. However, thermal degradation does not start under environmentally relevant temperatures. All investigated test objects are commonly used food packaging items from these three plastic materials bought in a local supermarket (Table 2 and Figure 6). The size of the samples determines the minimum size of the shaking vessels (see chapter 5.1.2), especially their opening. PS cup samples have a colourless protective coating, which causes the surface to appear glossy. All samples were emptied and cleaned with tap water prior use in the experiments.

Since plastic objects entering the environment by intentional littering are mostly whole objects such as complete bags, foils, bottles and cups, samples were exposed to the ex-

perimental conditions in their original form. This included the LDPE bottle caps screwed onto the PET bottles.

**Table 2:** Description of the examined plastic samples.

| Material | Item | Thickness [mm] | Colour | Sample area [cmxcm] | Sample size | Experiment |
|---|---|---|---|---|---|---|
| **PET** | Bottles | 0.35 *Medium* | transparent | - | Large | EINP* |
| **HDPE** | Bottle cap | 1.04 *Thick* | orange with black imprint logo on top | - | Small | EINP* |
| **PS** | Yoghurt cup | 0.18 *Medium* | outer layer: red/purple/yellow inner layer: white | - | Medium | EINP* |
| **LDPE** | Carrier bag | 0.01 *Thin* | transparent | 21 x 47 | Very large | EINP* |
| **PS** | Yogurt cup part | 0.18 *Medium* | outer layer: red inner layer: white | 2 x 2 | - | EFP** |
| **LDPE** | Garbage bag part | 0.028 *Thin* | pinkish | 5 x 5 | - | EFP** |
| **LDPE** | Carrier bag part | 0.01 *Thin* | transparent | 5 x 5 | - | EFP** |

*EINP: Experiments to investigate the influence of natural parameters on plastic debris

**EFP: Experiments to investigate the fragmentation pattern over the time

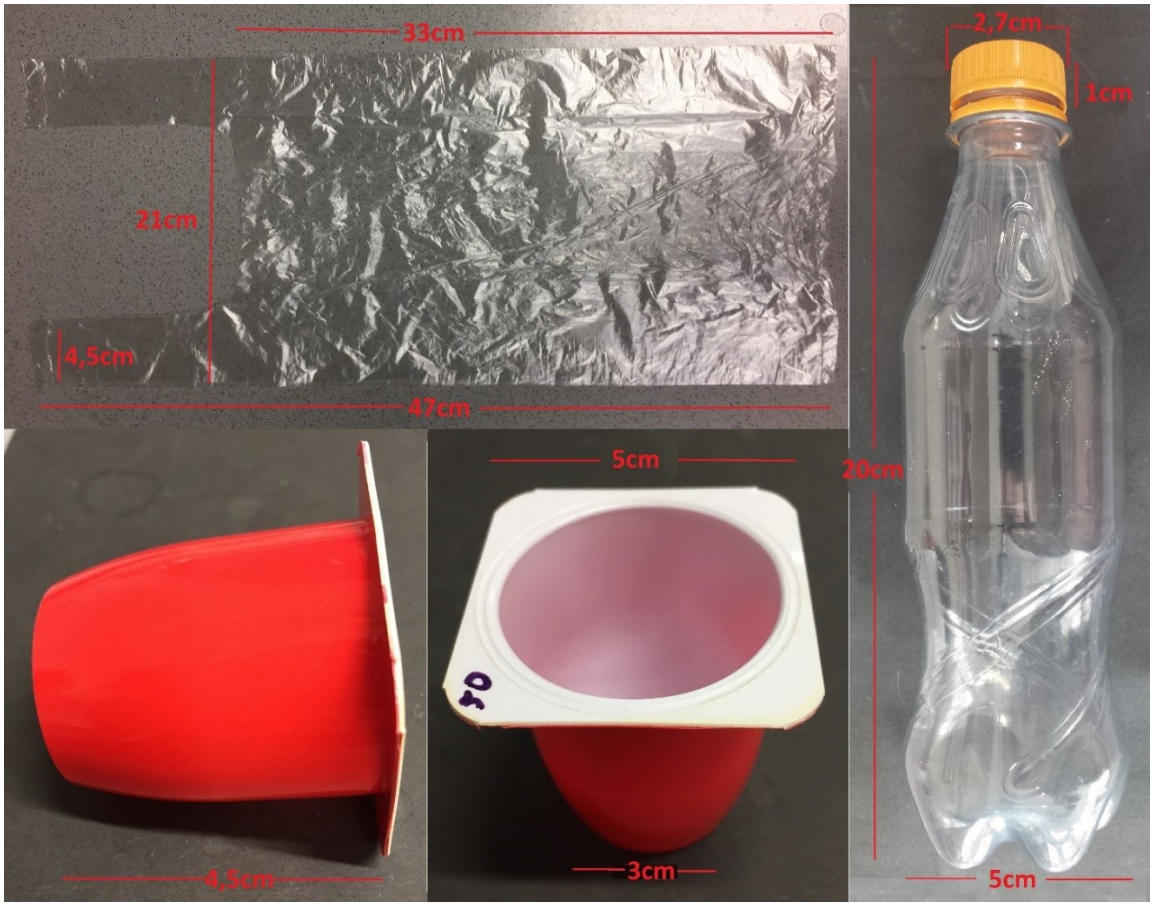


**Figure 6:** Sample dimensions.

Due to the 30 days run time of the experiments, several objects were exposed to the different experimental conditions together in one batch sample in order to generate as much results as possible in the available time. The samples were selected to differ in colour, because the colour does not affect the abrasion and fragmentation behaviour but facilitates visual recognition and attribution of fragments to the original objects in the mixed approach.

The surface of all samples was smooth at the start of the experiments to allow for evaluation of abrasion by inspecting changes in surface roughness. Reproducible quantitative determination of surface roughness with a scattered light sensor was planned, but proved inapplicable, since this technique requires flat samples which were not available from the investigated objects. Surface roughness of the samples was thus visually analysed using a stereomicroscope and a scanning electron microscope (SEM) for selected subsamples.

Material thickness of samples was measured (see chapter 5.5.1) and samples were categorized according to their measured thickness as thin (≤0.01 mm), medium (1 mm-0.01 mm) and thick (> 1mm).

Since samples are manufactured by moulding the materials into their provided shapes (bottles, cups, or caps) internal stress of the samples may occur. Due to their low thickness, PE bags are very flexible.

### 5.1.2 Experimental design

All experiments were conducted on a universal shaker with a horizontal amplitude (SM-30; Edmund Bühler GmbH) to simulate shear stress conditions at the beach and in the low tide surf- and swash zone. Investigated plastic objects were exposed to sand, artificial seawater and a seawater/sand mixture (Table 3).

**Table 3:** Experimental shaker setup of the fragmentation experiments.

| Experimental shaker setup | Environmental situation |
|---|---|
| **Sand + plastic objects** | Beach, wind-induced friction |
| **Seawater + plastic objects** | Open seawater |
| **Sand/Seawater + plastic objects** | Low tide surf zone / swash zone |

Pre-experiments showed that under open seawater conditions neither abrasion nor fragmentation was to be expected within 30 days of exposure to friction stress. Due to the result that no visual signs of mechanical stress were observable in pre-experiments, the final experiments were performed only under beach and breakwater conditions.

Aquarium sand of two different grain sizes was purchased from Hornbach Baumarkt AG. Medium sand substitute (0.2-0.6 mm) and coarse sand substitute (1-2 mm) were

pre-washed with deionized water to minimize contamination with organic or inorganic impurities. The sand was then dried in a laboratory oven chamber at 150 °C.

Artificial seawater was prepared according to (Zaroogian et al., 1969) and stored in the refrigerator at 5 °C until use.

**Table 4:** Constituents of artificial seawater after Zaroogian et al. (1969).

| Constituents | Chemical formula | Amount [g] |
|---|---|---|
| **Potassium bromide** | KBr | 0.1 |
| **Potassium chloride** | KCl | 0.7 |
| **Calcium chloride dihydrate** | $CaCl_2 \times 2H_2O$ | 1.47 |
| **Sodium sulfate** | $Na_2So_4$ | 4.0 |
| **Magnesium chloride hexahydrate** | $MgCl_2 \times 6H_2O$ | 10.78 |
| **Sodium chloride** | NaCl | 23.5 |
| **Sodium hydrogen carbonate** | $NaHCO_3$ | 0.2 |
| **Pure Water** | $H_2O$ | 1L |

The EINP experiments were conducted in 3500 mL glass bottles (ø:15 cm, height: 28 cm) and an aquarium-like tub (50 cm x 42 cm) made of acrylic glass (PMMA) to allow for investigation of whole objects. The size of the bottles restricted the number of parallel setups on the shaker to two (bottles) or one (tub).

Since in the EFP experiments, at least eight time points under identical conditions were necessary, smaller glass bottles (250 mL) had to be used. These did not allow for investigation of whole objects such as cups or bottles. Thus, smaller parts were cut out of the respective objects and exposed.

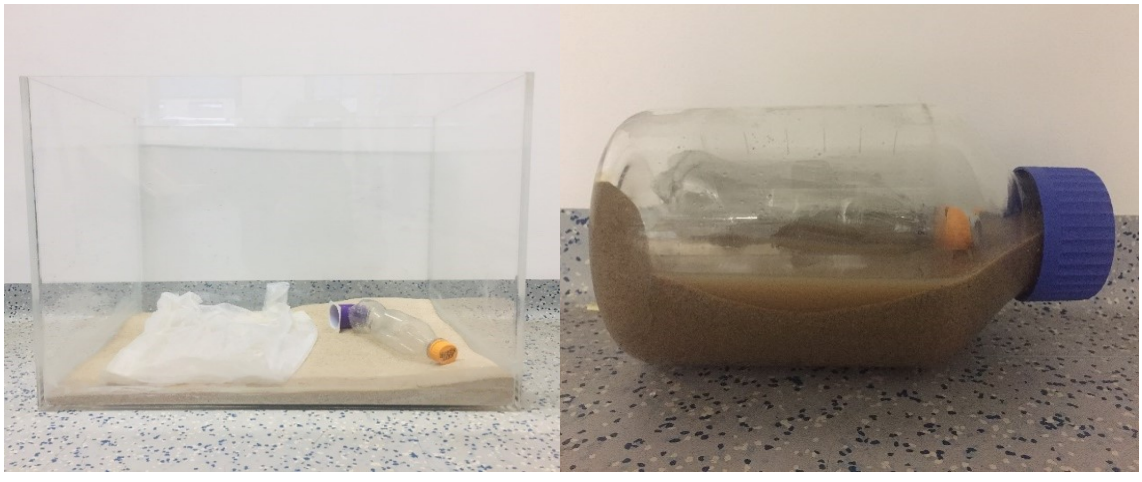

**Figure 7:** Wave tub (left side) and 3.5L glass bottle (right side) as shaking vessels.

Originally, the aquarium experiment was meant to simulate more turbulent wave movement, giving it the term wave tub. However, due to the restriction of the shaking frequency, turbulent movement with waves breaking at the inner walls of the aquarium could not be achieved. Higher frequencies could be used in the bottle experiment (BE), where they induced movement of the plastics and the matrix in the bottles at all. The

large volume of the wave tub together with the restricted shaking frequency prevented steady collisions of the samples with the inner walls of the tub. Thus, wave tub experiments simulate wind-induced friction and wave movements in the swash zone (Table 5).

**Table 5:** Description of the environmental situation simulated by the fragmentation experiments.

| Experimental design | Matrix | Environment |
|---|---|---|
| **Bottle experiment** | Beach conditions | Environmentally not relevant |
| | Breakwater conditions | Environment with high collisions potential like rocky coasts, reefs, surf zone high tide |
| **Wave tub experiment** | Beach conditions | Wind induced friction on the beach |
| | Breakwater conditions | Wave runup in the swash zone |

Due to the smaller volume of the bottles and the higher shaking frequency, collisions were achieved in bottle experiments. Thus, they simulate environmental conditions with high collision potential like rocky coasts or reefs (Table 5). Generally, experiments in small vessels (relative to the sample dimension) are not representative for simulating the abrasion and fragmentation behaviour of plastic objects on beaches but may represent effects of collision forces typical for conditions like cliffs or rocky coastlines.

The objects were placed in the vessels together with the respective medium (Table 3) and then the vessels were fixed on the orbital shaker. The shaking frequency was adjusted to resemble friction stress for plastic objects under environmental conditions on the beach or in the low tide surf- and swash zone. For the glass bottle experiments, 275 rpm proved necessary to move the objects within the bottles, while in the wave tub 150 rpm was sufficient. To investigate the influence of the shaking frequency, two glass bottle experiments were repeated with a lower frequency of 150 rpm (beach and breakwater conditions, non-UV irradiated samples). The shaker was then operated continuously for 30 days.

The grain size of the sand matrix potentially affects the abrasion of small microplastics from plastic samples (Hypothesis 4). Chubarenko et al. (2020) observed a connection between sediment size and the number of fragments generated. It is conceivable that gravel (particles >2 mm), coarse sand (2 mm >particle >0.63 mm) and medium sand (0.63 mm >particle >0.2 mm) determine the size of formed microplastic particles. This hypothesis was investigated in parallel experiments with coarse sand (1 to 2 mm) and medium sand (0.2 to 0.6 mm).

#### 5.1.2.1 Experiments to investigate the fragmentation pattern over time (EFP)

An important issue in the analysis of the abrasion and fragmentation behaviour of plastics in the environment is not only the fragmentation itself, but also the timeframe, in

which the process proceeds. This was investigated by analysing weekly samples during selected fragmentation experiments lasting for eight weeks.

The experiments were conducted on the horizontal shaker in 250 mL glass bottles at a shaking frequency of 275 rpm. Five different plastic samples were exposed, namely:

- Irradiated and non-irradiated polystyrene (PS) parts
- Irradiated and non-irradiated garbage bags of polyethylene (LDPE) parts
- Non-irradiated polyethylene (LDPE) carrier bag parts

The setup was restricted to resembling breakwater conditions using 100 g of medium sand (0.2 to 0.6 mm) and 40 mL artificial seawater as matrix. The sand was pre-cleaned by wet sieving over a 63 µm soil sieve to remove matrix particles smaller than 63 µm prior to the experiment.

### 5.1.3 UV irradiation

As pointed out in chapter 3.4, weathering of plastics can weaken the chemical structure backbone leading to higher vulnerability against mechanical stress. A crucial factor, which affects the stability of plastics in the environment, is UV radiation from sunshine. Especially on the beach, plastic objects lying on the sand surface are exposed to natural sunlight. Additionally, the temperature of the surrounding environment is often relatively high since sand heats up when exposed to sunlight.

To analyse the influence of sunlight radiation, all fragmentation experiments were conducted with the original samples and identical samples irradiated with artificial sunlight prior to the fragmentation experiment.

Samples were continuously irradiated with artificial sunlight in the irradiation chamber of a *Suntest* CPS+ (Atlas Material Testing Technology GmbH) for 10 or 15 days, respectively. The apparatus simulates average global outdoor sunlight in the wavelength region between 300 and 800 nm. Irradiation energy was set to 700 $Wm^{-2}$, which results in a total power of 16.8 $kWhm^{-2}$ over one day of continuous irradiation. PE carrier bags were irradiated for 10 days and PET bottles, PE caps and PS yoghurt cups for a total of 15 days. The reduced UV irradiation time for PE carrier bags was necessary since the samples became too brittle to be transferred to the experimental vessel without disintegration/damage if they were irradiated for longer than 10 days.

The temperature in the test chamber was held at about 40°C due to the use of a water-cooling system.

### 5.1.4 Overview of conducted experiments

In total, 16 different fragmentation experiments (EINP) were conducted. In each setup, all selected plastic items were investigated together due to time constraints. To facilitate

later separation of plastic fragments, all items had different colors. The results of the experiments were compared to prove or disprove the hypotheses listed in chapter 4. Figure 8 shows the cascade of experiments.

Furthermore, four separate experiments over a period of eight weeks (EFP) were performed to analyse the temporal development of the fragmentation pattern. For practical reasons, only small parts cut out of three of the samples (PS cup, LDPE bags) were investigated.

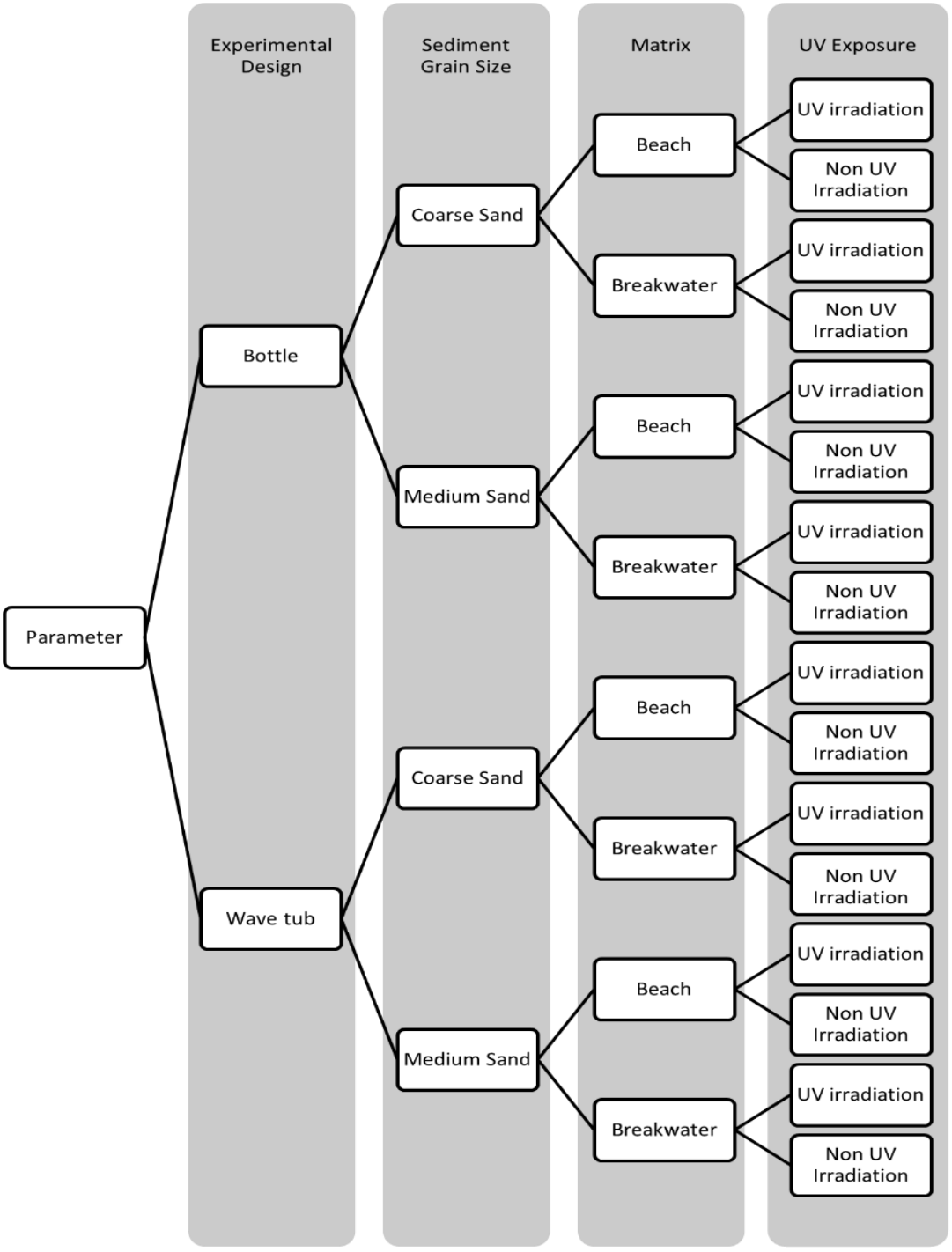


**Figure 8:** Presentation of the variable parameters of 16 experiments EINP.

In the following table (Table 6), all parameters and boundary conditions of the fragmentation experiments are summarized:

**Table 6:** Experimental conditions for fragmentation experiments (EINP) and fragmentation pattern experiments (EFP).

| | **Fragmentation Experiments (EINP)** | | **Fragmentation Pattern (EFP)** | |
|---|---|---|---|---|
| **Vessel** | 3.5 L Bottle | 275 rpm | 250 mL Bottle | 275 rpm |
| | Wave Tub | 150 rpm | | |
| **Samples** | All items together<br>Original Form | | One sample at a time<br>Cut-out parts | |
| **Shaking Duration** | 30 d | | Different durations up to 56 d | |
| **Conditions** | Beach | 2-3 kg sediments | Breakwater | 100 g sediment |
| | Breakwater | 5-6 kg sediment | | 40 mL seawater |
| | | 3 L seawater | | |
| **Sediment types** | Coarse sand | particles [<63 µm] excluded | Medium sand | particles [<63 µm] included |
| | Medium sand | | | |
| **Irradiation** | UV | Non-UV | UV | Non-UV |
| **Extraction** | Large volume samples | | Small volume samples | |

### 5.1.5 Sample processing

Samples should be ideally analysed for plastic particle numbers separated into different size classes. Therefore, the sample had to be processed to remove as much matrix and background as possible.

#### 5.1.5.1 EINP

In a first step (see chapter 5.3.3.3), the samples were sieved into different size fractions using a standard sieve stack for soil analysis with mesh sizes 2 mm, 630 µm, 200 µm, and finally 63 µm (Retsch; DIN-ISO 3310/1). To minimize transfer loss of plastic particles the sample vessel was rinsed three times with pure water. The sieve stack was then placed on a mechanical shaker (AS200 basic; Retsch) for 15 minutes under a gentle stream of pure water (wet sieving) to accelerate the sieving process.

Large, visible fragments and not fragmented plastic objects were taken off the top sieve, dried at room temperature, photographed, visually categorized by size, and inspected for visual signs of mechanical stress on the surface. All remaining size fractions were dried in the sieves in a drying oven at 50 °C for 72 hours. An overview over the sample pro-

cessing shows Figure 9. The fractions were then transferred to glass beakers and stored until extraction with the method for large sample volumes (see chapter 5.3.3).

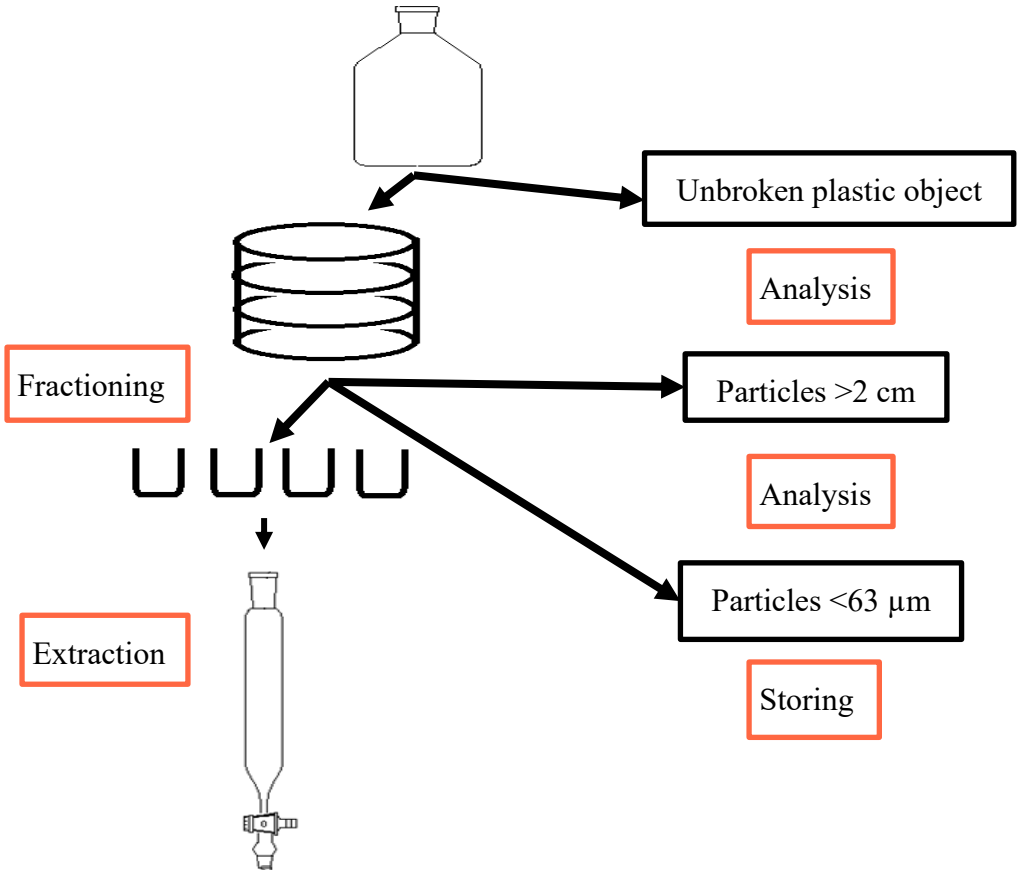


**Figure 9:** Overview Sample Processing EINP.

The smallest particles (<63 µm) present in the filtrate of the bottom sieve were collected by filtration over a cellulose-nitrate filter (8 µm). However, it turned out that the filtrate contained a large amount of very small particles, which led to long filtration times and the need for further sample clean up. Since no practical method was available for this additional purification step articles smaller than 63 µm (sediment particles as well as microplastics) could not be considered in the following analyses with a few exceptions.

#### 5.1.5.2 EFP

Here, the artificial seawater was vaporized slowly by about 50 °C in a drying chamber. Plastic samples bigger than 1 cm were taken out, dried and stored. Then, the sample was dispersed in a sodium chloride solution and five internal standard plastic particles were added (Table 9). Extraction was conducted with the extraction method developed for small sample volumes (see chapter 5.3.2).

## 5.2 Quality control

To avoid contamination of the samples from airborne microplastics, all glassware and other materials used were pre-cleaned in a dishwasher, rinsed with deionized water and

covered with aluminium foil prior to use. The use of plastic items in the experiments and subsequent treatments and analyses steps was avoided (exceptions: shaking vessel bottle cap, blue PP; extraction method: PTFE tube). During all experiments and sample handling, cotton clothes and laboratory cotton coats were worn. No commercial plastic gloves for laboratory use were used, since they are suspected to be a potential source for plastic blanks (Witzig et al., 2020). The use of a clean bench for the analysis of microplastics in this study was not required since all experiments were designed to allow for unequivocal distinction of MPP under investigation (due to color and material type) from potential airborne contaminants.

For the analysis of environmental samples, the use of ultrapure water is recommended in the literature, since there are hints that tap water and even demineralized water may contain particle blanks in the low µm range (Koelmans et al., 2017). Since the focus of the laboratory experiments in this study was on particles larger than 100 µm, demineralized water was considered sufficiently clean to be used.

Blank samples of tap water, demineralized water and distilled water were analysed by filtering 10L over 0.45 µm cellulose-nitrate filter and visual inspection under a stereomicroscope. Blanks were almost exclusively composed of fibres of different length giving no cause for concern. Since the experiments were targeted at microplastic fragments, fibre blanks were simply ignored during data evaluation.

All samples were weighed prior to exposure. After each experiment, the visual remains of the plastic objects were weighed again to ensure that inexplicable mass loss had not occurred. Few samples increased in weight, which is only imaginable if intercalation of matrix constituents into the surface structure had occurred.

To identify individual plastic fragments formed during the experimental process that could not be assigned unequivocally to a polymer material by visual inspection, it was possible to analyse their chemical composition by pyrolysis (Pyr) in combination with gas chromatography (GC) coupled with mass spectrometry (MS) or by Fourier-transform infrared spectroscopy (FTIR).

## 5.3 Optimization of extraction methods

Most methods described in literature are based on the principle of density separation by flotation. However, due to their complex experimental setup they are expensive, often very time consuming and not practical for high volume samples. For small volume samples (50-250 g), a density separation was developed based on the air-induced overflow (AIO) method from Nuelle et al. (2014). For the EINP in this study, the extraction of samples up to 6 kg was necessary (see chapter 5.1.2). Thus, the development of a more practical high-throughput extraction method for large volume samples was necessary.

### 5.3.1 Recovery experiments

To evaluate the effectiveness of the extraction methods, recovery experiments were performed with eight different types of plastics. Low-density plastics (PE, PP and EPS) as well as high-density plastics (PS, PA, PET, PVC and PUR) were tested with a focus on PET and PVC particles, which have the highest densities. Microplastic particles were produced by cutting different plastic items (Table 7) into small pieces of a size between 600 µm and 1500 µm. For better visual identification of the particles, items of different colours were used. 20-30 particles of each plastic material were added per kg sand and homogeneously mixed with the sand. The resulting sample was completely extracted with the respective method. For evaluation of the small volume method 100 g sand were used, while for the large volume method, the amount of sand was 1 kg.

**Table 7:** Selected plastic items for recovery test.

| Microplastic | Average Density [g/cm³] * | Origin of the Material | Colour |
|---|---|---|---|
| **PA** | 1.078 | Industrial pattern | white |
| **PE** | 0.854 | spray bottle | Red |
| **PET** | 1.333 | bottle | green |
| **PP** | 0.861 | bottle top | blue |
| **PS** | 1.052 | Yoghurt cup | yellow |
| **PUR** | 1.26 | Industrial pattern | dark yellow |
| **PVC** | 1.338 | pipe | orange |

* Densities from https://polymerdatabase.com/home.html [17.11.2021];
Copyright © 2021 polymerdatabase.com;
inter alia: https://polymerdatabase.com/polymers/polyethylene.html

### 5.3.1 Separating fluids

Three different separating fluids were tested for the different extraction methods (Table 8). A saturated sodium chloride (NaCl) solution was prepared, dissolving 360 g household salt in 1 L ultrapure water. A simple salt/sugar solution was made from mixing a saturated sodium chloride solution (NaCl) in ultrapure water with household sugar until the intended density was reached (1.30 g/cm³). Both ingredients were purchased in a local grocery store in food quality.

A zinc chloride solution ($ZnCl_2$) (55%, weight/weight) was prepared with a density of 1.30 g/cm³ at 20 °C. 550 g $ZnCl_2$ (analytical grade, Grüssing GmbH, Germany) were added to 1000 ml of ultrapure water in a 2 L glass beaker, stirred and heated until it was fully dissolved. All solutions were prepared in ultrapure water and filtered prior to use (Cellulose-acetate; 0.45 µm; Sartorius AG, Germany). Due to its hazardous properties and high cost, the zinc chloride solution was purified and reused after its use.

**Table 8**: Separating fluids.

| Solution | Concentration [g/mL] | Density [g/cm³] | Prize per L [Euro] |
|---|---|---|---|
| **Water** | - | 1 | - |
| **Sodium-chloride (sat)** | 0.36 | 1.19 | 0.36 |
| **Salt-Sucrose** | 0.36 (NaCl) + 0.5 (Sucrose) | 1.3 | 0.70 |
| **Zinc-chloride** | 0.55 | 1.3 | 10.00 |

### 5.3.2 Small volume sediment samples

To separate LDPE and PS microplastic particles from 150 g of sediment matrix, the method of Nuelle et al. (2014), which is based on fluidisation in a sodium chloride (NaCl) solution with air-induced overflow of the low-density particles and was adapted to the current sample requirements.

A closed system has been developed to reduce airborne blank values. A 2 L conical flask (Figure 10d) with socket NS 29/32 equipped with a magnetic stir bar is filled with the sample and the separating fluid and placed on a magnetic stirrer (Figure 10e). The solution is connected to a reservoir (Figure 10a) via a gas wash bottle head (Figure 10h).

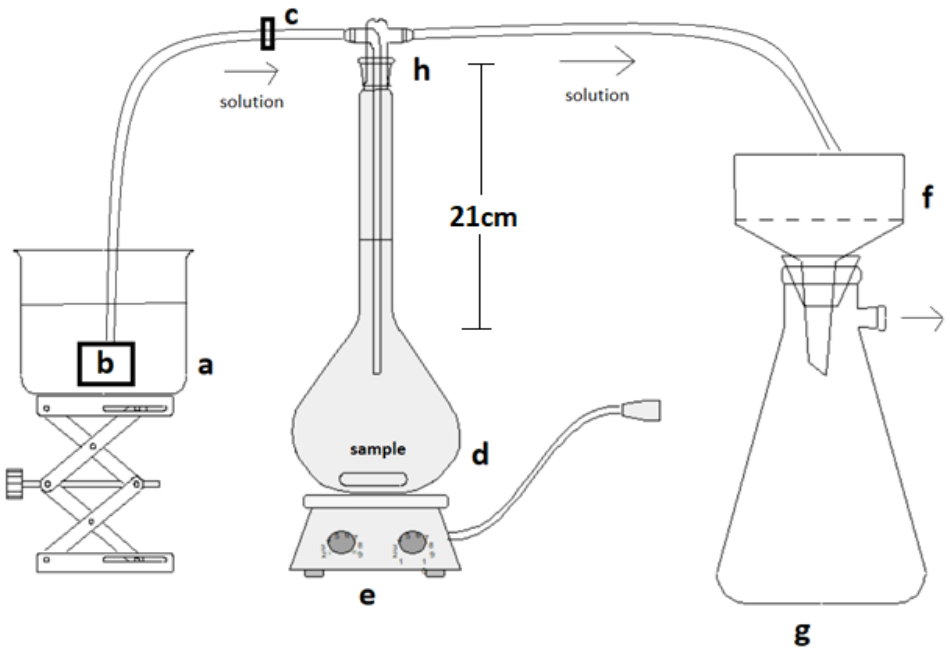


| | |
|---|---|
| a) Fresh Solution Tank | e) Magnetic Stirrer |
| b) Water Pump | f) Microplastic Filter |
| c) Hose Clamp | g) Vacuum Filtration unit |
| d) Floating Tank with Sample | h) Head of a Gas Washing Bottle |

**Figure 10**: Experimental setup of the settling approach for small volume samples

Using a conventional water pump for aquaria (Eheim compact ON 300, 7W; Figure 10b), fresh solution is continuously pumped through the sample from the reservoir (Figure 10a). The connection tube can be blocked with a hose clamp (Figure 10c) to prevent solution backflow when the pump is switched off. Surplus solution including floating microplastics leaves the flask via the outlet and is directly filtered through a pre-weighted 8 µm filter (cellulose nitrate) placed on a vacuum filtration unit (Figure 10f, g).

The sample is initially stirred for about 5 minutes without pumping so that lighter particles float upwards to the surface of the density solution. Heavier particles, which have also been suspended by the movement of the stir bar, are then allowed to re-settle for about 4 hours. This settling time has been selected to ensure complete settling of sediment particles in the micrometre size range. Transfer of the microplastics from the solution surface is then initiated by switching on the water pump and opening the hose clamp. Approximately 100 mL of the density solution is pumped through the separating system onto the filter for filtration (pump speed for Hmax for 0.2 m = about 0.8 L/min). These three steps (mixing, settling and pumping) are repeated three times to allow MPP buried under the sediment load to be freed. After switching of the pump, the fluid inside the head of the gas wash bottle is decanted carefully onto the filter and removed. All parts of the extractor are rinsed with bi-distilled water and added to the filter to catch MPP possibly adhered to the glass surfaces. About 10 cm of the remaining solution in the flask are also decanted on the filter. Then the flask is refilled with fresh solution and decanted again in order to transfer particles adhered onto the inner walls of the flask on the filter. After filtration, the filter is dried for 48 hours at 40°C and the remains on the filter (filter cake) are analysed for microplastics.

To make sure that the full range of MP particles can be extracted, the separating fluid must have a higher densitiy than the largest density of MP present in the sample. In this study, the small volume sample method was applied only to experimental setups with low density particles, so that a NaCl solution could be used. This has the advantage that no purification for recycling the solution was necessary. For samples, which contain MPP with higher densities, a solution with a higher density is necessary.

#### 5.3.2.1 Microplastic recovery

For evaluation of MP recovery, samples are spiked with an internal MP standard (Table 9) before processing. Standard particles were of bright colours different from the sample objects to allow for easy identification.

**Table 9:** Characteristics for internal MP standards.

| Sample Type | Sample Colour | Sample Density [g/cm³] | Standard Type | Standard Colour | Standard Density [g/cm³] |
|---|---|---|---|---|---|
| **PS** | red/white | 1.04 | PS | blue | 1.04 |
| **PE** | pink | 0.93 | PP | blue | 0.91 |
| **PE** | transparent | 0.93 | PP | blue | 0.91 |

Recovery tests were performed with plastic materials with a low density since only low-density materials have been processed in small volume samples in this study. Recovery rates from 88% for PE up to 100% for PP (Figure 11).

The developed method for the extraction of small volume samples using a NaCl solutions is well applicable for low density samples.

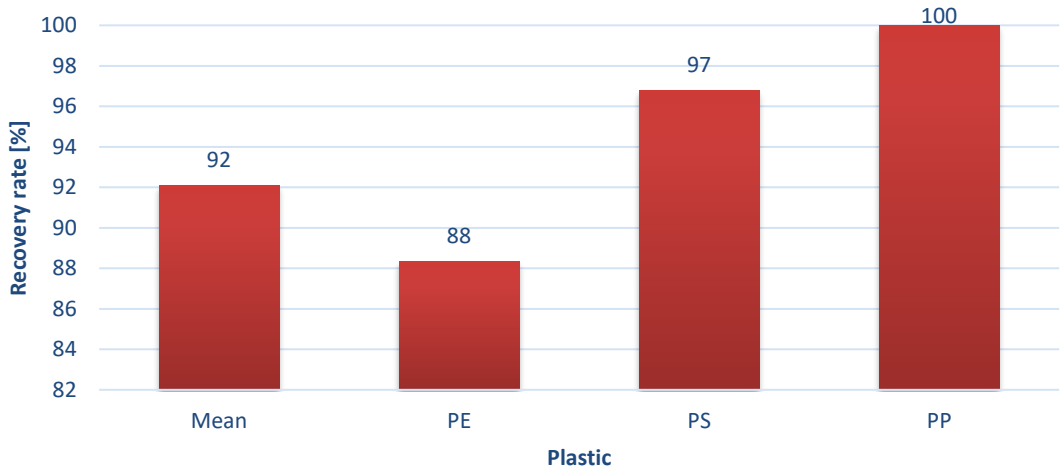


**Figure 11:** MP and sediment recovery rates for small sample method.

### 5.3.3 Large volume sediment samples

Large sample volumes of up to 6 kg sand bear the risk of insufficient recovery in flotation approaches where the sample is just stirred with the separating fluid, because microplastics may be buried under the sand layer preventing them from floating upwards to the solution's surface. Thus, a settling approach was tested, in which the sample was added to the top of the separating fluid in a column setup. This allows for settling of the denser sand particles while the lighter microplastics would float or at least remain suspended in the top liquid layer.

#### 5.3.3.1 Experimental setup

The experimental setup is shown in Figure 12. The method is appropriate for extraction of up to 3 kg sediment sample requiring a total of 2800 mL of separating fluid. A glass column (length 105 cm, i.d. 5.5 cm, Figure 12a) equipped with a stopcock (i.d. 0.8 cm, Figure 12c) at the bottom is filled with about 1600 mL of separating fluid. The column is connected to a collection vessel (volume 1200 mL, Figure 12f) via a connector

(Figure 12d) with an additional outlet (Figure 12e) to allow outflow of surplus solution into a waste collector. At the bottom of the column, an air dispenser (Figure 12b) is introduced creating a continuous gentle upward airflow. By reduction of the surface tension of the separating fluid, this shall prevent matrix and plastic particles from aggregation at the surface and support the separation of the plastic particles from the matrix in suspension by adherence of very fine air bubbles at the particle surface fortifying the density differences and supporting the buoyancy of the lighter particles. Since on the other hand, these bubbles can cause foaming of the separating fluid if airflow was too high, which hampered sample introduction, the optimum flow rate between 6 and 8 ml/sec was determined as most practicable with sufficiently high recovery rates. Higher flow rates led to extensive foaming of the solution.

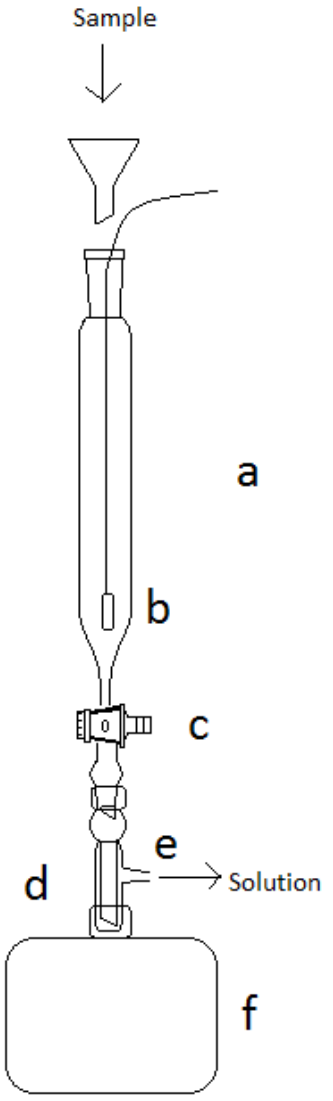


a) Separation column
b) Fine air diffuser
c) Valve / Discharge
d) Connecting piece for draining the solution
e) Discharge
f) Collecting vessel

**Figure 12:** Experimental setup of the settling approach for large volume samples.

The sediment sample to be extracted is introduced manually with a spoon in portions of 10 g with an introduction frequency of 6 spoon per min for medium sand and 1 spoon

per min for coarse sand into the column from the top via a funnel, while the stopcock valve is open. Particles with high density are transferred into the collecting vessel by settling, while lighter particles remain floating in the column. The sediment supplants the separating fluid in the system, which is drained via the outlet into a beaker. This outflow has an influence on the extraction time since the surplus solution does not pass the connector. If the outflow is too big, a negative pressure is created so microplastic particles floating in the separating fluid can be pulled down.

After the sand sample has been completely filled into the column system, the air diffuser is held open for another 5 minutes and then closed. The solution is allowed to rest for about 45 minutes until no more visible particles settle. Then, the valve (Figure 12c) is closed and the solution in the column is filtered through a pre-weighed cellulose-nitrate filter (8 µm, Sartorius AG, Germany) and a cellulose acetate filter (0.45 µm) and dried for 48 hours at 40 °C.

Small particles especially organics and microplastics tend to adhere on the surfaces of the inner glass walls. In extraction pre-experiments, such behaviour was also observed. When the separating fluid is drained after settling, particles visibly adhere onto the inner walls of the extraction column possibly because of electrostatic forces. Thus, all glass vessels including the separating column have to be thoroughly rinsed to minimize the loss of microplastic particles by surface adhesion. This rinsing step should be made with water followed by ethanol, because these liquids partly break up the adhesive forces. Subsequently, the remains on the filter (filter cake) are analysed for microplastics.

The size of the valve (Figure 12c) determines the maximum size of particles in the sample that can be extracted. Particles with a size close to the valve opening will lead to clogging of the valve. Using a valve with an inner diameter of 8 mm allowed for extraction of MPP from sample matrices with a grain size below 2 mm. Larger particles - although smaller than 8 mm - sometimes caused clogging problems due to wedging when their spherical form was irregular.

#### 5.3.3.2 Optimization of extraction parameters

For an efficient use of the extraction method, an optimisation of different method parameters was necessary. The determination of extraction parameters resulting in the best MPP recovery considering minimum interference by co-extracted matrix constituents was conducted by performing recovery experiments under different parameter settings.

Choice of separating fluid

The efficiency of the different separating fluids considering practicability was tested at constant airflow. Best MPP recovery rates (average: 92%) were achieved with zinc-chloride solution. Using deionized water or sodium chloride resulted in much lower recoveries of 59% and 66%, respectively. Salt-sucrose solution proved to be inappropri-

ate due to handling problems. The solution's viscosity is very high, which increases the filtration time exponentially.

Effect of matrix particle size

The extraction of microplastics from large volume sediment samples by flotation is impeded by the possibility of MP particles being buried under the sediment matrix preventing them from floating upwards into the top liquid layer. The potential influence of the sediment particle size was tested for three size fractions (0.063 mm-2 mm, 1-2 mm, 0.063-1 mm) from a commercial sand sample gained by sieving according to ISO 14688-1:2002. Additionally, a mixture of MPP without sand matrix was investigated to observe the unaffected sinking behaviour of MPP in the separation fluid.

MPP recovery was shown to be independent of the particle size of the matrix (grain size of sand). However, the amount of matrix particles not separable from the MPP with the method was higher for sand with small grain sizes. The settling time of particles in the column is not only dependent on the particle density, but also on the particle diameter. It could thus be useful to increase the holding time for MP extraction from samples with small matrix particles.

Settling time

In the density separation approaches, settling velocity of MP particles and matrix particles are important parameters that determine the definition of the minimum required holding time for an efficient separation. Very small sediment particles (fine sand and smaller) were suspected to require up to 24 hours for complete settling in the extraction column (1 m height) depending on the separating fluid. For independent estimation of settling times of particles Stokes-Law formula is often used. However, this formula is not valid over the full range of density differences and particle sizes in MP separation. Furthermore, it is only valid for non-turbulent flows. This can be distinguished by the Reynolds number (R1), which depend on the density and dynamic viscosity of the fluid as well as the characteristic flow length and velocity.

$$Re = \frac{\rho_f \cdot v \cdot d}{\eta} \qquad \text{(R1)}$$

For estimating settling times, the approach described by Dietrich (1982) was applied, which additionally considers the effect of particle characteristics such as shape and roundness (equations (D1) – (D7)). It uses the Corey shape factor (CSF) and the Power roundness index ($P_r$) as additional parameters. This approach can be used independently of Reynolds numbers.

Equation (D1.a) was used for calculation of the settling velocity $w_s$ combining the effects of density difference between the fluid and the particle, the fluid kinematic viscosity (ν) and the shape characteristics described by the sum parameter $w_*$ (D1.b).

$$w_s = 3\sqrt{\frac{w_* \cdot (\rho_s - \rho_f) \cdot g \cdot \nu}{\rho_f}} \qquad \text{(D1.a)}$$

$$w_* = R_3 \cdot 10^{R_1 + R_2} \qquad \text{(D1.b)}$$

Parameter $w_*$ combines the effect of three different processes represented by parameters $R_1$, $R_2$ and $R_3$.

$R_1$ is the uncorrected settling velocity derived from the dimensionless particle size $D_*$ according to equation (D2):

$$R_1 = 3.76715 + 1.92944 \cdot (logD_*) - 0.09815 \cdot (\log D_*)^2 - 0.00575 \cdot (\log D_*)^3 - 0.00056(\log D_*)^4 \qquad \text{(D2)}$$

$D_*$ (equation D3) was estimated from the standardised particle diameter $D_N$ and must be in the range between 0.05 and 5 x $10^9$ to be used with equation (D2).

$$D_* = \frac{(\rho_s - \rho_f) \cdot g}{\rho_f \cdot \nu^2} \cdot {D_N}^3 \qquad \text{(D3)}$$

The effect of the particle shape in general is considered by $R_2$ calculated from the Corey shape factor (CSF) and the dimensionless particle size D* according to equation (D4):

$$R_2 = \left(\log\left(1 - \frac{1 - CSF}{0.85}\right)\right) - (1 - CSF)^{2.3} * \tanh\,(logD_* - 4.6) \qquad \text{(D4)}$$

CSF (equation D5) represents the ratio of the shortest diameter $d_{min}$ and the square root of the product of the two other dimensions.

$$CSF = \frac{d_{min}}{\sqrt{d_1 \cdot d_2}} \qquad \text{(D5)}$$

For natural sediment particles, a CSF of 0.7 is assumed (Dietrich, 1982).

The Powers roundness index ($P_r$) was used as indicator for the particle roundness in calculation of $R_3$ by equation (D6). $P_r$ is between 1 (perfect angular) and 6 (perfectly round); sediment particles are generally attributed a $P_r$ –value of 3.5 (Dietrich, 1982).

$$R_3 = [0.65 - (\frac{CSF}{2.83} \cdot \tanh(logD_* - 4.6))]^{1 + \frac{3.5 - P_r}{2.5}} \qquad \text{(D6)}$$

For particles with low values ($D_*$ <0.05) outside the application domain of equation (D 3), shape and roundness play only a minor role. In this case, an alternative estimation equation (D7) for W* can be used.

$$W_* = 1.71 \cdot 10^{-4} {D_*}^2 \qquad \text{(D7)}$$

Large particles (very high $D_N$) with exceptionally high D*-values (>5 x $10^9$) cannot be treated with this approach at all.

**Table 10:** Parameters of the determining equations for settling velocity after Dietrich (1982).

| Parameter | Unit | Value |
|---|---|---|
| **d** | cm | Flow length |
| **v** | cm/s | Flow velocity |
| **$W_s$** | cm/s | Settling Velocity |
| **$\rho_s$** | g/cm³ | Particle Density |
| **$\rho_f$** | g/cm³ | Fluid Density |
| **g** | cm/s² | Gravity of Earth |
| **ν** | cm²/s | Kinematic Viscosity |
| **η** | Pa*s | Dynamic Viscosity |
| **$W_*$** | - | Dimensionless Settling Velocity |
| **$R_1$** | - | Uncorrected Settling Velocity |
| **$R_2$** | - | Shape Factor |
| **$R_3$** | - | Roundness Factor |
| **$D_*$** | - | Dimensionless Particle Size |
| **CSF** | - | Corey Shape Factor |
| **$P_r$** | - | Powers Roundness Index |
| **$D_N$** | cm | Standardised Particle Diameter |

The efficiency of the extraction method can be enhanced by better separation of MPP and small sediment particles. The more interfering matrix particles were present in the final extract, the more difficult the MP detection was. To get an idea of the holding times necessary to allow for complete settling of different matrix particles, their sinking speed was estimated depending on density and size. Theoretical settling times were then calculated by multiplication of the sinking speed with the column height (105 cm).

Figure 13 illustrates that the influence of the density of the separation fluid is more pronounced in the small particle size range, while it almost vanishes for particles with diameters larger than 750 µm. For example, particles of a size of 63 µm have six times higher settling times in zinc-chloride than in sodium chloride.

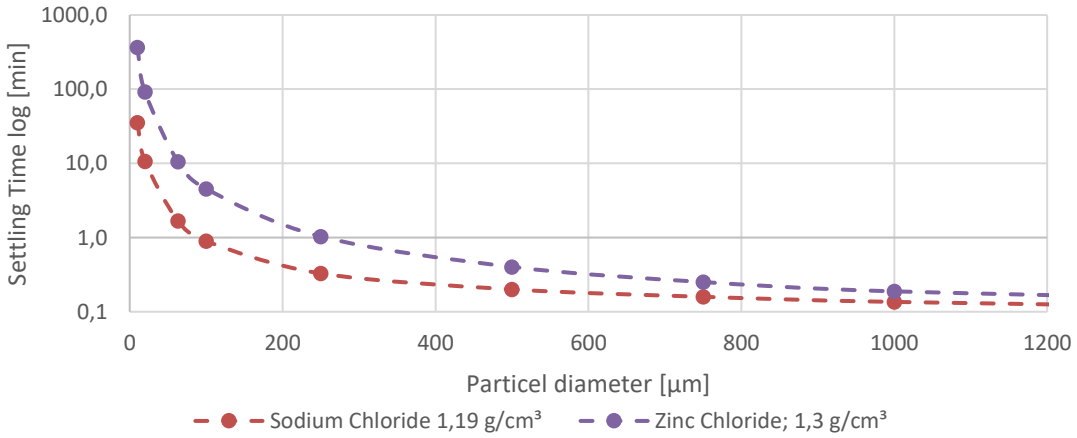


**Figure 13:** Estimated settling time of standard sediment particles (Form:3.5; CSF:0.7) for zinc-chloride and sodium-chloride. The y-axis is log-scaled.

Generally, settling times of particles increase exponentially with decreasing size. For example, 20 µm standard particles need 1.5 hours to settle in $ZnCl_2$- solution in the 105 cm separating column, whereas in NaCl- solution this takes only 11 minutes. Very small particles (10 µm) may require around 6 hours of settling time in $ZnCl_2$- solution, which would explain incomplete matrix settling within the standard holding time of 45 minutes. Thus, settling time was increased to 24 hours for the extraction of respective samples. To check whether this settling was feasible to keep PET (1.37 g/cm³) sufficiently long in suspension, settling time of a standard PET particle was compared with sediment (Figure 14).

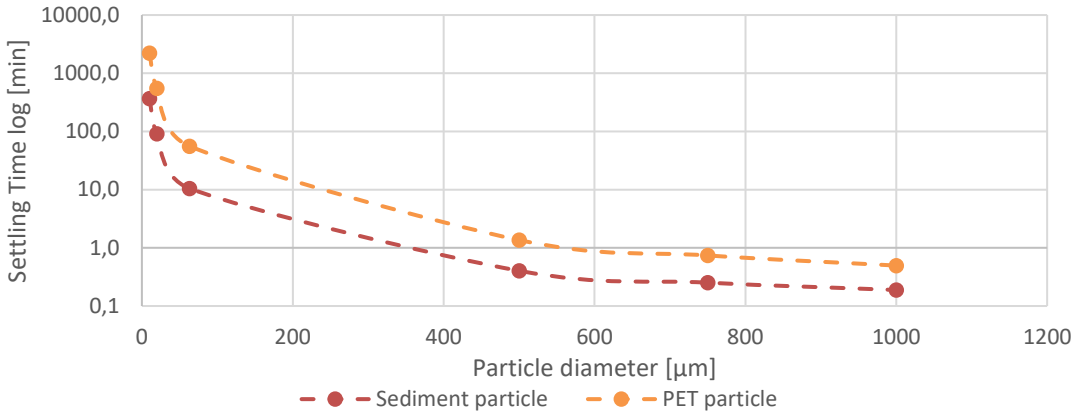


**Figure 14:** Settling times [min] for sediment and PET particles [µm] in zinc-chloride (Form:3.5; CSF:0.7; Separating way: 105 cm). The y-axis is log-scaled.

At a settling time of 24 hours, PET particles smaller than about 22 µm were completely settled, which means that if such small PET particles were formed by abrasion processes, they could not be extracted with the proposed method. All other plastic materials (PE, PP and PS) have lower densities than the separating fluids preventing them from settling at all.

#### 5.3.3.3 Pre-sieving of samples

Kedzierski et al. (2016) introduced a pre-sieving step for sediment samples in their density separation to enhance the MP extraction. This step reduced the particle size variability of the sediment and should lead to a more efficient separation of microplastic from the sediment particles in the separation column. Since the diameter to volume ratio of particles in one size fraction was levelled off, the possibility of larger sediment particles dragging down small MP particles was minimized. (Cashman et al., 2020) also described that removing the smallest sediment fraction (<45 µm) prior to analysis improves the extraction efficiency.

To explore the influence of such a pre-separating step, 1 kg samples were divided into different size fractions following the ISO 14688-1:2017 classification of soil (>2 mm, 2 mm-630 µm, 630 µm-200 µm, 200 µm-63 µm) in a stainless-steel sieve stack on a

mechanical shaker (about 15 minutes, dry and wet sieving). The smallest fraction (<63 µm) was discarded and the remaining sediment was spiked with microplastics before sieving. Each fraction was extracted separately but subsequently in the same separation column with the standard method (zinc-chloride solution, airflow: 6-8 mL/sec (see Figure 15).

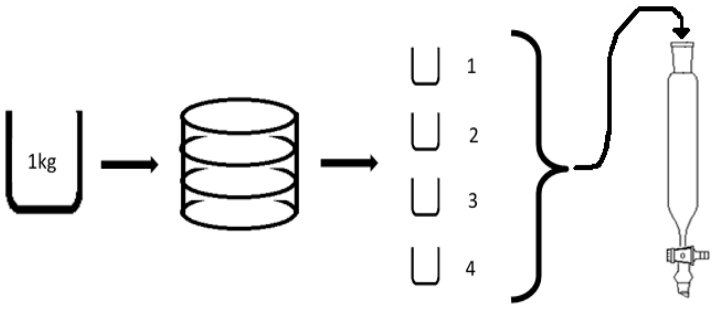


**Figure 15**: Description of pre-sieving experiments.

Figure 16 shows the results for the MPP recovery for the tested pre-sieving steps. Of the different plastic materials, EPS was the only one showing lower recovery after pre-sieving. This might be explained by the pressure exerted on the material during wet sieving, causing EPS particles to stick in the sieve. Recovery rates of all other materials were increased up to 100 %. The pre-sieving process also reduced the amount of sediment still co-extracted on the filter hindering MP identification.

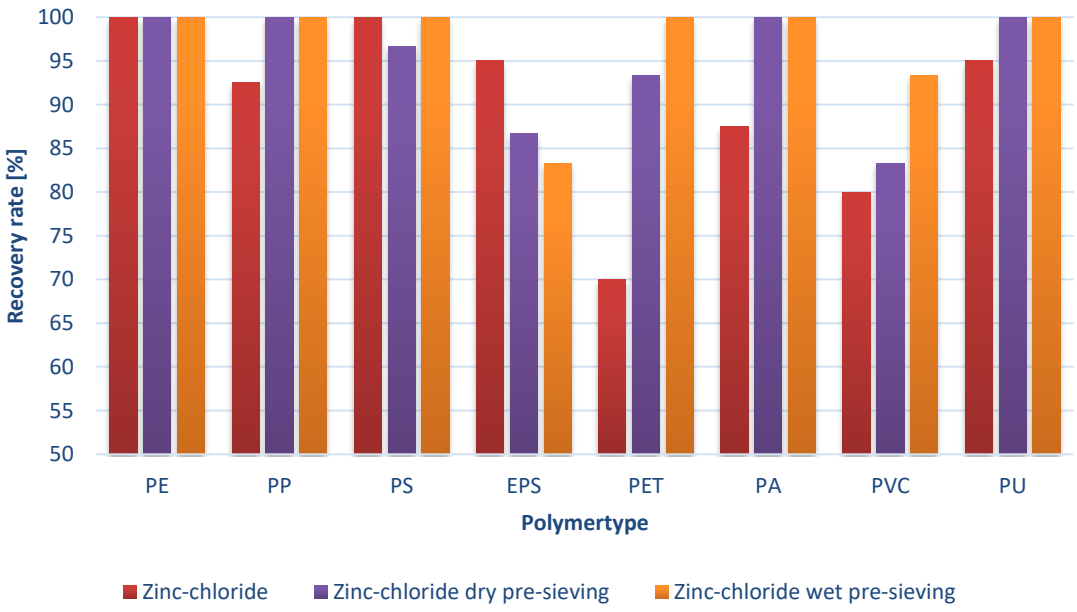


**Figure 16**: Microplastic recovery of pre-sieving steps [%].

Pre-sieving was thus considered a useful pre-processing step to achieve better microplastic particle recoveries. It improves the average recovery rate from 91% to 97%.

### 5.3.4 Sample clean-up for samples with large numbers of particles

After the extraction of the sample with the developed methods, a filter cake consisting of plastic particles of all size classes and co-extracted sediment particles was formed. Microplastic identification and MP particle counting proved impossible when too many sediment particles were still present due to insufficient separation efficiency of the extraction step. In this case, an additional clean-up step had to be filled in. The filter cake was carefully removed from the filter and visible particles were transferred into petri-dishes for identification and counting. The filter and the sample cake were analysed under a stereo microscope at a magnification of 6.5x up to 40x to detect small microplastics by the naked eye. Then, the sample cake was further analysed for particles <350 µm as described in chapters 5.4.3 and 5.4.4.

Figure 17 shows the sample processing for sample cakes with large numbers of particles. Instead of transferring the countable particles into petri dishes, they are separated into size fractions by dry sieving in a sieve stack column (>2 mm, 2 mm-1 mm, 1 mm-500 µm, <500 µm). In the individual size fractions, the lighter polymers (PE and PP) were density separated from PS and PET in 250 mL beaker glasses using water as separating fluid. After 4 hours settling time, the solution was carefully decanted and filtered through cellulose nitrate filter (8 µm). The remains were analysed in a second step: PS and PET were separated using a saturated sodium chloride solution (1.19 g/cm³) and likewise processed. Again, the remains containing PET and sediment particles were subsequently filtered under rinsing with deionised water. Finally, all plastic particles on the filters were transferred into petri dishes, photographed and (if possible) counted.

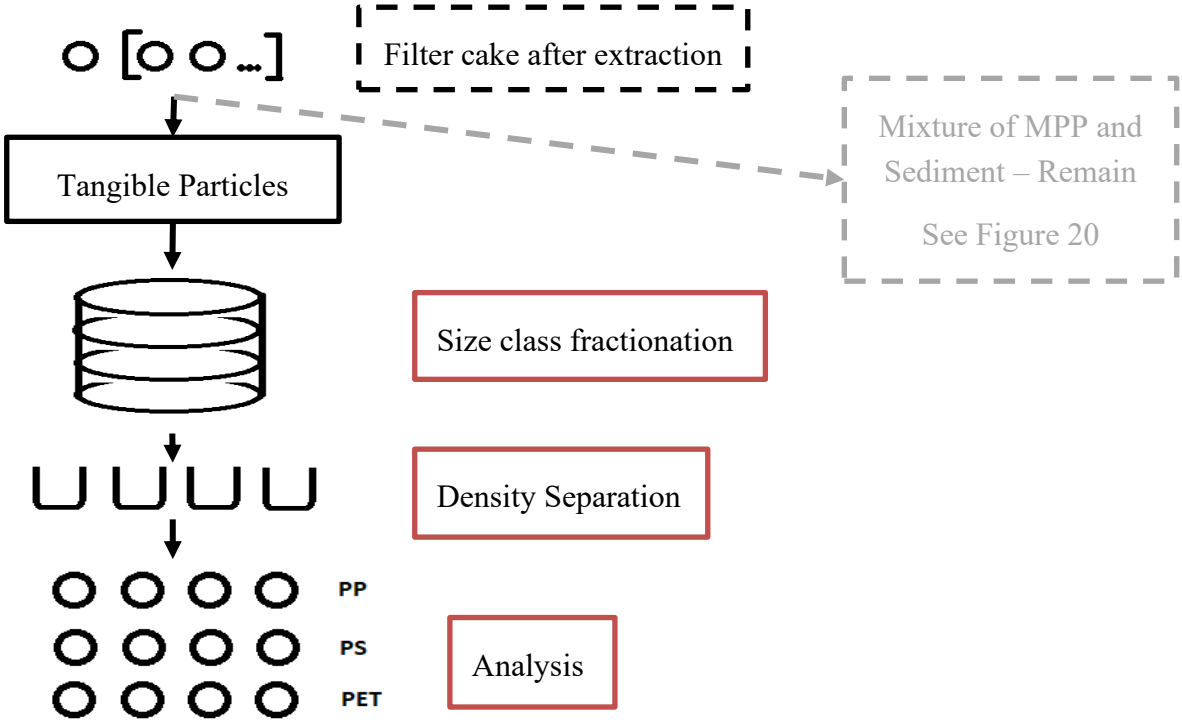


**Figure 17:** Sample Clean-up for samples with large numbers of particles.

In some experiments, LDPE bag samples fragment completely into meso- and microplastic particles of two different forms (thin-long shaped or squared shaped). The removal of such particles was impossible due to the enormous particle numbers. The LDPE particles from such sample cakes were not separated from sediment particles and further analysed by a thermogravimetric analysis (see chapter 5.4.3).

Surprisingly, LDPE bag samples sometimes disintegrated into long-shaped meso- and microplastic fragments, which formed entanglements hardly separable from the sediment matrix and other small plastic particles after extraction (Figure 18). These entanglements were carefully removed from the bulk sample before the above described clean up step was applied for the other three sample types. Entanglements were carefully released with tweezers (Figure 18b). Unlike PET, PS and HDPE samples, counting individual LDPE particles was not possible due to the entanglements and the large number of particles (Figure 18c).

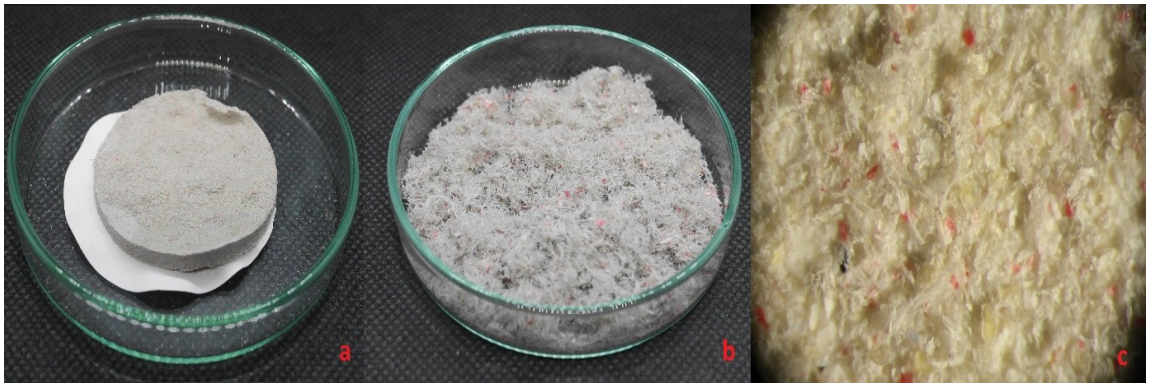


**Figure 18:** PE bag sample cake forming an entanglement after extraction (a). Entanglement was carefully released (b). Sample section with a x40 magnification (c). Red particles were PS sample microplastics trapped in the LDPE-entanglement.

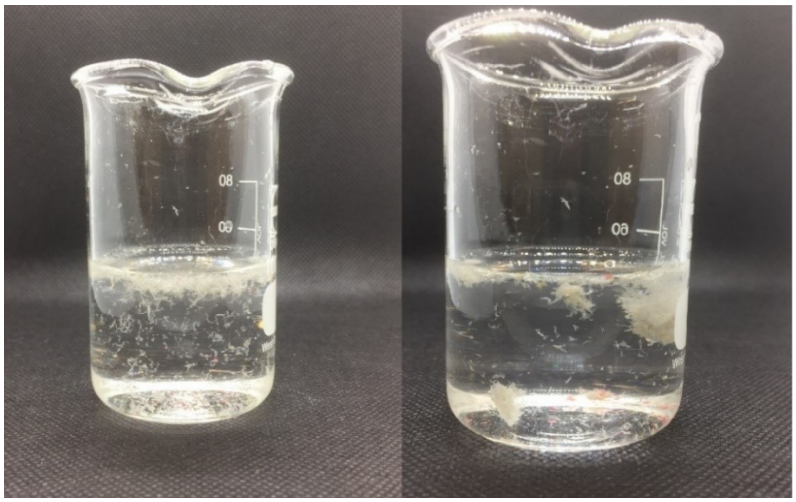

**Figure 19:** PE-matrix particle entanglements suspended in ultra-pure water before sonification (left) and after sonification (right).

Separation of the PE particles from the entanglements with ultrasonic treatment (Figure 19) did not succeed as well. Free-floating meso- and microplastics formed more or less globular entanglements again after sonification for only 10 seconds. Therefore, these samples were analysed by a thermo-gravimetric analysis as described in chapter 5.4.3 and µ-Raman analysis of suspended sub-samples described in chapter 5.4.4 (Figure 20).

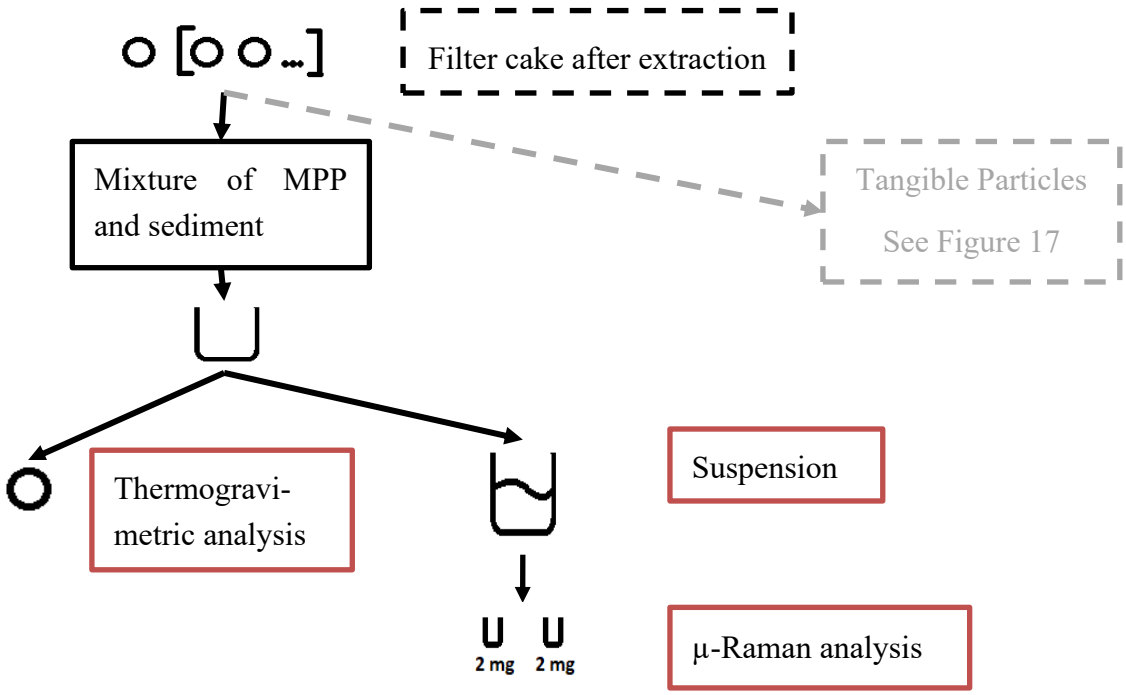


**Figure 20:** Analysis of microplastic <350µm.

## 5.4 Analysis and counting of microplastic particles

### 5.4.1 Microscopic particle counting

Ideally, particle numbers for different size classes in the meso- and microplastic range should have been determined for the different experimental setups. Large particle numbers indicate a high grade of destruction of the samples due to abrasion and/or fragmentation. Observed particle numbers are important for the evaluation of the effect of experimental boundary conditions.

For each sample type, larger fragments manually collected were pre-sorted by size and then photographed. With the help of graph paper, fragments were measured (largest side) and divided into five particle-size categories (>2.5 cm-macroplastic; 2.5 cm-5 mm-mesoplastic; 5-2 mm-large microplastic; 2-1 mm - small microplastic; 1 mm-350 µm - very small microplastic). Smaller particles were analysed by µ-Raman analysis (see chapter 5.4.4).

For microplastic microscopic analysis, collected particles were optically analysed under a stereo microscope Wild M3Z (Leica Microsystems GmbH, Wetzlar, Germany) at a magnification of x6.5 up to x40. This allowed for unequivocal identification of particles larger than 350 µm to 5 mm in at least one dimension with the help of a measuring eyepiece. If possible, the identified particles were allocated to the polymer material according to their unique colour.

### 5.4.2 Particle number estimation by weight

Some sample extracts had too high MPP numbers to be counted manually. For these samples, an estimation was made by weighing. For each size fraction, the average weight per particle was estimated by weighing a defined number of particles (5-10) representing the size distribution as best as possible. Total MPP weight of the fraction was then used to estimate the total MPP number in the fraction.

### 5.4.3 Thermo-gravimetric analysis

The sample cakes consisting of PE and matrix entanglements were subjected to a thermo-gravimetric analysis in form of an incineration at 600 °C. Organic material undergoes thermal decomposition under these conditions leaving behind inorganic constituents. Since we assume that natural organic matter is not present in the sample extracts, this fraction represents the amount of plastic material solely, while the inorganic fraction is composed of the sediment matrix. Incineration of weighed sub-samples was conducted in porcelain crucibles, which had been burnt out before adding the sample. Combustion of flammable ingredients was performed with a Bunsen burner under a fume hood. Complete incineration was then achieved by placing the crucible in a muffle furnace at 600 °C for about 2 hours. The remains were cooled down in a desiccator and then its weight was determined. The weight of the residue was used to estimate the amount of inorganic sand matrix (residue) and plastic material (ignition loss) in the different samples.

### 5.4.4 µ-Raman analysis

The sample cake residue was analysed using µ-Raman analysis to gain insight into the number and size distribution of small MP particles not identifiable under a microscope (5 µm - 350 µm). The analyses were kindly conducted by an external project cooperation partner (TZW: DVGW-Technologiezentrum Wasser; Karlsruhe). Due to restricted capacities during the Corona pandemic, only a limited number of samples could be analyzed.

Sample cakes were removed from the filter and suspended in distilled water. The suspension was stirred with a magnetic stirrer to achieve homogeneous distribution. A subsample (2 mg sample weight) was taken with an Eppendorf pipette and vacuum-filtered through 25 mm PTFE filters (1-2 µm, sintered, Pieper Filter GmbH) using a stainless

steel in-line filter holder (Pall Corp.). The rest of the suspension was subsequently filtered through a cellulose nitrate filter (8 µm) and dried in a desiccator.

The subsamples were analysed by µ-Raman using a Horiba LabRAM HR Evolution system (Horiba Jobin Yvon) equipped with a Syncerity EMCCD camera (Horiba Jobin Yvon) and a confocal BXFM-ILHS microscope (Olympus). As µ-Raman analysis is very time consuming, two "piece of cake" sections per filter (Schymanski et al., 2021) were analysed, which corresponds to approx. 30% of the filter area. Particles were measured using the *ParticleFinder* tool of the software LabSpec (ver. 6, Spectroscopy Suite Software, Horiba Jobin Yvon). Measurements were performed using x20 and x10 magnification in the wavenumber range 50-3300 $cm^{-1}$. The excitation wavelength was 532 nm (air cooled solid-state laser kit). 600 gr/mm spectral grating, 50 to 150 µm pinhole, 2-3 seconds acquisition time, automatic baseline-correction and 1 accumulation were used. For polymer identification, acquired spectra were compared with a spectra database using the software TrueMatch (WITec GmbH). Spectra match was manually verified by experienced lab personal. The number of polymers detected on the two filter sections ("piece of cake") was subsequently extrapolated to the entire filter.

These numbers were then extrapolated by an extrapolation factor derived from the proportion of the amount (g) of the subsample to the total amount of sample cake. The factors ranged from 26 to 450 (see Table 27.) Original sample counts and extrapolated data are listed in the appendix (see Table 36 to Table 40, Appendix).

### 5.4.5 Sample Treatment - Process diagram

As discussed in the previous chapters, it was not useful to treat all samples from the different experimental setups in the same way. Depending on the outcome of the experiments, different extraction steps, processing and further clean-up were necessary. Also, analytical methods applied to characterize the extent of abrasion and fragmentation were different. Figure 21 shows an overview of the different treatment schemes applied and in Table 11 the treatments are assigned to the different experimental setups (EINP). All EFP samples passed process scheme 3 or 4 as the number of plastic fragments produced was manageable, so clean up steps were not necessary.

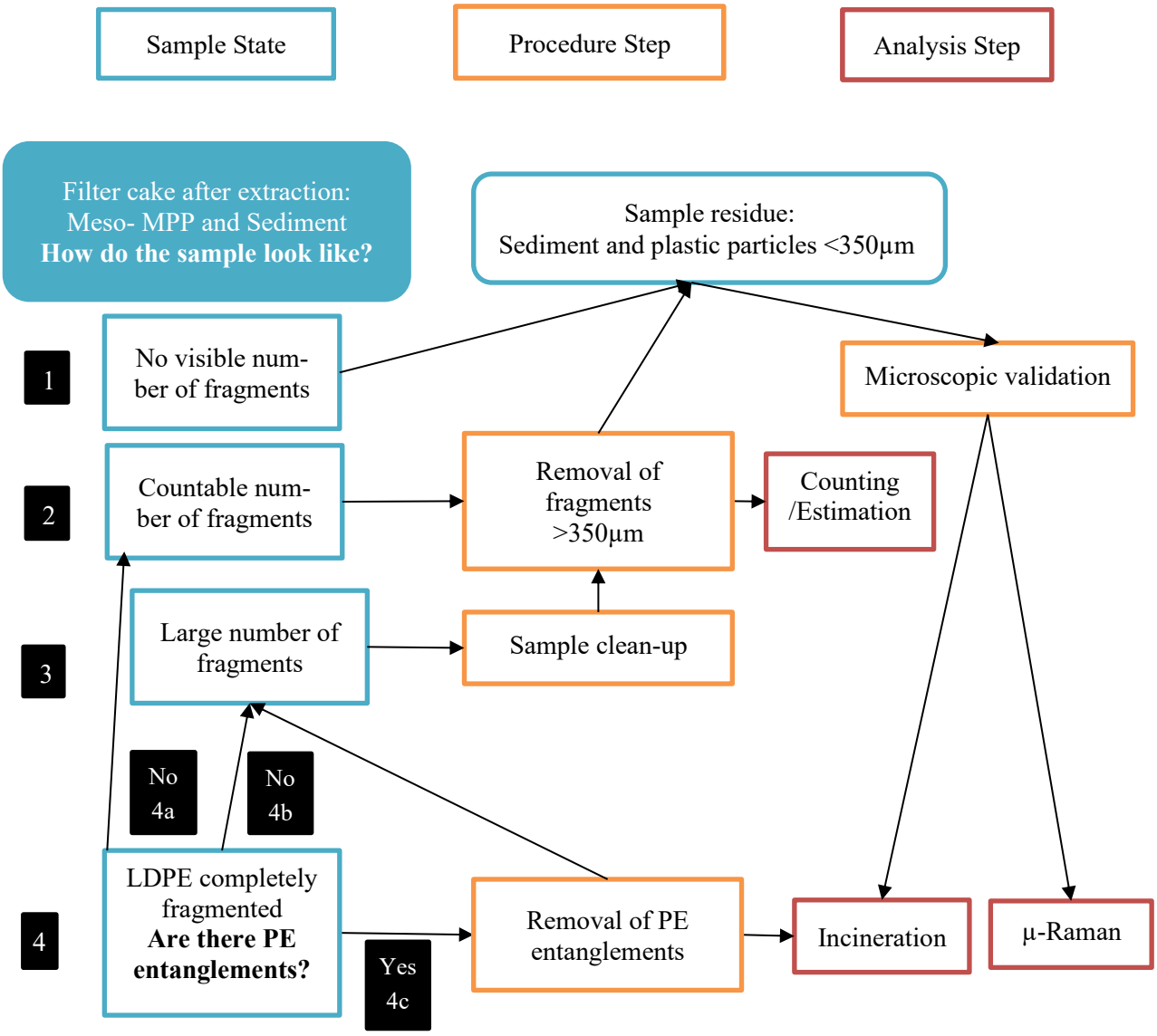


**Figure 21:** Process diagram. The illustrated process starts with the filter cake after the extraction. Black boxes show the number of process scheme.

**Table 11:** Analysis process for samples from EINP.

| Experimental design | Sediment grain size | Matrix | UV-Exposure | Process number |
|---|---|---|---|---|
| **Bottle** | Coarse sand | Beach | UV irradiated | 4b |
| | | | Non-UV irradiated | 2 |
| | | Breakwater | UV irradiated | 4b |
| | | | Non-UV irradiated | 4c |
| | Medium sand | Beach | UV irradiated | 4b |
| | | | Non-UV irradiated | 2 |
| | | Breakwater | UV irradiated | 4a |
| | | | Non-UV irradiated | 4c |
| **Wave tub** | Coarse sand | Beach | UV irradiated | 2 |
| | | | Non-UV irradiated | 2 |

| Experimental design | Sediment grain size | Matrix | UV-Exposure | Process number |
|---|---|---|---|---|
| | Medium sand | Breakwater | UV irradiated | 2 |
| | | | Non-UV irradiated | 1 |
| | | Beach | UV irradiated | 2 |
| | | | Non-UV irradiated | 1 |
| | | Breakwater | UV irradiated | 2 |
| | | | Non-UV irradiated | 1 |

## 5.5 Evaluation of abrasion and fragmentation

### 5.5.1 Visual inspection

All samples were visually inspected for signs of mechanical stress and abrasion. Objects were photographed before the experiments and thereafter and all scratches, abrasion traces, cracks and changes of surface roughness were noted.

To enable the comparison of effects on the investigated objects by the experimental conditions, a categorization system based on observed signs of mechanical stress i.e., visible signs of fragmentation and abrasion was developed. Samples were categorized using several descriptive statements for signs of abrasion and fragmentation (Table 12) including the most important observations from chapter 6.1.

**Table 12:** Signs of fragmentation and abrasion used for sample categorization.

| **Signs for fragmentation** | |
|---|---|
| Sample object is original without breaches | F0 |
| Sample is torn into several fragments | F1a |
| Original sample shape is still clearly identifiable | F1b |
| Plastic object is perforated or cracked | F2 |
| Mesoplastic and microplastic fragments have been generated | F3 |
| **Signs for abrasion** | |
| Sample shows no visible signs of mechanical stress on the surface | A0 |
| Surface is visibly affected (change in light reflection) | A1 |
| *Thickness has measurably decreased* | *A2* |

Based on the observations from Table 12 a decision tree (Figure 22) was developed resulting in a categorisation of the samples according to their degree of destruction from 0 (no visible fragmentation or abrasion was observed) to 5 (the sample was fragmented into meso- and microplastics), henceforth referred to as the destruction category. Since abrasion and fragmentation often occur simultaneously, the system considers both processes.

This categorization system, however, does not consider different levels of abrasion. Thus, an additional classification of abrasion was introduced ranging from 0 (no abra-

sion) to 2 (strong abrasion) based on surface texture damages like scratches and asperities which affects the surface haze. Figure 23 exemplary shows the three stages of abrasion as observed for a PS cup sample. For all samples that allowed for thickness measurements of the object before and after exposure, this information was used for confirmation.

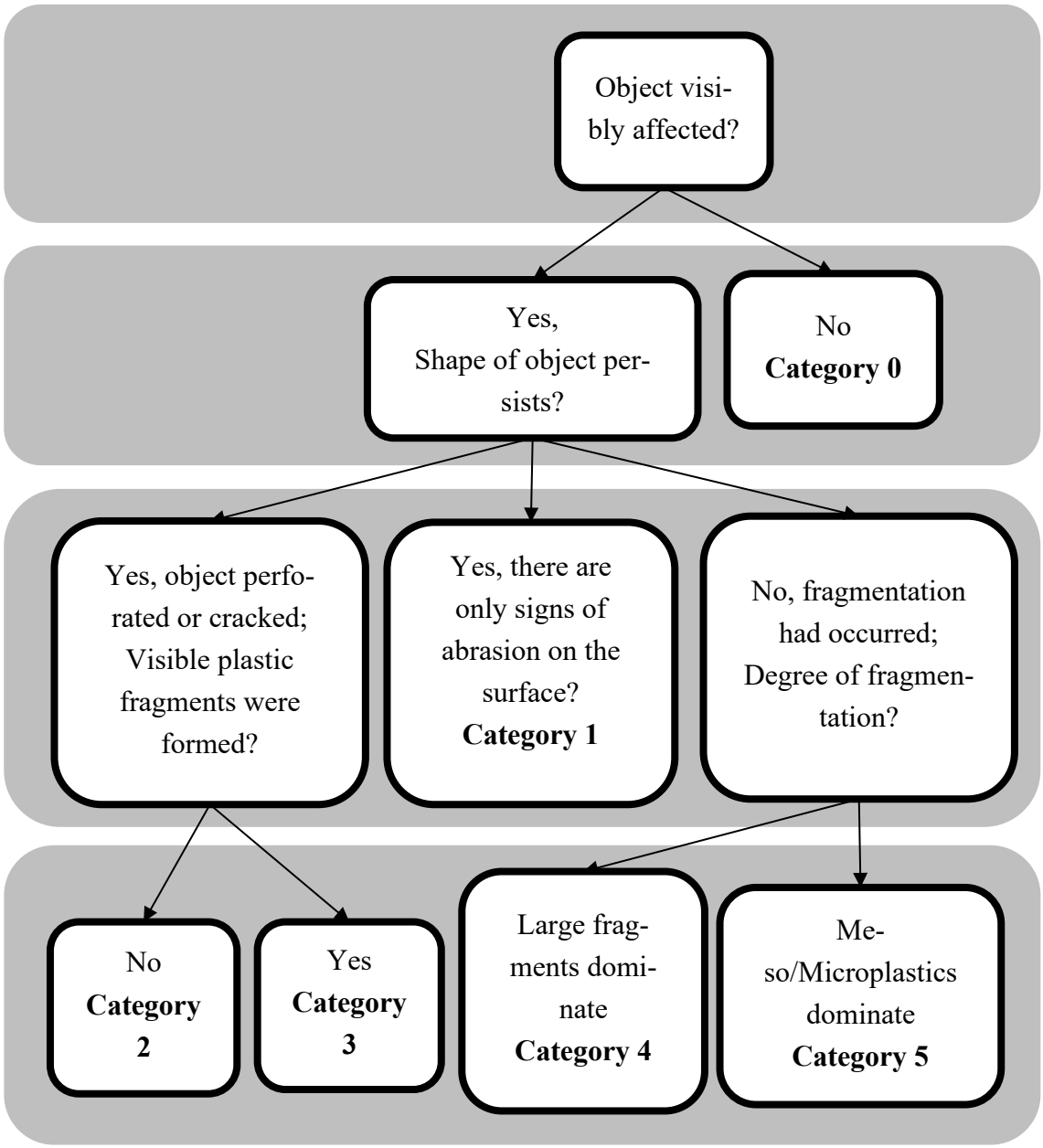


**Figure 22:** Decision tree for classification of samples into destruction categories.

**Figure 23:** Example of PS cup samples in the three different abrasion categories. Red sample: Abrasion category 0; Purple sample: Abrasion category 1; Yellow sample: Abrasion category 2.

### 5.5.2 Sample thickness

Material thickness of selected sample objects was measured with a digital Digimatic CD-15CPX calliper from Mitutoya (Japan) with a resolution of 0.01 mm. The average value from three aliquots (1 cm x 1 cm) of each sample was determined.

Samples were selected for their signs of surface abrasion. A distinction was made between high, medium or low level of abrasion (Table 13).

**Table 13**: Selected samples for thickness analysis.

| Sample type | Experimental design | Sediment grain size | Matrix | UV-Exposure | Level of abrasion |
|---|---|---|---|---|---|
| **PET** | BE | Medium Sand | Beach | UV | Low |
| **PET** | WTE | Medium Sand | Beach | UV | Low |
| **PET** | BE | Coarse Sand | Breakwater | Non-UV | High |
| **PS** | BE | Coarse Sand | Beach | Non-UV | Low |
| **PS** | WTE | Medium Sand | Beach | UV | Low |
| **PS** | BE | Medium Sand | Breakwater | UV | High |

### 5.5.3 Sample surface analysis

For the evaluation of the destruction level of the sample surface by abrasion, a scanning electron microscope (SEM) analysis was performed for selected objects (HDPE cap, PS cup and PET bottle samples). This method delivers surface images from a focused electron beam. The surface is scanned in a raster pattern leading to spatial representations of the sample morphology. The microscopic principle is easy: High energy electrons hit the sample and interact with sample atoms at various depths within the sample producing so-called secondary electrons (backscattered electrons) and characteristic X-rays, which are detected and displayed on a computer screen. Its high resolution makes SEM useful for the analysis of microplastic generation from plastic debris (Schwaferts et al., 2019).

A high vacuum SEM (Joel JSM-IT 200, JEOL GmbH) with a 10kV electron accelerating voltage and a 30° sample tilt was used. Sample preparation was conducted as following: About 1 cm x 0.5 cm sample parts were transferred onto a conductive and adhesive carbon tape mounted on an aluminium SEM sample holder. Before introducing the samples in the high vacuum chamber, they were sputter-coated with gold to make the plastic electrically conductive preventing accumulation of electrostatic charge.

Sample-selection was made based on the visually evaluated level of destruction (Table 14) categorized into high, medium and low level.

**Table 14:** Selected samples for SEM.

| Sample type | Experimental design | Sediment grain size | Matrix | UV-Exposure | Level of destruction |
|---|---|---|---|---|---|
| **HDPE** | BE | Coarse Sand | Beach | UV | High |
| **HDPE** | WTE | Medium Sand | Beach | UV | Low |
| **PET** | BE | Coarse Sand | Breakwater | Non-UV | High |
| **PET** | BE | Medium Sand | Beach | UV | Medium |
| **PET** | WTE | Coarse Sand | Breakwater | Non-UV | Low |
| **PET** | WTE | Medium Sand | Beach | UV | Low |
| **PS** | BE | Medium Sand | Breakwater | UV | High |
| **PS** | WTE | Medium Sand | Beach | UV | Low |

### 5.5.4 Cluster analysis

To divide a set of objects into homogeneous groups (clusters) a cluster analysis can be performed. Objects in a cluster should be more similar in selected properties to each other than to objects in other clusters. Resulting clusters can highlight the influence of test parameters (experimental design, sediment grain size, matrix condition, UV irradiation) by grouping samples/objects together due to their signs of fragmentation and abrasion.

Cluster analysis is not a direct procedure, but a collective term for statistical procedures that allow for structuring a data set by assigning individual samples to groups. There are numerous clustering models (connectivity model, centroid model etc.) available using different algorithms and proximity measures for discovering a cluster structure. The success of the application depends on the appropriate combination of data and model (Wiedenbeck, 2010). Here, the connectivity model "*Hierarchical clustering"* was used since the aim of the process is to create groups of objects with similar signs of fragmentation and abrasion. Hierarchical clustering can be divided in agglomerative (Ward, Complete Linkage, Single Linkage etc.) and divisive algorithms. While agglomerative algorithms start with the number of examined objects, divisive algorithms group objects by division of a totality into groups (Backhaus et al., 2016). The choice of the proximity measure is dependent on the scale of measure of the variables (Finch, 2021; Tzeng et al., 2009). A distinction is made between similarity (Dice, Simple match, Jaccard etc.)

and distance measures (Euclidean distance). The former reflects the similarity between two objects, the second measures the dissimilarity between two objects. Here, data grouping is based on binary variables and the similarity between the objects is sought.

Hierarchical cluster analyses via SPSS (IBM SPSS statistic 26) were conducted with binary variables (0 and 1; absence or presence) for the selected properties for each sample type and for all samples together. A complete linkage algorithm with the simple matching coefficient (M-coefficient) as proximity measure was applied. A single linkage algorithm was used to identify outliners to which the complete linkage algorithm is susceptible. The seven included variables, which are based on visual signs of abrasion and fragmentation of the samples, are listed in Table 15. An overview of the data for all sample objects is shown in Table 41 in the appendix. Resulting dendrograms are analysed for clusters and connections between the investigated parameters (Figure 60).

**Table 15:** Separating variables of the cluster analysis.

| Variables for cluster analysis | Number |
|---|---|
| Sample is visibly affected | 1 |
| Original sample shape is destroyed | 2 |
| Surface haze | 3 |
| Plastic object is perforated or cracked | 4 |
| Mesoplastic particles (5 mm-25 mm) emerged | 5 |
| Large MPP (1 mm-5 mm) emerged | 6 |
| Small MPP (<1 mm) emerged | 7 |

### 5.5.5 Fragmentation model approaches

The particle size distribution (PSD) of plastics in our ecosystem plays a key role in the definition of effective measures for removal of plastics from our environment. The smaller the particles are, the more difficult it is to clean the marine ecosystem from the plastic particles. Modelling the size distributions of MPP may help to understand sources, transport pathways and accumulation sinks in natural water bodies. Such a model could also help to overcome the problem of insufficient comparability of MPP exposure data between different studies applying different sampling procedures and analytical methods.

To date, only few studies on the use of models in this research field are existing. A promising approach for modelling the size distribution of plastic particles in a sample or a compartment has been published by Kooi and Koelmans (2019). They adopted the well-known power law (Bader, 1970; Patterson et al., 1999) to describe particle size distributions in environmental samples.

$$N(d \geq l) = K * l^{-\alpha} \quad (P1)$$

With N as number of particles larger than particle size *l, K* as scaling factor (*K* >0) and alpha (α) as exponential growth factor (α >0). α as the exponent of the power law function has an influence on the slope of the function.

This equation describes the particle size distribution in systems where milling or fragmentation processes induced particle breakdown into smaller pieces. It represents the exponential increase in total number of smaller particles by fragmentation. The more fragmented the original objects are, the more pronounced the sum function is shifted to lower particles.

Equation P1 describes the cumulative number of particles with respect to the minimum size *l.* It can thus be directly used to estimate the total number of particles within a defined size category $G = \{l \in \mathbb{R} | \, l_1 \leq l < l_2\}$

$$N_G = N(d \geq l_1) - N(d \geq l_2) = K * ({l_1}^{-\alpha} - {l_2}^{-\alpha}) \quad (P2)$$

Another formulation of the power law is given by equation P3 where again *l* constitutes the particle size; A is the scaling factor and β the exponential growth factor.

$$\frac{dN}{dl} = A * l^{-\beta} \quad (P3)$$

This equation represents the negative slope of the sum function, because total particle number N decreases with increasing (exclusion) size. Equation P3 is thus equivalent to the derivative of equation P1 with $A = -(\alpha * K)$ and $\beta = \alpha + 1$. Note that since $\alpha$ and $K$ are positive numbers, the new scaling factor $A$ must be negative.

Observations of particle size distributions in the environment can be best fitted with equation P2, when the particle numbers of sufficient size categories G have been counted. Kooi and Koelmans (2019), however, have chosen an approach, where equation P3 is used as an approximation. In this case, the local derivative at the mean of the size class is interpreted in terms of average slope. Important pre-requisites for application of this approximation to environmental data, is that the size class borders are on a logarithmic scale and due to the exponential relationship of slope with size, the size class widths have to be reasonably small. In how far this pre-requisite is fulfilled by existing datasets as used by Kooi and Koelmans (2019) is at least debatable.

Since environmental data are reported for relatively large size class categories often defined by practical restrictions (e.g. sampling equipment), in this thesis all size distribution data are directly fitted to equation P2. Parameter fitting of α and K was performed using an iterative optimisation method minimizing the sum of squared residues (SSR) between observation ($N_{obs}$) and prediction ($N_{pre}$) (equation P4).

$$SSR = \sum (N_{obs} - N_{pre})^2 \quad (P4)$$

For practical reasons, the evaluation of the experiments allowed only particle counts for relatively broad size categories and a minimum size of 350 µm (5 cm / 2.5 cm / 0.5 cm /

0.2 cm / 0.1 mm / 0.035 mm). Only for a few selected experiments, particle numbers for smaller size classes were available from µ-Raman analysis. Here, the SSR of the logarithmic values is minimised since in these cases the particle numbers in the individual size classes differed by orders of magnitude introducing a bias towards the smaller size classes with extremely high numbers in the optimization step.

$$Log(N_G) = Log\left(K * ({l_1}^{-\alpha} - {l_2}^{-\alpha})\right) \quad (P5.1)$$

$$Log(N_G) = Log\ (K) + Log({l_1}^{-\alpha} - {l_2}^{-\alpha}) \quad (P5.2)$$

However, in these experiments, abrasion was most likely the main process, which is not consistent with the power law. Unusual high particle numbers in the small size classes are thus an indicator that besides fragmentation also abrasion had occurred. The model will most likely fail to describe the observed particle size distribution. In this way, the model can be used to distinguish between fragmentation and abrasion processes.

For statistical analysis of the goodness-of-fit, the dimensionless efficiency coefficient (NSE-value) introduced by (Nash & Sutcliffe, 1970) for hydrological models was additionally calculated (Ritter & Muñoz-Carpena, 2013).

$$NSE = 1 - \frac{\sum(N_{pre} - N_{obs})^2}{\sum(N_{obs} - \overline{N_{obs}})^2} \quad (P6)$$

with $N_{obs}$ and $N_{pre}$ as the observed and predicted numbers of MPP and $\overline{N_{obs}}$ as the mean of the observed numbers. The denominator gives the total variance of the observations and the enumerator represents the remaining variance not explained by the model. Full agreement between prediction and observation was achieved at NSE = 1 (no remaining variance). Negative values suggest, “that the mean of the observed values is a better predictor than the evaluated model itself” (Ritter & Muñoz-Carpena, 2013).

# 6 Results and Discussion

## 6.1 Visible analysis

Mechanical stress can lead to different states of destruction depending on the sample type and experimental conditions. In the following chapter, visible signs of destruction are described separately according to the four sample types, considering the experimental conditions.

### 6.1.1 PET bottles

250 mL PET bottles (height: 20 cm) had been selected as representative sample. The wall thickness was measured to be 350 µm. Results of the visual inspection are shown in Table 16 and Table 18 separated in bottle and wave tub experiments.

**Table 16:** Categorisation results of PET bottle samples exposed in bottle experiments.

| Experimental design | Sediment grain size | Matrix | UV Exposure | Destruction Category | Abrasion Category |
|---|---|---|---|---|---|
| Bottle | Coarse sand | Beach | UV irradiated | 3 | 1 |
| | | | Non-UV irradiated | 3 | 1 |
| | | Breakwater | UV irradiated | 3 | 1 |
| | | | Non-UV irradiated | 3 | 1 |
| | Medium sand | Beach | UV irradiated | 3 | 1 |
| | | | Non-UV irradiated | 2 | 1 |
| | | Breakwater | UV irradiated | 3 | 1 |
| | | | Non-UV irradiated | 3 | 1 |

Effects of mechanical stress were much more pronounced in the bottle experiments (BE) than in the aquarium. Moderate abrasion of the sample bodies was observed for all samples (abrasion categories 1). Fragmentation had also occurred recognizable from the perforations (Figure 24). Holes at the bottleneck and the base with uneven edges indicating that material cracking leads to their expansion and the formation of plastic fragments (Figure 24a, Table 17). In addition, some holes were formed, that exhibited smooth edges (Figure 24b) indicating that abrasion leads to material removal resulting in sample perforation. Based on these observations the samples were classified in destruction category 2 or 3, respectively.

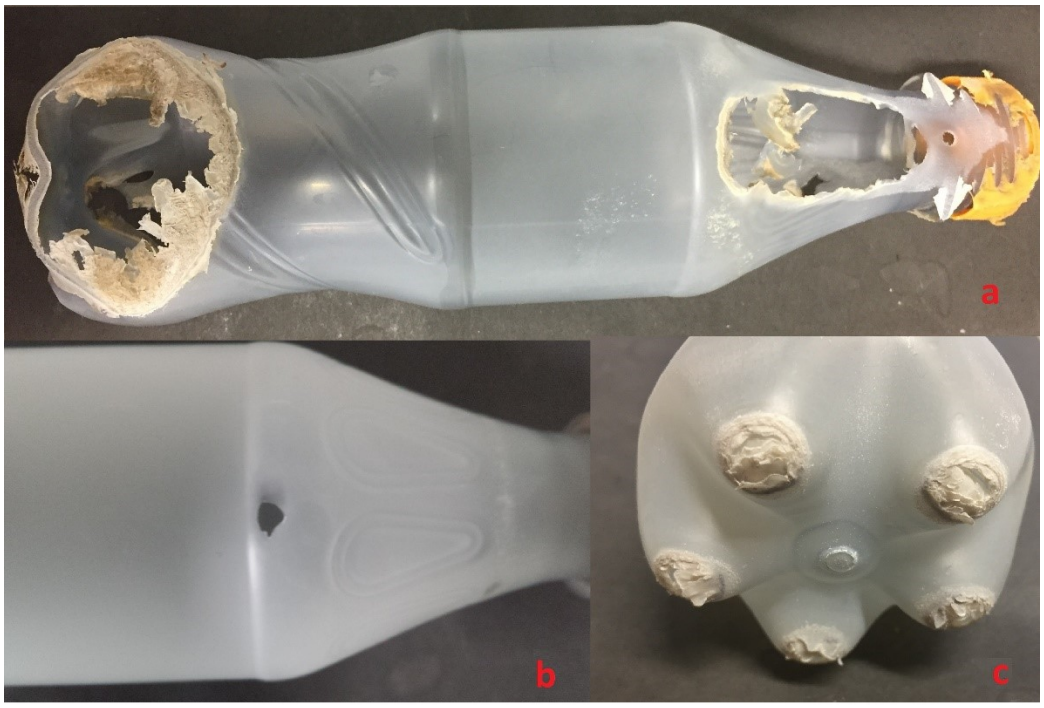


**Figure 24:** Effects of mechanical stress detected by PET bottle samples exposed in BE.

Thickness measurements and SEM images were taken in regions with increased surface haze (Figure 24a) and next to the perforated regions (Figure 24b). Thickness had decreased by up to 50 µm (16%) proving that material removal took place in regions where the surface haze was increased. Next to perforation holes, thickness decrease was even higher (150 µm corresponding to 40%). This large material loss by abrasion weakened the molecular structure making the bottle partly fragile. Most likely, this was the trigger for the subsequent perforation.

**Table 17:** Number of meso- and microplastic PET bottle particles formed in bottle experiments.

| Experimental design | Sediment grain size | Matrix | UV-Exposure | 2.5 cm-5 mm | 5 mm-2 mm | 2 mm-1 mm | 1000 µm-350 µm | Total |
|---|---|---|---|---|---|---|---|---|
| Bottle | Coarse sand | Beach | UV irradiated | 1 | 4 | 6 | 3 | 14 |
| | | | Non-UV irradiated | 0 | 2 | 1 | 0 | 3 |
| | | Breakwater | UV irradiated | 5 | 114 | 22 | 100 | 240 |
| | | | Non-UV irradiated | 9 | 142 | 10 | 200 | 376 |
| | Medium sand | Beach | UV irradiated | 1 | 4 | 3 | 6 | 14 |
| | | | Non-UV irradiated | 0 | 0 | 0 | 0 | 0 |
| | | Breakwater | UV irradiated | 25 | 78 | 31 | 1 | 135 |
| | | | Non-UV irradiated | 4 | 37 | 119 | 58 | 218 |

PET bottles were only little smaller than the 3 L glass bottles leading to many collisions of the PET bottles with the inner walls of the glass bottles during the experiment. This repeatedly occurring mechanical collision stress must be seen as another reason for the

observed fragmentation. Since all PET samples exposed in bottle experiments showed the same degree of destruction, an influence of sample matrix, sediment grain size and UV irradiation could not be identified. However, numbers of MPP formed during exposure may give a deeper insight (Table 17). Generally, it was difficult to detect PET bottle particles visibly because of their transparency. Numbers clearly indicate that exposure under breakwater conditions result in a higher number of fragments than under beach conditions (Figure 25). In the sand/water matrix, the samples seem to be exposed to higher collision forces.

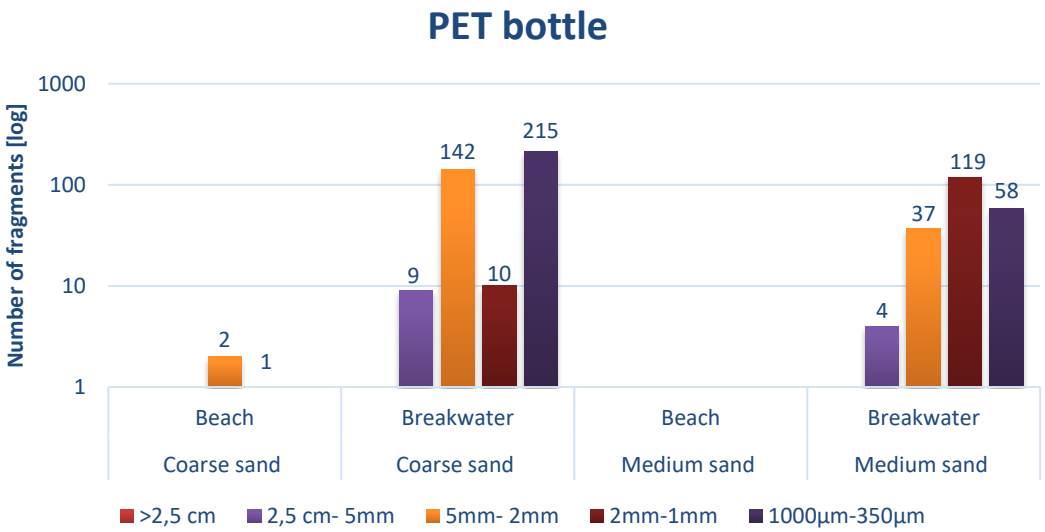


**Figure 25:** Particle size distribution of non-UV irradiated PET bottle samples exposed in BE under different experimental conditions. The y-axis is log-scaled.

In the wave tub experiments (WTE), no fragmentation of the samples was observed at all. They were thus classified in destruction category of 0 or 1, respectively (Table 18).

**Table 18**: Categorisation results of PET bottle samples exposed in WTE.

| Experimental design | Sediment grain size | Matrix | UV-Exposure | Destruction Category | Abrasion Category |
|---|---|---|---|---|---|
| Wave tub | Coarse sand | Beach | UV irradiated | 1 | 1 |
| | | | Non-UV irradiated | 1 | 1 |
| | | Breakwater | UV irradiated | 1 | 1 |
| | | | Non-UV irradiated | 0 | 0 |
| | Medium sand | Beach | UV irradiated | 1 | 2 |
| | | | Non-UV irradiated | 1 | 2 |
| | | Breakwater | UV irradiated | 0 | 0 |
| | | | Non-UV irradiated | 0 | 0 |

Almost all samples exposed to breakwater conditions were not visibly affected (destruction category 0) without visible fragments being formed. Only one UV-irradiated sample exhibited increased surface haze (category 1). Probably, direct contact of the bottle

with the sand layer was reduced by the water leading to less friction stress for the samples.

The surface texture of samples exposed to beach conditions showed signs of moderate abrasion (Figure 26). Two bottles exposed to medium sand (beach setup) were stronger affected with circular traces of abrasion around the bottleneck and the base (Figure 26; red arrows).

**Figure 26:** Effects of mechanical stress detected by PET bottle samples exposed in WTE.

Friction stress during the experiment could have been concentrated here if the bottles were always moved in the same direction over the sand. This highlights that random factors play a role for the extent of abrasion of plastic objects in the environment making general predictions of their fate almost impossible. SEM images of the surface of the virgin bottle and objects from different experiments with different stages of surface impairment confirm the influence of the boundary conditions (Figure 27).

Original PET bottles had a smooth surface making the recording of a SEM image difficult since the camera needed a focus point. Only some small grooves could be observed (Figure 27a, magnification x170).

Figure 27b shows a sample with increased surface haze from BE. The surface texture exhibited linear flat grooves with flaked edges, and deeper and longer fractures. The whole sample was also covered with small curvy grooves. In addition to wide grooves, small and flat impact sites, so-called pits (Cooper, 2012), probably caused by sediment particles heavily hitting the plastic surface were also observed. Pits might be caused by ploughing, as surface asperities can result from squeezed layers of material due to the hitting forces of sediment particles. In comparison, the surface of the sample cut out next to a perforated area was completely covered with curved grooves of varying depths (Figure 27c). The surface was fissured with long, deep fractures. These observations of surface texture damage along with a reduction in thickness support the assumption that perforation is induced by abrasion will generate small microplastic particles.

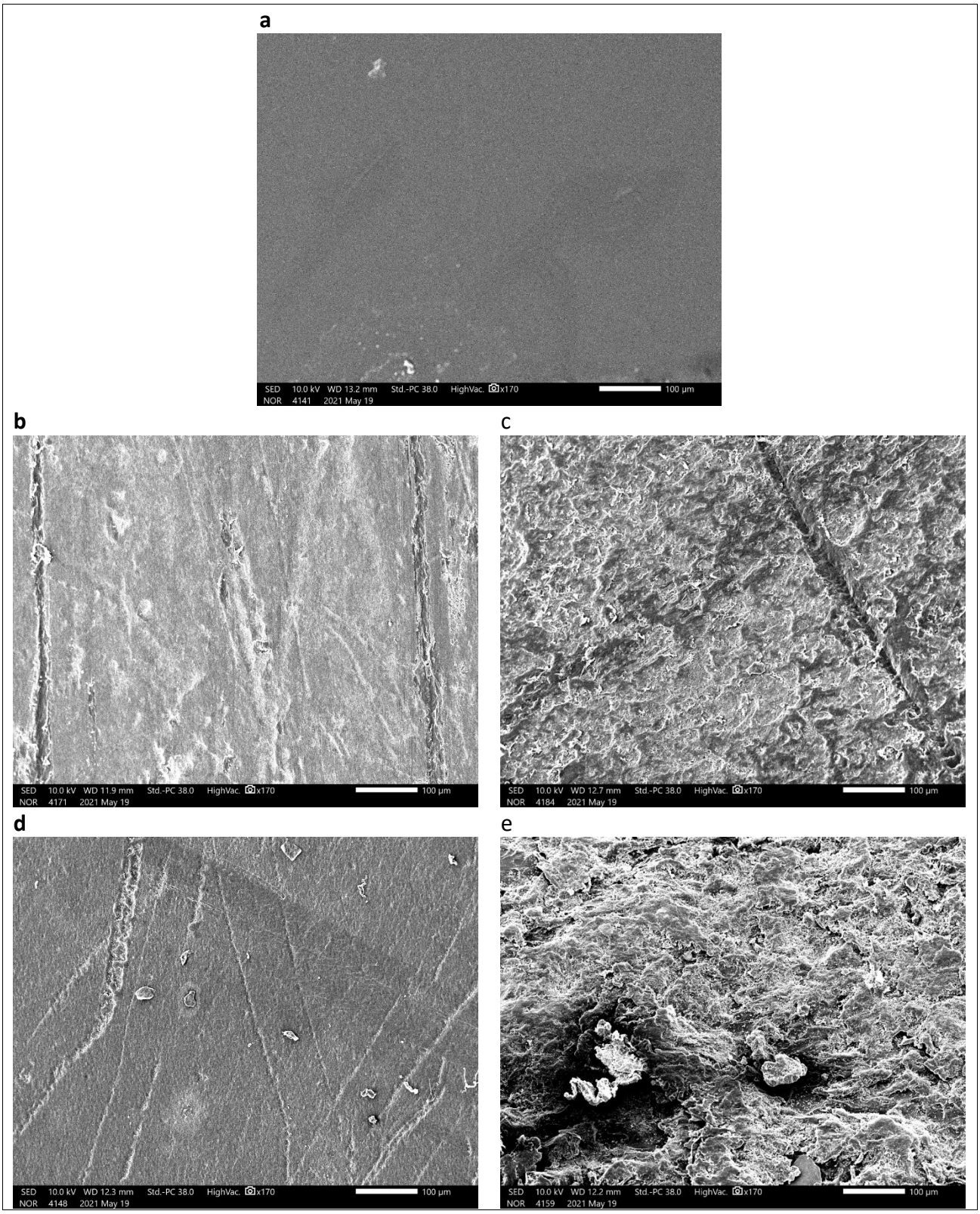


**Figure 27:** SEM images of PET bottle samples (magnification x170). The original PET surface (a) in comparison to samples exposed in BE with abrasion category 1 (b and c) and from WTE with abrasion category 1 (d) and category 2 (e).

Samples from WTE exposed under beach conditions exhibited long linear fractures in different directions (Figure 27d). Wide grooves of about 25 µm indicate dragging of sediment particles along the plastic surface. The picture also confirms that adherence of

(sand) particles to the surface occurs. SEM images of the circular abrasion area (see Fig. 26) supports the visible categorization into abrasion category 2. Surface texture was much more spoilt showing curved grooves of different depth (Figure 27e). The surface texture of the sample was fissured proving a more effective abrasion.

In conclusion, PET bottles showed signs of abrasion under all experimental conditions, while fragmentation occurred only in the bottle experiments. The 30 days exposure time, however, was not long enough to lead to a complete breakup of the bottles.

### 6.1.2 HDPE caps

PET drinking bottles are often equipped with PE caps consisting of high-density polyethylene (HDPE). If such drinking bottles enter the environment by littering, the caps are often still screwed on the bottle. Thus, PE caps (height:1 cm; diameter: 3 cm) were exposed in the experiment together with the PET bottles. There, the bottles oriented themselves horizontally in the shaking vessels reducing the contact time with the sediment and thus the friction stress of the caps.

HDPE caps were visibly affected in almost all experiments mainly due to abrasion in form of scratches on the surface. (Figure 28, Figure 29). Table 19 (BE) and Table 20 (WTE) summarize the observations of the 16 experiments.

**Table 19:** Categorisation results and total number of meso- and microplastic of HDPE cap samples exposed in BE.

| Experimental design | Sediment grain size | Matrix | UV-Exposure | Destruction category | Abrasion category | Total number of particles |
|---|---|---|---|---|---|---|
| Bottle | Coarse sand | Beach | UV irradiated | 1 | 1 | 0 |
| | | | Non-UV irradiated | 1 | 1 | 2 |
| | | Breakwater | UV irradiated | 4 | 2 | 526 |
| | | | Non-UV irradiated | 4 | 2 | 322 |
| | Medium sand | Beach | UV irradiated | 1 | 1 | 0 |
| | | | Non-UV irradiated | 1 | 1 | 0 |
| | | Breakwater | UV irradiated | 4 | 2 | 213 |
| | | | Non-UV irradiated | 4 | 2 | 286 |

In the bottle experiment, fragmentation and material shrinkage occurred under breakwater conditions resulting in an emergence of meso- and MPP (destruction category 4; Figure 28), whereas in the beach setup only surface abrasion was observed (destruction category 1). Samples exposed under breakwater conditions also exhibited a higher abrasion (abrasion category 2) in comparison to samples exposed under beach conditions (abrasion category 1). This indicates that breakwater conditions support abrasion processes.

**Figure 28:** Effects of mechanical stress detected by PE cap samples exposed in BE.

In WTE, the samples were visibly less affected and fragmentation did not occur (Table 20).

**Table 20:** Categorisation results of HDPE cap samples exposed in WTE.

| Experimental design | Sediment grain size | Matrix | UV-Exposure | Destruction category | Abrasion category |
|---|---|---|---|---|---|
| Wave tub | Coarse sand | Beach | UV irradiated | 1 | 1 |
| | | | Non-UV irradiated | 1 | 1 |
| | | Breakwater | UV irradiated | 0 | 0 |
| | | | Non-UV irradiated | 0 | 0 |
| | Medium sand | Beach | UV irradiated | 1 | 1 |
| | | | Non-UV irradiated | 1 | 1 |
| | | Breakwater | UV irradiated | 0 | 0 |
| | | | Non-UV irradiated | 0 | 0 |

Samples exposed under breakwater conditions were not affected (destruction category 0, Figure 29a). This indicates that the samples did not have contact with sediment particles due to their position on the bottle neck, so abrasion did not occur. Meso- and MPP were not observed (Table 35, appendix). Under beach conditions, all samples exhibited surface scratches (destruction category 1; Figure 29b) independent from the experimental design. The size of the matrix particles and the previous UV irradiation did not seem to have any influence.

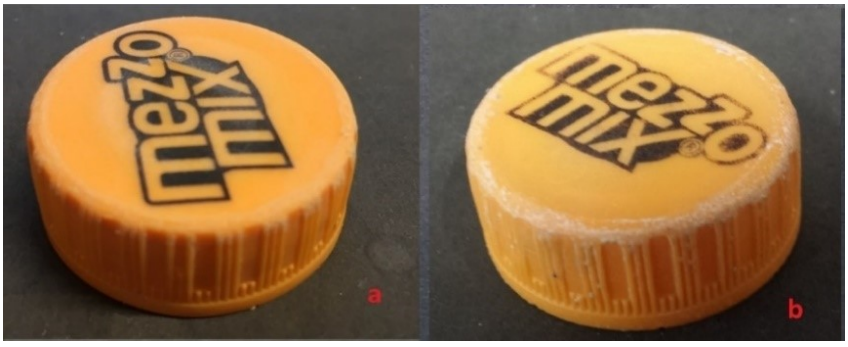

**Figure 29:** Effects of mechanical stress detected by PE cap samples exposed in WTE.

Comparisons in surface texture between cut out sample parts with abrasion category 1 and 2 classifications were made using SEM images. Surface structure of original HDPE samples exhibited a characteristic pattern. Figure 30a (magnification x270) shows the wavy structure in irregular smooth partitions extending over the entire sample area. Samples classified in abrasion category 1 showed the same wavy patterns on the surface, but elevation edges lost their smoothness and were sharper (Figure 30b). In addition, deep elongated troughs and deep scratches or linear fractures appeared making the texture pattern more irregular. Destruction of the surface was even more pronounced for samples with an abrasion category 2 classification (Figure 30c). The original wavy surface texture was no longer recognizable. No linear fractures appear, but curvy grooves of different depth emerged. Furthermore, the surface seems to be brittle. This indicates that the upper surface layer was almost completely removed by experimental procedure.

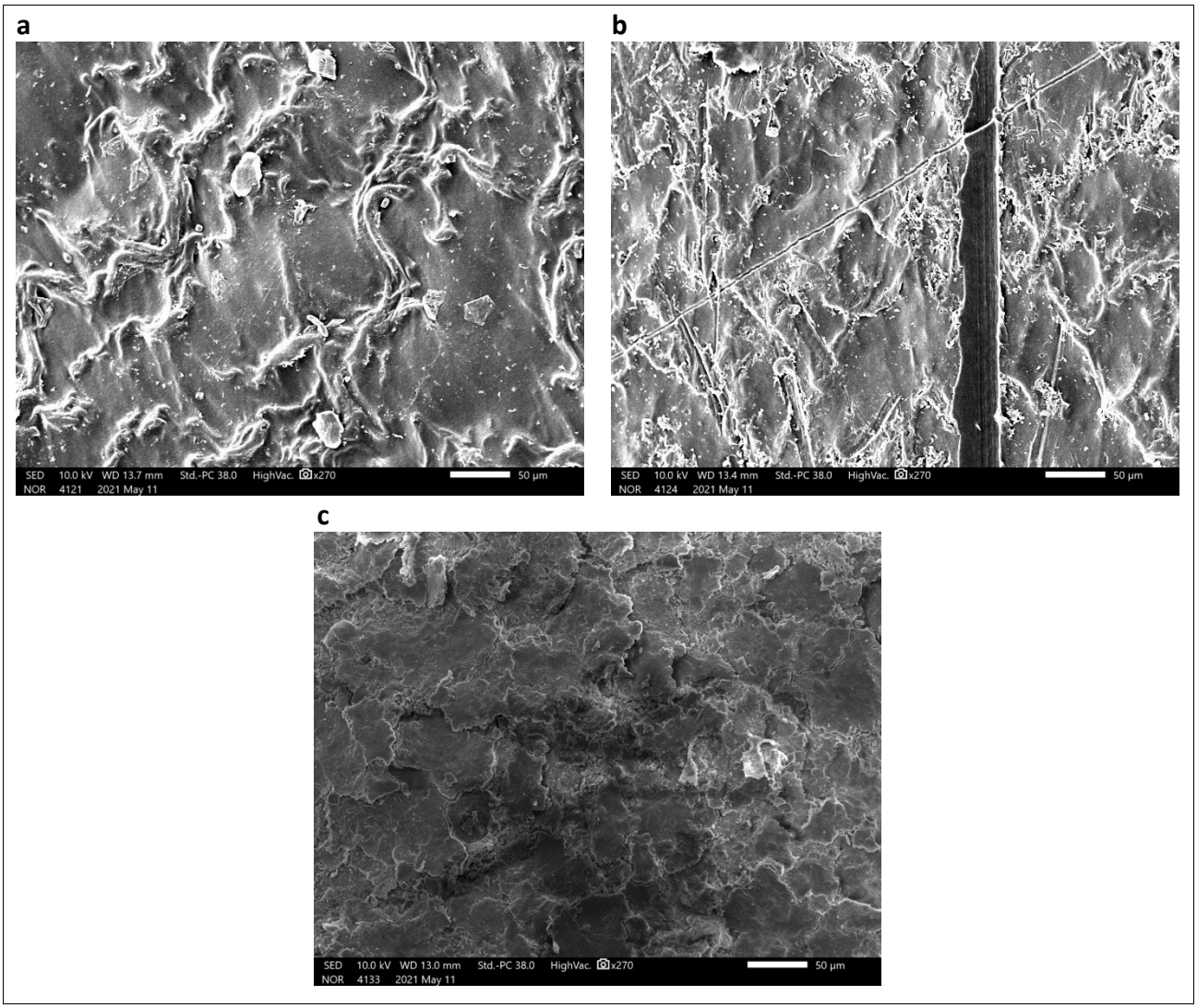


**Figure 30:** SEM images of HDPE samples (magnification x270). The original HDPE surface (a) in comparison to samples with abrasion category 1 (b) and category 2 (c) classifications.

Due to their compact shape and material thickness, the caps are more resistant against mechanical stress so fragmentation played a minor role. However, during the 30 day-

exposure, the material was obviously sufficiently weakened, e.g. by abrasion, so that it can break under certain conditions with strong collision energy.

**Box 1**
**Does the position of the HDPE cap during the experiments affect fragmentation processes?**

It is assumed that HDPE caps collide more often with the inner walls of the glass bottle when fixed on the PET bottle compared to motile single caps.

To check this assumption, BE under breakwater conditions were repeated with single PE caps not screwed onto the bottles. Observed destruction was much less than for caps screwed onto the PET bottles (Figure 31). Moving freely protected the samples from hard collisions with the glass wall so that only abrasion was observed (scratched surface). This experiment highlights, that mechanical collisions with hard materials increase the destruction level of plastic debris significantly.

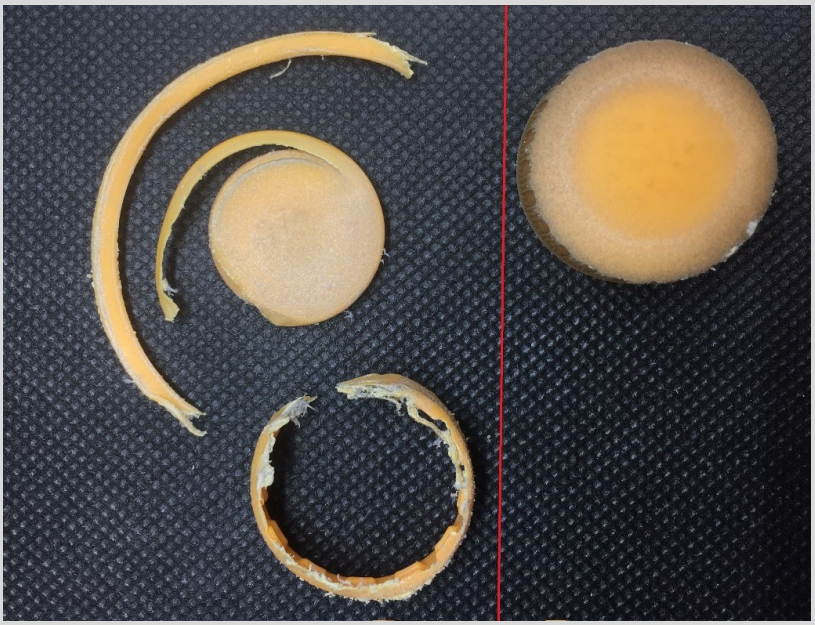

**Figure 31:** PE cap samples after exposing to similar breakwater -BE. Sample was screwed onto PET bottles during experiment (left side) or motile in the 3L glass bottle (right side).

### 6.1.3 PS cups

Commercial PS yoghurt cups (h: 4.5 cm; d: 3 cm) with a polymer wall thickness of 0.18 mm were selected as samples. Depending on the experimental design, PS cups showed signs of abrasion and fragmentation from destruction category 0 to 5 (Table 21 and Table 23).

**Table 21:** Categorisation results of PS cup samples exposed in BE.

| Experimental design | Sediment grain size | Matrix | UV-Exposure | Destruction Category | Abrasion Category |
|---|---|---|---|---|---|
| Bottle | Coarse sand | Beach | UV irradiated | 4 | 2 |
| | | | Non-UV irradiated | 3 | 2 |
| | | Breakwater | UV irradiated | 5 | 2 |
| | | | Non-UV irradiated | 5 | 2 |
| | Medium sand | Beach | UV irradiated | 4 | 2 |
| | | | Non-UV irradiated | 3 | 2 |
| | | Breakwater | UV irradiated | 3 | 2 |
| | | | Non-UV irradiated | 3 | 2 |

In the bottle experiments, samples were generally more destructed exhibiting perforations and longitudinal cracks. Half of the samples fragmented into macroplastics (Figure 32c) and/or formed a large number of long shaped meso- and microplastics (Figure 32d). It is assumed that the form of the fragments was caused by the longitudinal cracks, which can extend over the whole sample body before splitting (Figure 32c). All BE samples showed strong abrasion (class 2), which weakened the structure of the plastic object and eventually led to fragmentation. This was corroborated by the observation that holes in the cups were surrounded by white edges, where the coloured layer was already abraded (Figure 32a and b). The perforation of the samples occurred due to the smaller thickness of the walls, which was proven by a thickness measurement (Figure 32a) that showed that the thickness was reduced by about 100 µm (56%). Since thickness measurements were performed next to the perforated regions (red square) a thickness decreases of around 55% down to less than 0.1 mm is necessary before perforation of the cup starts.


**Figure 32:** Effects of mechanical stress detected by PS cup samples exposed in BE.

Under beach conditions, UV irradiated PS cups fragmented into many large micro- and mesoplastics, whereas non-UV irradiated samples exhibited perforation but kept their cup shape. This supports the assumption that UV irradiation weakens the sample structure and facilitates fragmentation; PS cups seemed to be more affected than PET bottles or HDPE bags. Under breakwater conditions, no effect of UV irradiation was observed. It was also notable that in the breakwater experiment non-UV irradiated samples formed more particles than UV irradiated samples (Table 22), which hints an overlying effect of collision frequency and strength.

**Table 22:** Number of meso- and microplastic PS cup particles formed in bottle experiments.

| Experimental design | Sediment grain size | Matrix | UV-Exposure | >2.5cm | 2.5cm-5mm | 5mm-2mm | 2mm-1mm | 1000µm-350µm | Total |
|---|---|---|---|---|---|---|---|---|---|
| Bottle | Coarse sand | Beach | UV irradiated | 10 | 148 | 70 | 142 | 136 | 506 |
| | | | Non-UV irradiated | 0 | 7 | 36 | 29 | 10 | 82 |
| | | Breakwater | UV irradiated | 0 | 10 | 10 | 206 | 1900 | 2126 |
| | | | Non-UV irradiated | 0 | 47 | 26 | 700 | 5900 | 6673 |
| | Medium sand | Beach | UV irradiated | 8 | 180 | 204 | 245 | 300 | 937 |
| | | | Non-UV irradiated | 0 | 6 | 40 | 68 | 96 | 210 |
| | | Breakwater | UV irradiated | 0 | 2 | 29 | 14 | 1 | 46 |
| | | | Non-UV irradiated | 0 | 0 | 48 | 109 | 42 | 199 |

Under breakwater conditions, both samples in experiments with coarse sand fragmented into small MPP (destruction category 5), whereas in experiments with medium sand samples were only cracked and perforated (destruction category 3). This indicates that larger sand particles may support MP destruction under breakwater conditions.

PS cups exposed in WTE showed no signs of destruction or fragmentation (Table 23).

**Table 23:** Categorisation results of PS cup samples exposed in WTE.

| Experimental design | Sediment grain size | Matrix | UV-Exposure | Destruction Category | Abrasion Category |
|---|---|---|---|---|---|
| Wave tub | Coarse sand | Beach | UV irradiated | 0 | 0 |
| | | | Non-UV irradiated | 0 | 0 |
| | | Breakwater | UV irradiated | 2 | 1 |
| | | | Non-UV irradiated | 0 | 0 |
| | Medium sand | Beach | UV irradiated | 3 | 1 |
| | | | Non-UV irradiated | 0 | 0 |
| | | Breakwater | UV irradiated | 0 | 0 |
| | | | Non-UV irradiated | 0 | 0 |

Only 2 of 8 samples exhibited signs abrasion and fragmentation in form of cracks with the glossy coating being faded and only a low number of emerged MPP (<15 particles in total). Both affected samples were UV irradiated before experiments, indicating a weakening effect of UV irradiation. However, since they do not have any other experimental parameter in common, one was exposed under breakwater conditions in coarse sand and the other under beach conditions in medium sand, an explanation for their destruction is almost impossible to find. The thickness of one sample was measured (Figure 33 b, red square). It decreased about 20 µm (11%). Since the colour of this sample was still visible, it is assumed that the shiny layer which coated the PS cups was at least 20 µm thick. The other samples were not affected by the experiments (Figure 33a).


**Figure 33:** Effects of mechanical stress detected by PS cup samples exposed in WTE.

The surface of the original PS cup sample was very smooth which made the recording of a SEM image challenging, since the camera needed a focus point. Nevertheless, fine scratches were observable caused by transport and storing processes during lifetime. Also, a few small particles (<50 µm) and some fibres adhere to the surface probably due to air pollution (Figure 34a, magnification x170).

As described earlier, abrasion of the samples led to thickness reduction, followed by perforation and finally fragmentation due to cracking. Sample surfaces from samples where only the glossy coating was reduced, exhibited lots of cracks, scratches and grooves, probably caused by dragging sand particles over the plastic surface (Figure 34b). The damages of the surface proved a change in gloss since the reflection of the light of smooth surfaces is focused and thus more radiant. A grid of flat linear and crescent fractures covered the whole sample. Cooper (2012) described these kinds of textures as an “early indication of stresses occurring on particles which have been embrittled through photooxidative processes”. Since this sample was exposed to UV irradiation before experiments this kind of surface damage is conceivable.

The surface texture of samples where the colour was already abraded, showed less deep relatively wide grooves and scratches (Figure 34c). Additionally, it was covered with

small curvy grooves (<5 µm) of different depth making it uneven. Furthermore, dark shadowed areas were visible, where the surface edges of the elevations were smoother but of the same depth (Figure 34d, magnification x4500). This could be an effect of ploughing rather than abrasion with the dark area resulting from material squeezed by sediment grains. Although the sample was also UV irradiated no grid of fractures was observed explainable by the loss of the outer sample layer due to friction.

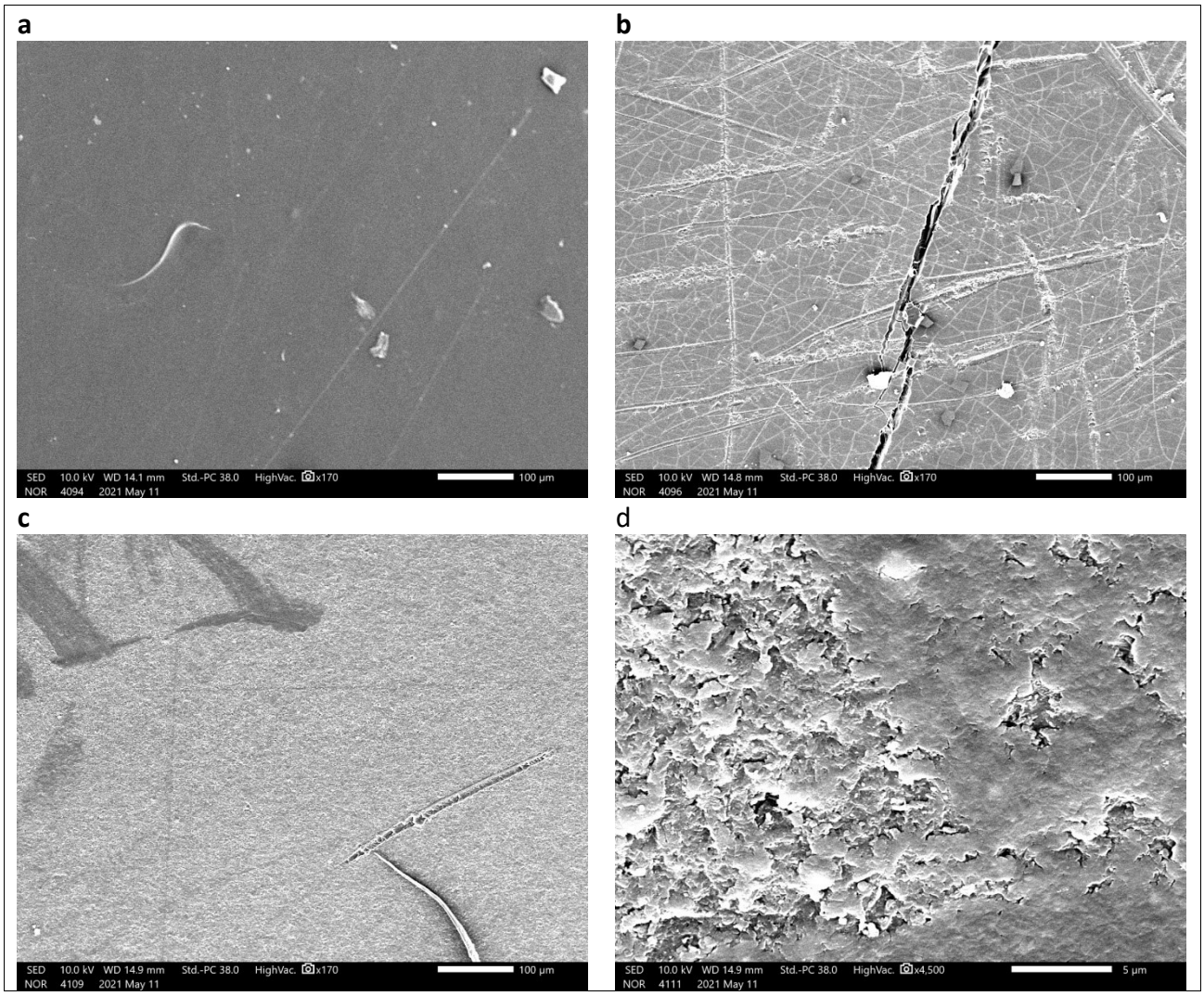


**Figure 34:** SEM images of PS cup samples (magnification x170) a) original sample, b) samples with reduced glossy coating and c) samples with abraded colour. d) shows the dark shadowed area with a magnification of x4500.

The PS cup is due to its hollow form and thin walls susceptible to abrasion leading to loss of thickness and subsequent fragmentation. Especially collisions with hard materials supports the fragmentation process.

Based on the observations, a fragmentation process for PS cups was developed (Figure 35). Depending on the test conditions, fragmentation starts after initial weakening by abrasion and/or other processes (UV). The cups initially break into large pieces (macroplastic) starting at the bottom of the cup, which forms a weak point due to the cup production process. Cups were form by injection moulding which means that the melted PS

foil is injected directly into a custom mould. As a consequence, the kink between the ground and the body is structurally weak. As a result, larger fragments were formed along the lateral cup surface often showing additional longitudinal cracks. These fragments break down into smaller long-shaped particles. Smaller fragments break off from the fragment edges and finally microplastics will emerge.

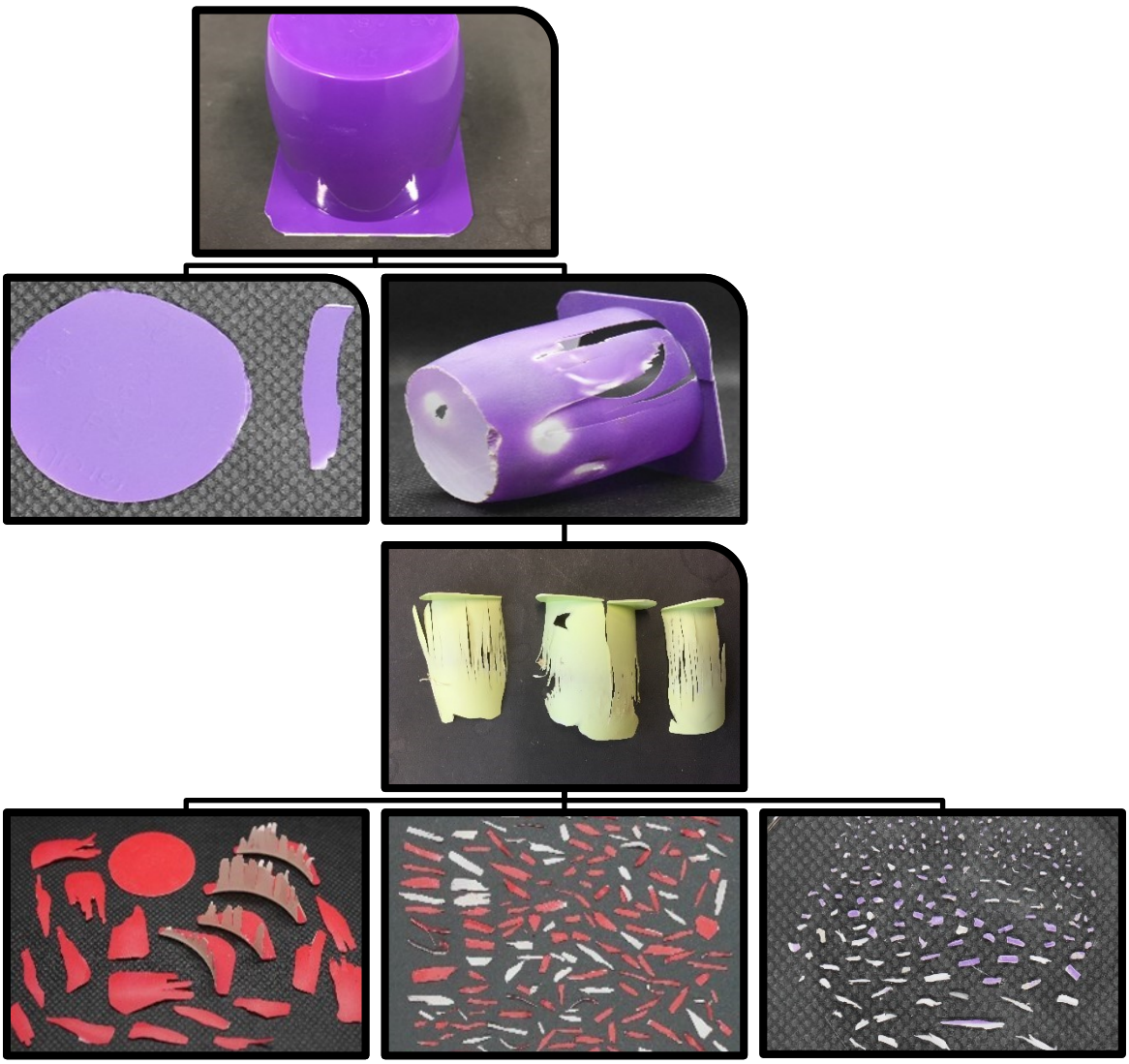

**Figure 35:** Theoretical fragmentation of a PS yoghurt cup.

### 6.1.4 LDPE bags

Transparent LDPE carrier bags (21 cm x 47 cm, 0.01 mm thick) from the supermarket were selected as samples.

LDPE bags exhibited higher destructions in form of perforation up to completely fragmentation into meso- and microplastics in comparison to the other sample types. It is assumed that the low thickness and the flexibility of the bags played an important role here.

Observations show that LDPE bag samples exhibited two damage patterns:

1. Samples did not fragment, the original shape was kept, abrasion and perforation occurred

2. Samples fragmented
   a) in macroplastic particles, countable
   b) in meso- and microplastics, particles build inseparable entanglements (Figure 36a and b)
   c) in microplastics, particles were to small and numerous to count (Figure 36c and d)

Since counting of fragments was almost impossible for the PE samples from damage pattern 2b and c, the fraction of PE in the sample cake after extraction was estimated via thermogravimetric analysis.


**Figure 36:** Fragmentation pattern of LDPE bag samples. In a and b (magnification of x25) sample cakes from LDPE bags with damage pattern 2b are shown. C and d (magnification of x25) show sample cakes from samples with damage pattern 2c.

Table 24 shows the categorisation of LDPE bag samples in destruction and abrasion categories exposed in BE. In addition, the damage patterns were listed.

UV irradiated samples fragmented completely into microplastics. UV irradiation seems to severely weaken the structure of the LDPE bags and make them brittle. Collisions subsequently lead to fragmentation of the samples. Emerged microplastics were too

numerous to count (damage pattern 2c). The colour of the particles changed from transparent to greyish/brownish depending on experimental conditions (Figure 36).

**Table 24:** Categorisation results of LDPE bag samples exposed in BE.

| Experimental design | Sediment grain size | Matrix | UV-Exposure | Destruction Category | Abrasion Category | Damage pattern |
|---|---|---|---|---|---|---|
| Bottle | Coarse sand | Beach | UV irradiated | 5 | 2 | 2c |
| | | | Non-UV irradiated | 3 | 2 | 1 |
| | | Breakwater | UV irradiated | 5 | 2 | 2c |
| | | | Non-UV irradiated | 4 | 2 | 2b |
| | Medium sand | Beach | UV irradiated | 5 | 2 | 2c |
| | | | Non-UV irradiated | 3 | 2 | 1 |
| | | Breakwater | UV irradiated | 5 | 2 | 2c |
| | | | Non-UV irradiated | 4 | 2 | 2b |

Non-irradiated samples, when exposed under beach conditions, were crumpled with wrinkled surfaces (Figure 37b and c). Crack formation and tearing was observed (Figure 37a and c) leading to smooth edged tears, tattering (Figure 37a and d) and the formation of long shaped macro- and mesoplastic fragments (in destruction category 3; damage pattern 1). Whereas non-irradiated PE bags exposed under breakwater conditions fragmented with a dominating number of long shaped mesoplastic particles leading to plastic entanglements in which sand as well as other material particles got caught (Figure 36a; damage pattern 2b).

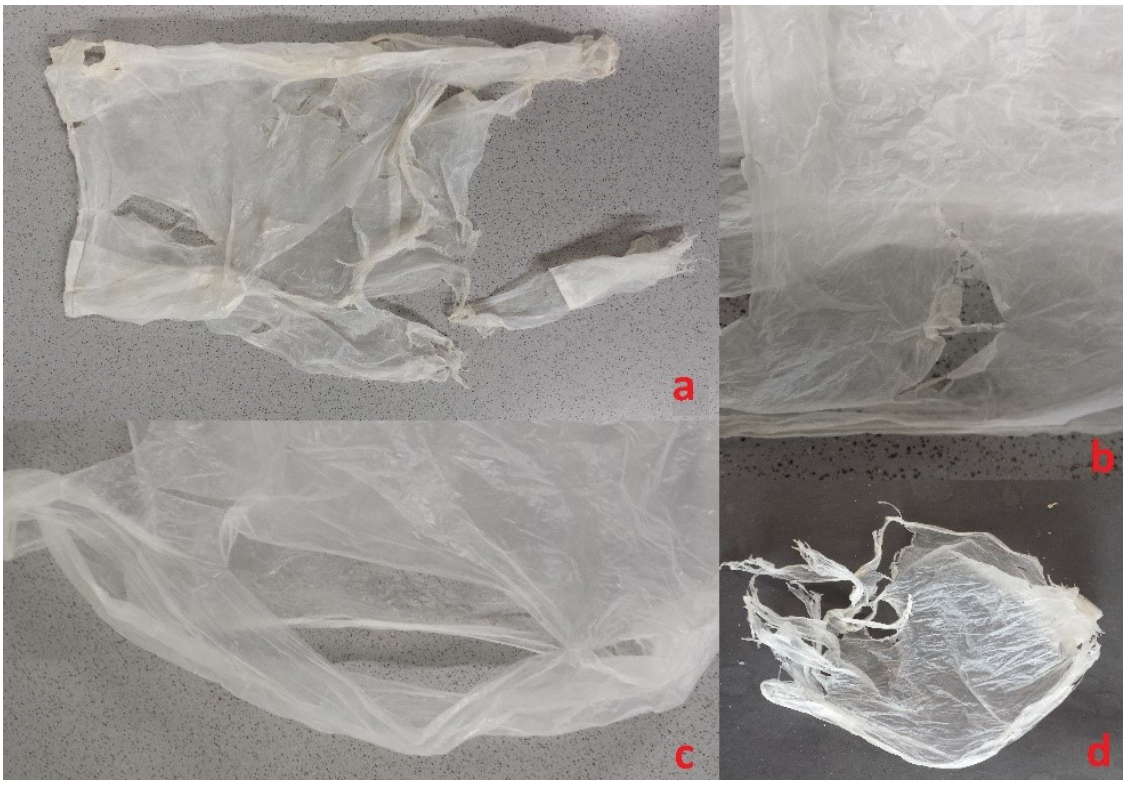


**Figure 37:** Effects of mechanical stress detected by unbroken LDPE carrier bag samples.

In WTE, the bag samples exhibited also relative high signs of fragmentation shown in Table 25.

**Table 25:** Categorisation results of LDPE bag samples exposed in WTE.

| Experimental design | Sediment grain size | Matrix | UV-Exposure | Destruction Category | Abrasion Category | Damage pattern |
|---|---|---|---|---|---|---|
| Wave tub | Coarse sand | Beach | UV irradiated | 3 | 1 | 1 |
| | | | Non-UV irradiated | 3 | 1 | 1 |
| | | Breakwater | UV irradiated | 4 | 2 | 2a |
| | | | Non-UV irradiated | 2 | 2 | 1 |
| | Medium sand | Beach | UV irradiated | 3 | 2 | 1 |
| | | | Non-UV irradiated | 2 | 2 | 1 |
| | | Breakwater | UV irradiated | 4 | 2 | 2a |
| | | | Non-UV irradiated | 2 | 2 | 1 |

The samples were less damaged overall compared to samples exposed in BE, but the same trends can be seen regarding to UV irradiation and matrix conditions. Under breakwater conditions, UV irradiated samples fragmented into large rectangular formed macroplastics (damage pattern 2a; Figure 37d) whereas non-irradiated samples exhibited tears and perforation (destruction category 2; damage pattern 1). Under beach conditions, samples were only torn and perforated, but fragmentation did not occur (damage pattern 1).

Visual determined surface abrasion of the samples exposed in BE and WTE was in the same range. It led to a loss of shine and increased surface haze resulting in a classification of all samples in abrasion category 2 (Figure 38b and d). The samples were opaque and the surface haze was further enhanced by small sharp wrinkles. Only two samples showed less signs of abrasion than all other samples (Figure 38a and c). They were exposed in WTE under beach conditions with coarse sand. The surface was less opaque in comparison to corresponding samples leading to an abrasion category 1 classification.


**Figure 38:** Comparison between LDPE bag sample with abrasion category 1 (a and b) and with abrasion category 2 classifications (b and c). C and d are magnified with x25.

Thermogravimetric analysis of the different filter cakes from LDPE bag fragmentation experiments should allow a rough estimation of the amount of LDPE fragments or MPP in the entanglements and in the non-separable mixtures of LDPE bag MPP and sand particles. Since the organic fraction in the cakes consists almost exclusively of LDPE fragments or MPP, the weight difference before and after incineration of a subsample can be equalled to its LDPE amount. Four sample cakes of the 16 experiments were too low in weight to apply the method; all contained samples were not broken (damage pattern 1).

First, blank samples of original sand were analysed confirming a low organic fraction of less than 0.4 %. Results of the thermogravimetric analysis of the other 12 experiments are shown in Table 26.

**Table 26:** Results of the thermogravimetric analysis.

| Experimental design | Sediment grain size | Matrix | UV-Exposure | Ignition Loss [%] | Incinerated filter cake amount [mg] | Proportion of the original LDPE bag in the filter cake [%] | Damage pattern |
|---|---|---|---|---|---|---|---|
| Bottle | Coarse sand | Beach | UV irradiated | 56 | 481 | 23 | 2c |
| | | | Non-UV irradiated | 40 | 120 | 6 | 1 |
| | | Breakwater | UV irradiated | 61 | 768 | 50 | 2c |
| | | | Non-UV irradiated | 77 | 3285 | 158 | 2b |
| | Medium sand | Beach | UV irradiated | 58 | 1419 | 69 | 2c |
| | | | Non-UV irradiated | 27 | 23 | 1 | 1 |
| | | Breakwater | UV irradiated | 76 | 452 | 30 | 2c |
| | | | Non-UV irradiated | 76 | 2233 | 108 | 2b |
| Wave tub | Coarse sand | Beach | UV irradiated | 33 | 20 | 1 | 1 |
| | | | Non-UV irradiated | - | - | - | 1 |
| | | Breakwater | UV irradiated | 64 | 183 | 12 | 2a |
| | | | Non-UV irradiated | - | - | - | 1 |
| | Medium sand | Beach | UV irradiated | 6 | 19 | 1 | 1 |
| | | | Non-UV irradiated | - | - | - | 1 |
| | | Breakwater | UV irradiated | 9 | 25 | 1 | 2a |
| | | | Non-UV irradiated | - | - | - | 1 |

Bags can be divided into four cases which corresponds with the previous determined damage pattern of the LDPE bag samples. In addition, results show that the separation from small sand particles was not possible since the amount of residue [%] proves the presence of sand particles in the filter cake.

1) Samples with damage pattern 1:

The proportion of the LDPE bag sample on the filter cake was <6% which is plausible since the sample showed no bigger fragmentation signs.

2) Samples with damage pattern 2a:

Macroplastics were emerged, the proportion of LDPE on the filter cake was <12% indicating that also a small proportion on plastic was generated in the experiments.

3) Samples with damage pattern 2b:

The content of plastic was over 100% of the original LDPE bag weight. Bags fragmented into elongated meso- and microplastics that had become entangled. The

height proportion of incinerated plastic indicates that other plastic material (PS cup, PET bottle and HDPE cap fragments) also got caught in the entanglements (see Figure 36a and b).

4) Samples with damage pattern 2c

Since the samples fragmented completely into small plastic particles during the experiments (Figure 39), it was assumed that the proportion of plastic on the sample cake was 100% of the original bag sample weight. Though, the proportion of the original weight was between 23-69%. This implies that about 1000 mg of these samples was lost during the extraction and treatment process. On the one hand, plastic particles might be drawn down by heavier sand particles during the extraction process ending up in the collecting vessel. On the other hand, small particles (<63 µm) might be washed out during the wet pre-sieving process before extraction. Further investigations of these two processing steps are needed.

Generally, results show that LDPE bag samples were extremely vulnerable to mechanical stress especially when exposed to UV irradiation. Due to their low thickness, they crack easily starting a fragmentation process. UV irradiation weakens the structure and makes them extremely brittle leading to a high number of small MPP. Abrasion occurred but seems not to play a major role for the fragmentation process since the plastics were weak anyway.

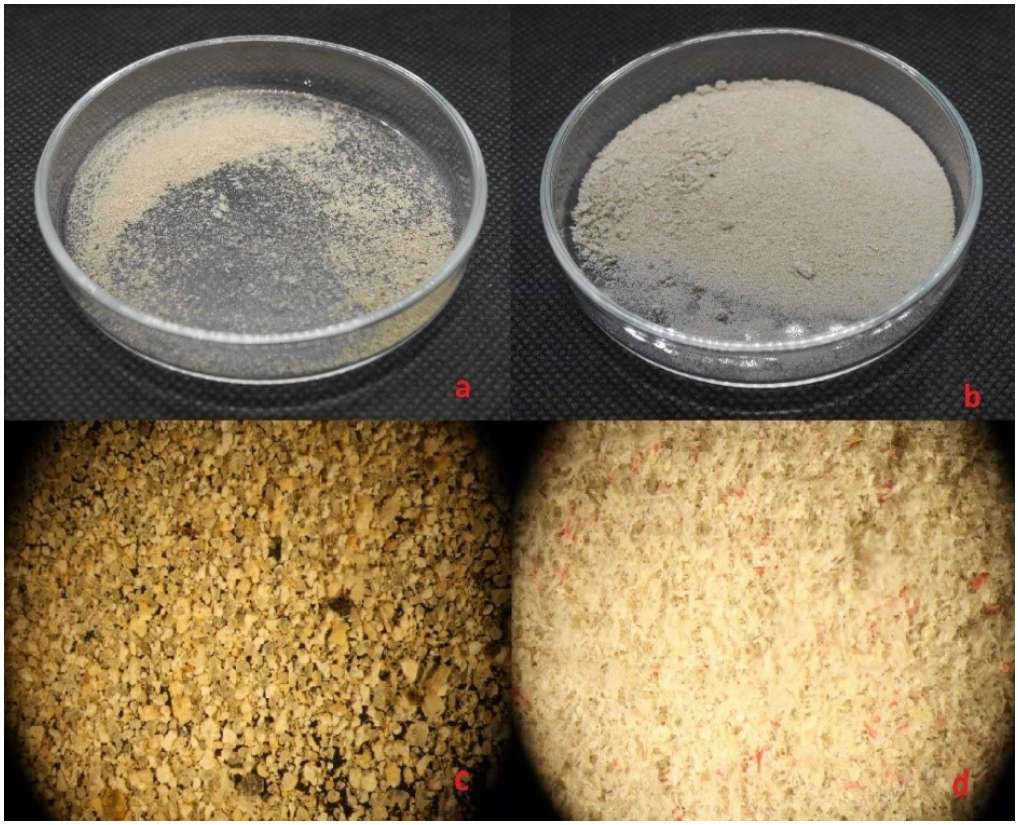


**Figure 39:** PE-sediment mixtures with ignition loss of under 10 % (a and c) and over 60% (b and d) before incineration. C and d are magnified in with x16.

PE bag particles are a serious problem for the environment. Sizes in micrometre ranges are not as plastic identifiable by eye anymore (Figure 39). This leads especially in the environment to problems since a distinction for animals between plastic and natural debris is not possible anymore. Also, the cleaning of beaches from not optically detectable fragments proofing difficult.

## 6.2 µ-Raman analysis

Due to the large effort and the restricted lab capacities caused by the Corona pandemic, only four selected samples could be examined by µ-Raman (Table 27). Samples were chosen for their level of destruction. A distinction was made between different levels: abrasion and fragmentation, only abrasion, no visible impairment of the surface.

**Table 27:** Selected samples for µ-Raman analysis.

| µ-Raman sample number | Experimental design | Sediment grain size | Matrix | UV-Exposure | Level of destruction | Extrapolation Factor |
|---|---|---|---|---|---|---|
| **1** | BE | Coarse Sand | Beach | UV | Abrasion and Fragmentation | 450 |
| **2** | BE | Coarse Sand | Breakwater | UV | Abrasion and Fragmentation | 160 |
| **3** | BE | Medium Sand | Beach | Non-UV | Only Abrasion, PS sample fragmented | 26 |
| **4** | WTE | Medium Sand | Breakwater | UV | no visible impairment of the surface | 112 |

In general, detection of MPP was hampered by the amount of inorganic particles in the sample cake. Sample clean-up was not sufficiently effective, so that large numbers of not clearly identifiable spectra (fingerprint peaks in the noise) were detected.

Particles of four polymer types were clearly identified (PE, PS, PET and PP), of which PP had not been used in the experiments. However, the cap of the glass bottles used for the bottle experiments was made of PP. It is well imaginable that during the experiment MPP were formed from the bottle cap through abrasion. Counted MPP from PP were not evaluated further, but this gives an additional hint that abrasion had occurred. Unfortunately, the µ-Raman detection method cannot distinguish between LDPE and HDPE so that the amount of PE particles cannot unequivocally be assigned to abrasion from the small bottle caps (HDPE) or the bag (LDPE).

Since samples had been pre-sieved through a 63 µm sieve prior to extraction and analysis (see chapter 5.3.3.3), detection of smaller particles was not expected. However, some MPP <63 µm were detected indicating that the wet sieving step does not fully remove them from the sample. Most likely some MPPs are associated with bigger matrix particles, e.g., by adhesive forces. Although these particle numbers do not fully represent the

MPP fraction below 63 µm, their existence corroborates that abrasion had occurred during the experiments.

Results of the Raman analysis of selected samples are presented in Table 28 together with the visual sample assessments.

**Table 28:** Overview of the µ-Raman analysis results.

| µ-Raman Sample number | Material | Destruction Category | Abrasion Category | Fragmentation | Abrasion | particles>350 µm | Extrapolated particles< 350µm |
|---|---|---|---|---|---|---|---|
| 1 | HDPE | 1 | 1 | x | ✓ | 0 | 14300* |
| | LDPE | 5 | 2 | ✓ | ✓ | yes | |
| | PS | 4 | 2 | ✓ | ✓ | 506 | 20300* |
| | PET | 3 | 1 | ✓ | ✓ | 14 | 21300* |
| 2 | HDPE | 4 | 2 | ✓ | ✓ | 518 | 1600 |
| | LDPE | 5 | 2 | ✓ | ✓ | High | |
| | PS | 5 | 2 | ✓ | ✓ | 2126 | 0 |
| | PET | 3 | 1 | ✓ | ✓ | 241 | 25000 |
| 3 | HDPE | 1 | 1 | x | ✓ | 0 | 0 |
| | LDPE | 3 | 2 | ✓ | ✓ | 15 | |
| | PS | 3 | 2 | ✓ | ✓ | 210 | 0 |
| | PET | 2 | 1 | x | ✓ | 0 | 3500 |
| 4 | HDPE | 0 | 0 | x | x | 1 | 7900 |
| | LDPE | 4 | 2 | ✓ | ✓ | high | |
| | PS | 0 | 0 | x | x | 4 | 0 |
| | PET | 0 | 0 | x | x | 0 | 0 |

*Mean value between two sub-samples

In all four investigated sample cakes, PE particles below 350 µm were detected. Although it was not possible to distinguish between LDPE and HDPE with the µ-Raman technique, it can be assumed that they were mostly formed from the LDPE bag, since the bags showed strong signs of fragmentation and abrasion, while the HDPE caps did predominantly not.

In the sample cake which belongs to unaffected samples (µ-Raman sample number 4) no PET and PS particles <350 µm were detected. This was in agreement with the observations during visual inspection.

PET particles were found in three of the sample cakes, although for µ-Raman sample number 3 no fragmentation of the PET bottle was observed. The assumption that abrasion leads to the release of small particles was supported. To distinguish between the two processes, particle numbers were analysed by the power law model (chapter 6.5).

PS particles were only detected in one sample cake, although three PS samples showed fragmentation (destruction categories >2) and visible signs of abrasion (category 2). It might be possible, that µ-Raman analysis failed in this case due to the relatively high concentrations of colorants of the PS cup objects (Figure 40). However, parallel microscopic analyses (magnification x100) of the two sample cakes in question gave the same result of MPP absence. Positive MPP detection in the third sample cake was supported by the occurrence of (red) PS particles identifiable with the naked eye. These particles could have theoretically been formed by fragmentation rather than abrasion.


**Figure 40:** PS cups from samples which sample cakes were analysed by µ-Raman spectroscopy. a) µ-Raman sample number:1; b) µ-Raman sample number:3; c) µ-Raman sample number:2

In conclusion, PE and PET samples which exhibited signs of fragmentation or abrasion generated particles in all size classes including MPP below 350 µm. Very small PS particles as were expected from an abrasion process could not be detected.

## 6.3 Cluster analysis

The appearance and structural destruction of the samples is a very good indicator for the influence of natural parameters on the fragmentation or abrasion of plastic debris. Cluster analysis forms a variety of possible group assignments which are described in a dendrogram (appendix; Figure 60).

Treating all 64 samples (4 objects in each of the 16 experiments) as one data set resulted in the smallest number of categories (clusters) of 2, while 13 was the highest number created (after 64 of course). The division into destruction categories by the decision tree yields (almost) the same result as the cluster analysis. Samples in the same cluster were

in the same or similar destruction categories. The division of both classification systems was based on the given data set resulting from the visually observed signs of abrasion and fragmentation, which explains the high level of correlation.

On the x-axis of the dendrogram (Figure 60), the heterogeneity within the clusters is plotted (standardized by SSPS from 0-25). Thus, a dendrogram shows the optimal number of clusters for a data set by looking at the x-axis since the greatest increase in heterogeneity usually determines the optimal number of clusters. For the 64-sample data set the greatest increase in heterogeneity occurs between a four-cluster solution and a two-cluster solution. This means that the dendrogram suggests a three-cluster solution. The decision tree classification, on the other hand, divides into 6 categories (destruction categories; 0-5) making some distinctions that a binary data set cannot reproduce. One example for that is the division into destruction category 4 and 5, which was made by the degree of fragmentation determined by size distributions of generated fragments. The cluster analysis can thus not divide samples from destruction categories 4 and 5. On the other hand, the cluster algorithm distinguishes between samples which differ in one variable entry. This was not given by following the queries of the decision tree, which ends once it reaches a category. These differences lead to minor discrepancies in the sample classification between the two division systems (even if the result of the cluster algorithm was set to 6 clusters).

The results of the cluster analysis did not provide any hidden effect pattern of a particular experimental parameter (experimental design, sediment sand grain size, matrix condition, UV irradiation) but supported the conclusions from the visual analysis. This was not completely surprising, since the visible signs of fragmentation and abrasion formed the basis of both methods. So, the cluster analysis is a helpful tool to support the categorisation system and to visualise destruction degrees of samples due to fragmentation and abrasion.

## 6.4 Fragmentation pattern over time

The evolution of fragments over time is important for estimating the particle distribution of plastic waste in the environment. Fragmentation of plastic objects is generally initiated when mechanical forces cause the objects to break into pieces. The time resolved experiments (EFP) were conducted in 250 mL glass bottles under breakwater conditions recording weekly time series up to 56d days. The results for artificial cut-out parts from the PS cup (2x2 cm) and the PE bag (5x5 cm) are described below.

### 6.4.1 Polystyrene cup samples

The PS parts did not fragment under the experimental conditions but showed signs of increasing abrasion and mechanical destruction over time in the 56 days exposure period. The edges of the samples were rounded and material loss was observed, but the

original part did not fragment (Figure 41). Surface roughness increased and the coloured side was visually affected (loss of colour), which must have led to formation of small microplastics with abrasion being the main process at the beginning. Perforation of one sample after 35 days of exposure (Figure 41, middle) was consistent with the weakening of the structure by abrasion.

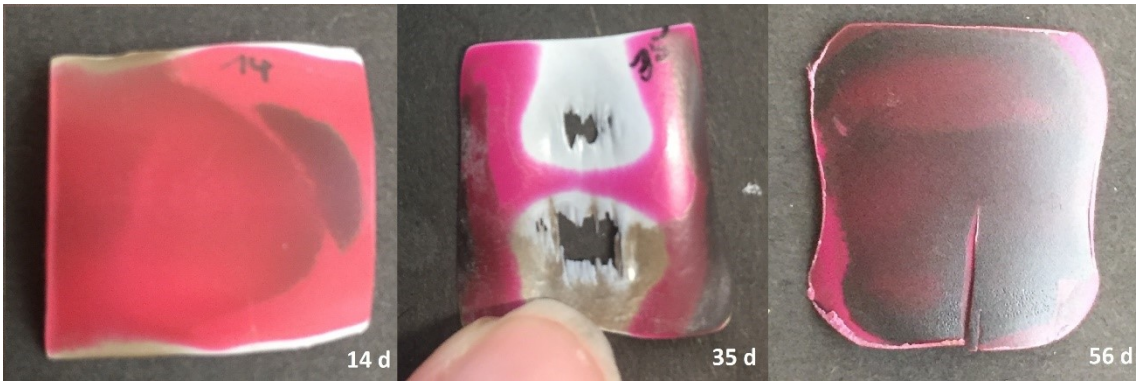


**Figure 41:** Fragmentation of PS parts over the time.

In general, the number of MPPs (350 µm-10 mm) showed increasing tendency over time, but no clear correlation (Figure 42). Although test conditions were held identical for all samples, mechanical stress was most likely variable because movement behaviour of the samples in the vessels cannot be controlled.

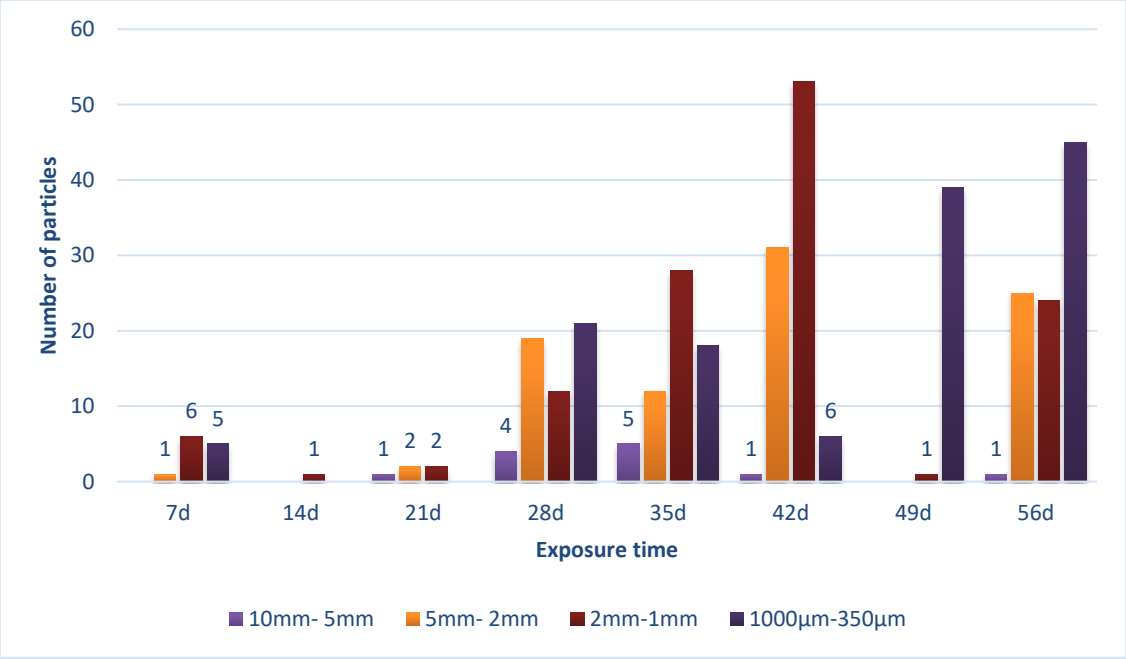


**Figure 42:** Visible MPP size distribution of the non-UV irradiated PS cups over time. The original parts were not included (see **Figure 41**).

Figure 42 shows the MPP size distribution for the non-UV irradiated PS samples. Particles bigger than 10 mm were not formed. Total number of MPP was low at the beginning (days 7 - 21). After longer exposure, the material was weakened leading to an in-

creasing number of MPP. However, from 28 days to 56 days no significant increase occurs; total numbers were in the range from 40 - 95 particles. Surprisingly, the particle size distribution of visible MPP was similar in all samples, with the exception of one sample (49d).

### 6.4.2 LDPE bag samples

Two different LDPE samples were tested differing in thickness (LDPE carrier bag, 0.01 mm; LDPE garbage bag, 0.028 mm). The thicker garbage bag was also investigated after UV irradiation for 10 days. Due to their flexibility, the LDPE samples often dug themselves in the sand matrix. This led to wrinkles on the surface due to folding.

The thicker garbage bag samples were not fragmented at all even after 56 days exposed under breakwater conditions (Figure 44a). Only visible signs of abrasion were detected. The thin LDPE carrier bags, on the other hand, were already completely wrinkled after 7 days (Figure 44c). After 21 days, the samples showed cracks and especially the sample edges were frazzled resulting in thin, elongated fragments. After 35 days, the sample remnants consisted only of several long, coherent fibre-like fragments. Figure 43 shows the generated MPP distribution for non-UV irradiated carrier bags. The number of emerged particles increased over the time. The size distribution of the plastic fragments also shifted to smaller ranges the longer the test time was set.

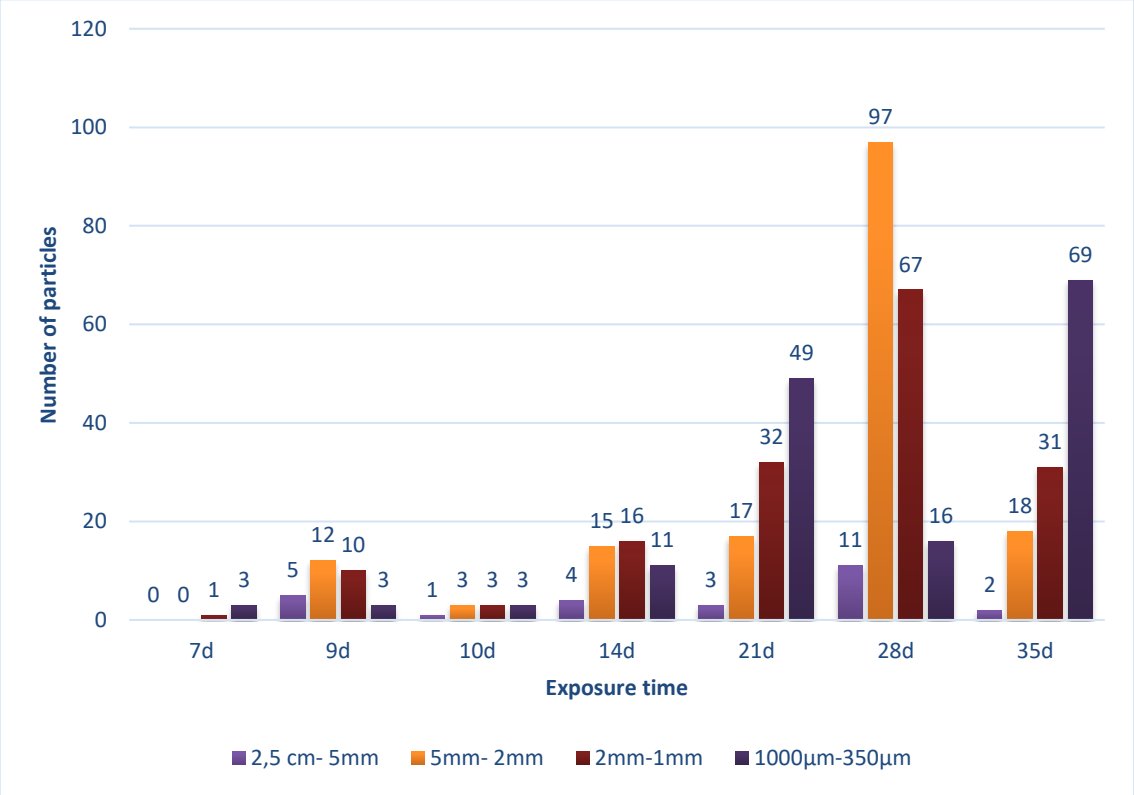


**Figure 43:** Visible MPP size distribution of the non-UV irradiated LDPE carrier bag over time.

Since the original PE garbage bag did not fragment over 56 days, the experiment was repeated with an UV irradiated sample. This could not be done with the PE carrier bag as well, because after more than 10 days of UV irradiation, the samples became brittle and broke into pieces even before they were exposed to mechanical stress (see chapter 5.1.3). Observed changes in colour and surface transparency of the carrier bags after irradiation gave reason to the assumption that the abrasion and fragmentation behaviour could be affected (Figure 44b). This was corroborated by the fact that these samples were fragmented already after five days of exposure (Figure 44b). The size distribution of plastic fragments was shifted to the smaller size categories with time (Figure 45). Most fragments had an elongated shape changing the ratio of length to width over time as they fragmented further.

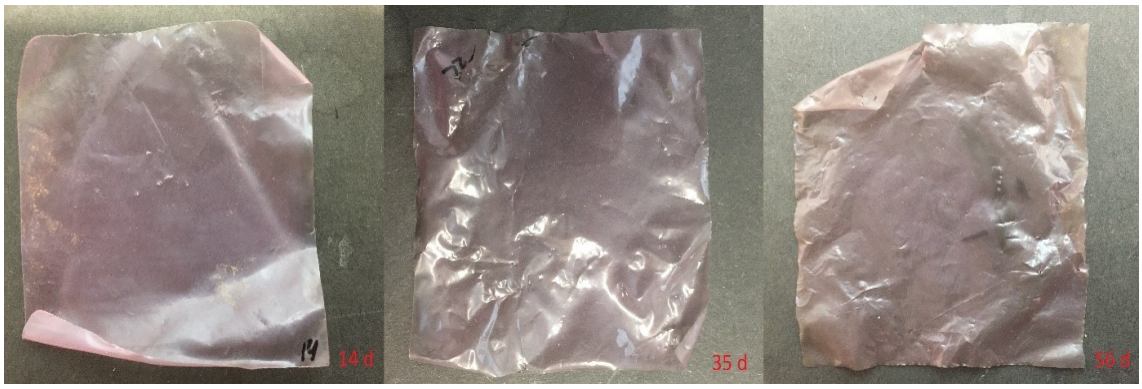


a) Non-UV PE Garbage Bag


b) UV PE Garbage Bag

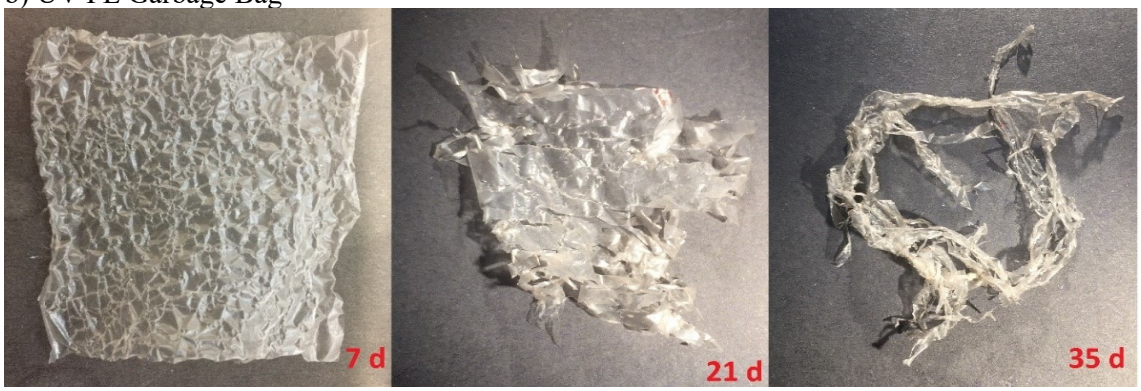


c) Non-UV PE Carrier Bag

**Figure 44:** Fragmentation of different LDPE samples over the time.

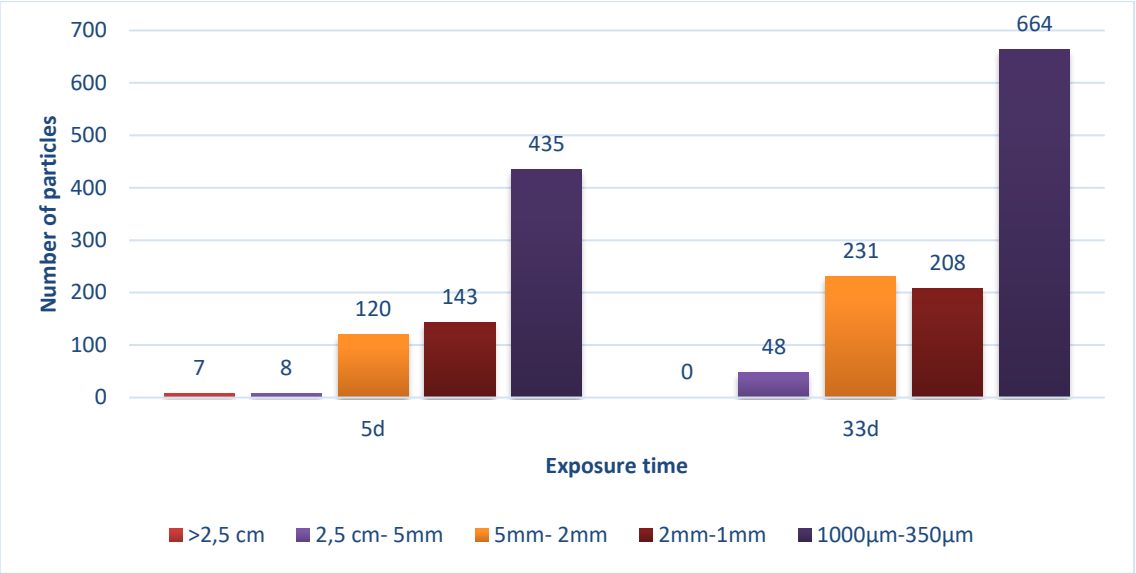


**Figure 45:** MPP size distribution of UV irradiated LDPE garbage bag over time.

UV light obviously weakens the LDPE bag enabling fragmentation in the experiment, which had not been observed for non-UV irradiated bags. This is in line with the irresistance of LDPE against UV-light leading to enhanced brittleness.

The results show that PE bags are prone to fragmentation in the environment. The extent and the time scale of the process depend on boundary conditions and thickness of the bags. The process starts by frazzling at the edges and formation of elongated fragments. These fragments break into smaller parts and finally end up as microplastics that can no longer be distinguished by eye from sediment particles or organic debris such as algae (see chapter 6.1.4). UV irradiation intensifies this process strongly.

## 6.5 Evaluation of fragmentation model approaches

The power law model is generally used to describe the state of fragmentation by the resulting size class distribution. It can be used to represent a particular MPP size distribution in a sample to allow a comparison of samples independent of their often pragmatically selected size classifications. The use of the model for evaluation of the fragmentation in conjunction with the abrasion process in this study is described below.

### 6.5.1 Application to experimental data sets

The model was applied to all experimental data with clear indication of fragmentation and a sufficiently high number of counted particles in at least four defined size categories. For this, the particle counts in the visual size range were fitted to the power law equation (P2) by minimization of the SSR. Since the number of particles for LDPE bag samples cannot clearly be identified, they were not taken into further consideration. From the 16 experiments only 16 samples (all from bottle experiments) had a sufficient-

ly high particle count, of which only 9 had a positive NSE value, while the model completely failed to describe the other seven datasets. Results are shown in Table 29.

**Table 29:** Results of the power law fitting of samples from BE with a sufficiently high particle count (> 45). Samples 1-9 have a positive while samples 10-16 have a negative NSE value inducing that the model fitting failed.

| Sample number | Sediment grain size | Matrix | UV-Exposure | Material | Total number of counted fragments >350µm | Total number of modelled fragments >350µm | α | K | NSE |
|---|---|---|---|---|---|---|---|---|---|
| **1** | Coarse sand | Beach | UV | PS | 506 | 514 | 0,2 | 662,2 | 0,60 |
| **2** | Coarse sand | Breakwater | UV | PS | 2126 | 2147 | 2,06 | 246,14 | 1,00 |
| **2 log** | | | | | | 1731 | 2,2 | 178,4 | 0,93 |
| **3** | Coarse sand | Breakwater | non-UV | PS | 6673 | 6741 | 2,0 | 837,7 | 1,00 |
| **3 log** | | | | | | 5043 | 2,05 | 588,60 | 0,96 |
| **4** | Medium sand | Beach | UV | PS | 937 | 863 | 0,4 | 617,3 | 0,69 |
| **5** | Medium sand | Beach | non-UV | PS | 210 | 205 | 0,6 | 109,6 | 0,79 |
| **6** | Coarse sand | Breakwater | UV | PET | 241 | 238 | 0,5 | 156,3 | 0,39 |
| **7** | Coarse sand | Breakwater | non-UV | PET | 361 | 339 | 0,8 | 144,4 | 0,62 |
| **8** | Coarse sand | Breakwater | UV | HDPE | 518 | 522 | 1,0 | 175,9 | 0,98 |
| **9** | Coarse sand | Breakwater | non-UV | HDPE | 285 | 279 | 1,2 | 153,1 | 0,92 |
| **10** | Coarse sand | Beach | non-UV | PS | 82 | 76 | 0,2 | 90,9 | -0,17 |
| **11** | Medium sand | Breakwater | UV | PS | 46 | 48 | 0,1 | 110,0 | -0,20 |
| **12** | Medium sand | Breakwater | non-UV | PS | 199 | 203 | 0,4 | 146,5 | -0,05 |
| **13** | Medium sand | Breakwater | UV | PET | 135 | 142 | 0,1 | 300,0 | -0,11 |
| **14** | Medium sand | Breakwater | non-UV | PET | 218 | 217 | 0,5 | 140,0 | 0,09 |
| **15** | Medium sand | Breakwater | UV | HDPE | 213 | 225 | 0,3 | 229,6 | -0,26 |
| **16** | Medium sand | Breakwater | non-UV | HDPE | 286 | 296 | 0,3 | 265,6 | -0,23 |

Figure 46 shows the particle size distributions of sample 1-9. Sample number 6 has the lowest NSE value, the power law model does not fit the counted PSD well. This resulted from the particle count in the size fraction 2-5mm, which was relatively high compared to the particle counts in the other size fractions, so the model failed to describe the

observed distribution. In general, the more uniform the size distribution of the particles, the worse the power law model fits. Data sets with a high number of small particles in comparison with the larger size fractions show a better model fit (for example sample number 8 and 9).

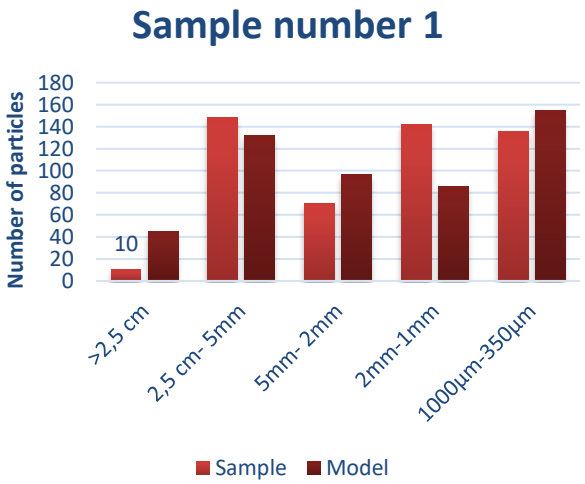


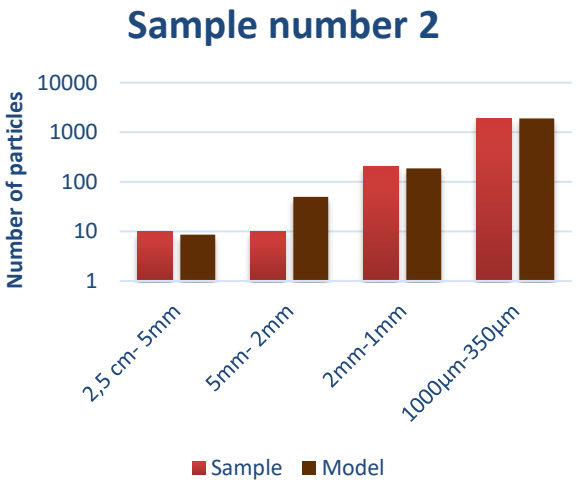


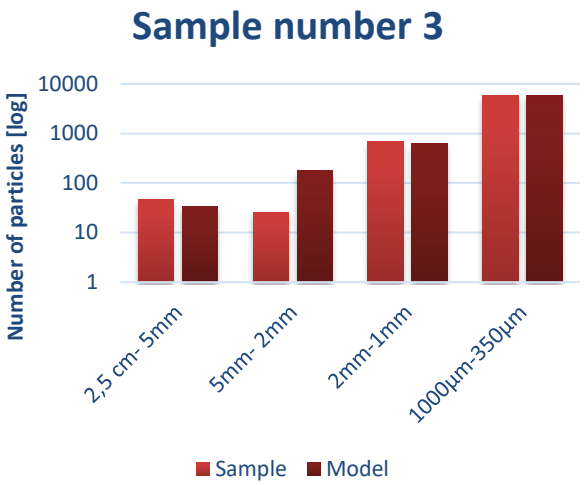


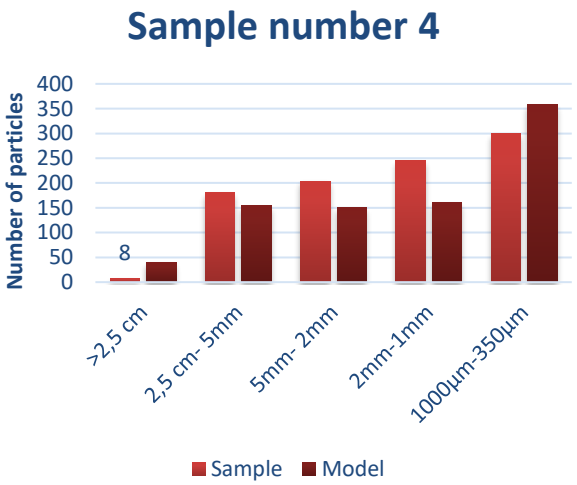


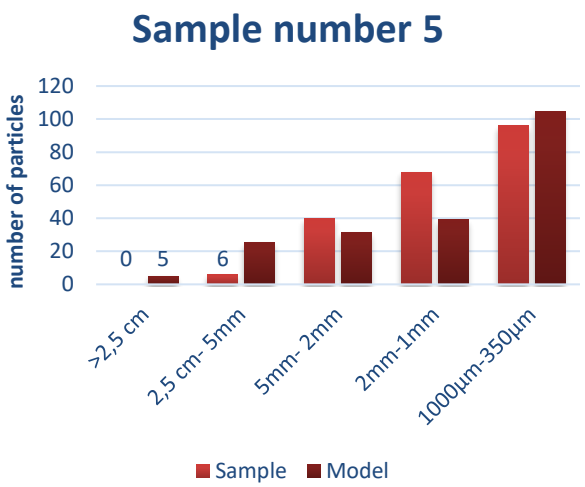


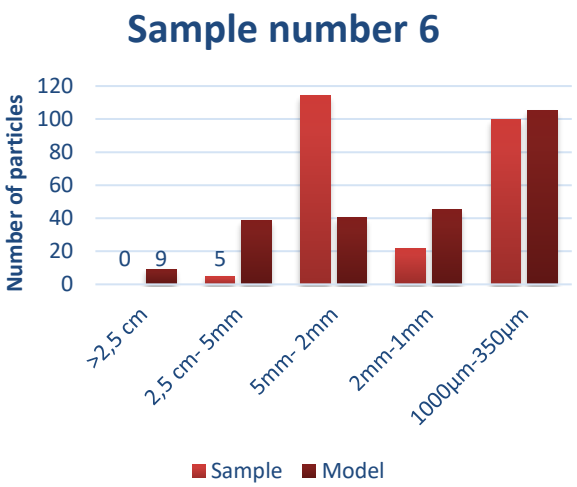

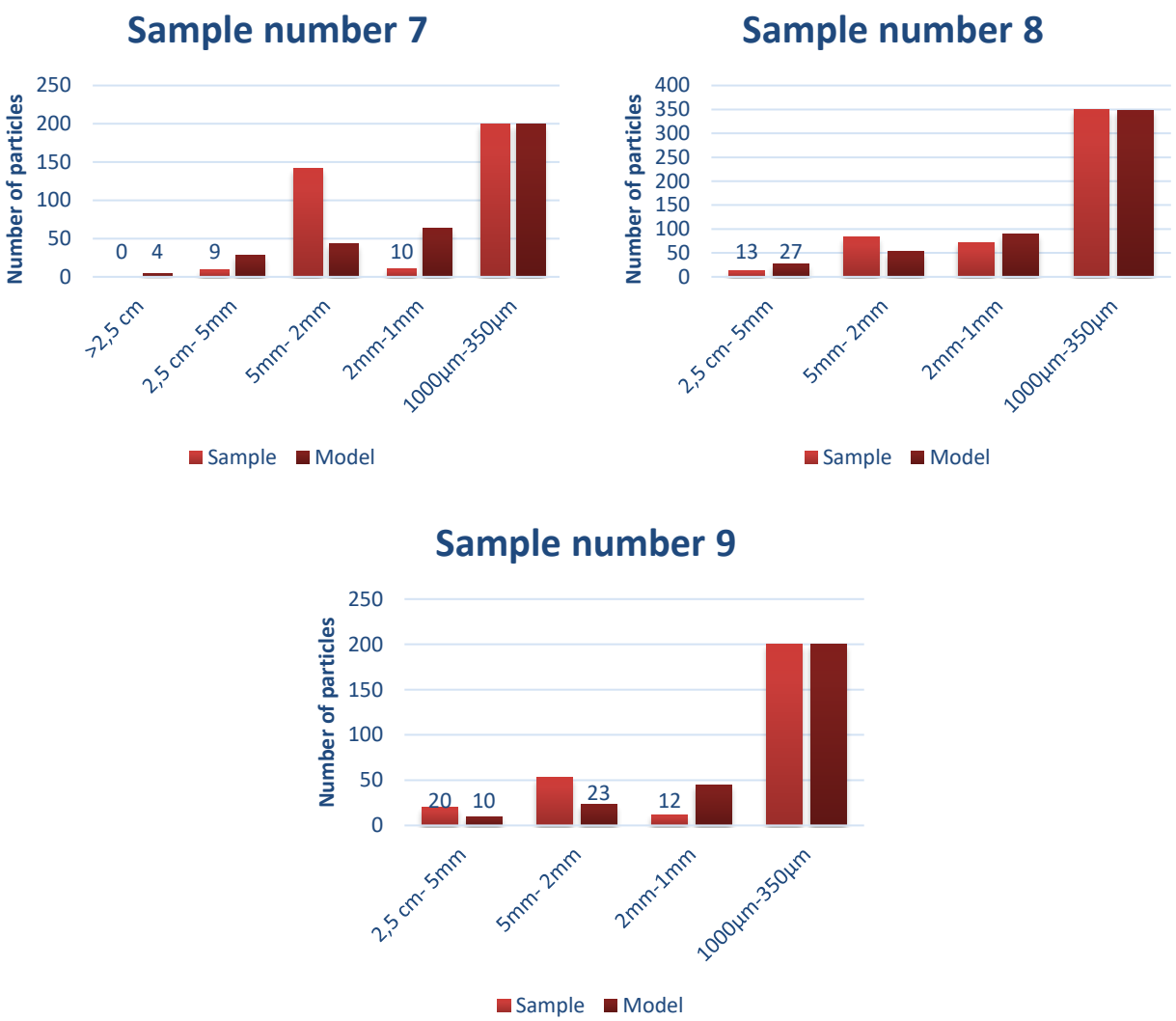


**Figure 46:** Counted particle size distribution of samples 1-9 in five four size classes, respectively, compared to distributions modelled with the power law model.

Since the numbers of particles in the smallest fractions for samples 2 and 3 were one magnitude higher than in the other size fractions, both samples were fitted both linearly and logarithmically using P2 and P5.2 to compare the influence of the SSR values of the dominant size fraction. Results show that alpha-values stay stable while K-values decreased by using logarithmical fitting. Since K has the function of a scaling factor in the model, the decrease of K by stable alpha results in a lower number of particles in the total particle amount. Here, decreasing the influence of the dominating size fraction (smallest fraction) results in better model fittings in bigger size fraction by decreasing the number of particles in the smallest. Since the power law can only show fragmentation, this was the first indication of an abrasion process.

### 6.5.2 Analysis of the α-values

The influence of α-values on the size distribution of particles is shown by varying α with a fixed K-value of 10 for the particle sum function (equation P1; Figure 47).

Curves intersect at (1000 µm/10 particles). For bigger α-values, a shift to higher numbers in smaller particles sizes was clearly observable. Furthermore, it can be observed that although the K-value remains fixed, the total particle number increases; the influence of large α-values was significant.

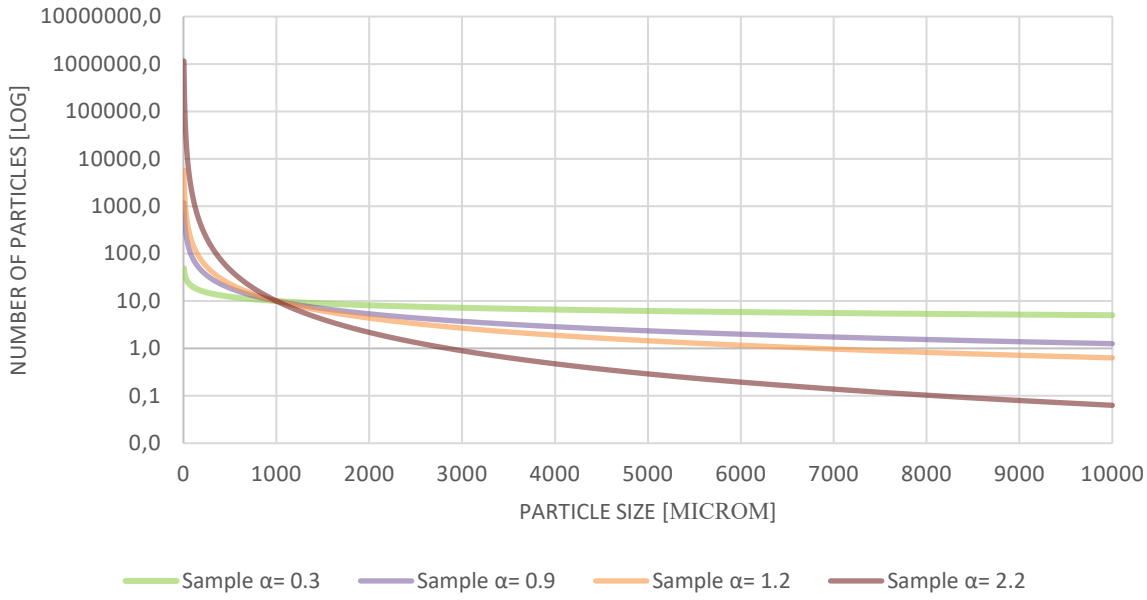


**Figure 47:** Sum function of particle numbers over their size with four different α-values and fixed K-value. The y-axis is log-scaled.

The experiments conducted in this work resulted in distributions with α-values between 0.2 and 2.2. A distinction can be made between the nine investigated data sets:

- α-values>1:
  Samples were fragmented with high numbers of small MPP in comparison with numbers in bigger sized fractions and destruction category classifications of 4 and 5 (sample number 2, 3, 8 and 9)
- α-values<1:
  Samples were fragmented in numbers of particles mainly uniformly distributed over the selected size classes (sample number 1 and 4-7)

Power law functions with α<1 have distributions with generally more meso- and large MPPs (up to 5 mm) than smaller particles while functions with α≥1 have a distribution with more smaller particles (Woyzichovski, 2020).

These observations lead to the assumption that the α-value for a power law fitting of a fragmentation process of a plastic object over a period of time increases, providing that the object breaks into smaller fragments. To analyse this, datasets from the EFP, which observed the development of PSDs over the time of 54 days, were fitted with the power law.

Unfortunately, there were no evaluable results with regards to emerged particle numbers. A trend for a slow increase in emerged particles over the time was observable, but the total number of particles was mostly small for applying the power law while data sets with positive NSE did not show a significant α-value pattern. The conditions in the EFP were not intense enough to cause progressive fragmentation within the observation period. Furthermore, the samples differed in their individual abrasion and fragmentation behaviour, although they were exposed under the same conditions in parallel approaches. The experimental forces were not controllable, an unidentified factor within the experimental approaches led to an inconsistent fragmentation. Thus, the effect of time cannot be separated from the effects of this factor. However, there are numerous factors that influence abrasion and fragmentation behaviour in the marine environment and that are also likely to lead to unpredictable fragmentation of plastic debris. The analysis of environmental data by using the power law is therefore complicated by influence factors induced by environmental conditions.

### 6.5.3 Including particles <350 µm to power law fittings

There were also reliable particle counts in the lower size range (<350 µm) available from µ-Raman analysis for sample 1 and sample 6. Both samples showed clear indications of abrasion, e.g. increased surface haze (see Table 30).

**Table 30:** Description of investigated samples with particles <350 µm by the power law model.

| Sample Number | Sample | Destruction Category | Abrasion Category | Description |
|---|---|---|---|---|
| **1** | PS cup | 4 | 2 | Fragmented completely into fragments of different sizes, glossy coating on the surface has faded |
| **6** | PET bottle | 3 | 1 | Perforation, Surface haze is increased |

The power law equation can be used to construct a continuous sum distribution of the plastic particle numbers for the samples. Extrapolation of the sum function to lower size classes allows for the estimation of expected MPP numbers in this range, if the fit describes the fragmentation process realistically. In this case, an unusual high number of small MPP (<350 µm) predicted by the model hints at an additional abrasion process overlaying the fragmentation.

Figure 48 shows the counted size distribution using µ-Raman for each sample, showing that number of particles below 350 µm calculated by the original model was for both samples much smaller than the counted one. The power law underestimates the particles numbers in the smaller size range significantly indicating that additional abrasion had occurred. However, particle counts were extrapolated from the mean value of a 2 g subsamples of the total sample introducing large uncertainties since each counted particle in

the subsample was grossed up to 450 respectively 160 particles in the total sample represented by “dilution factors”.

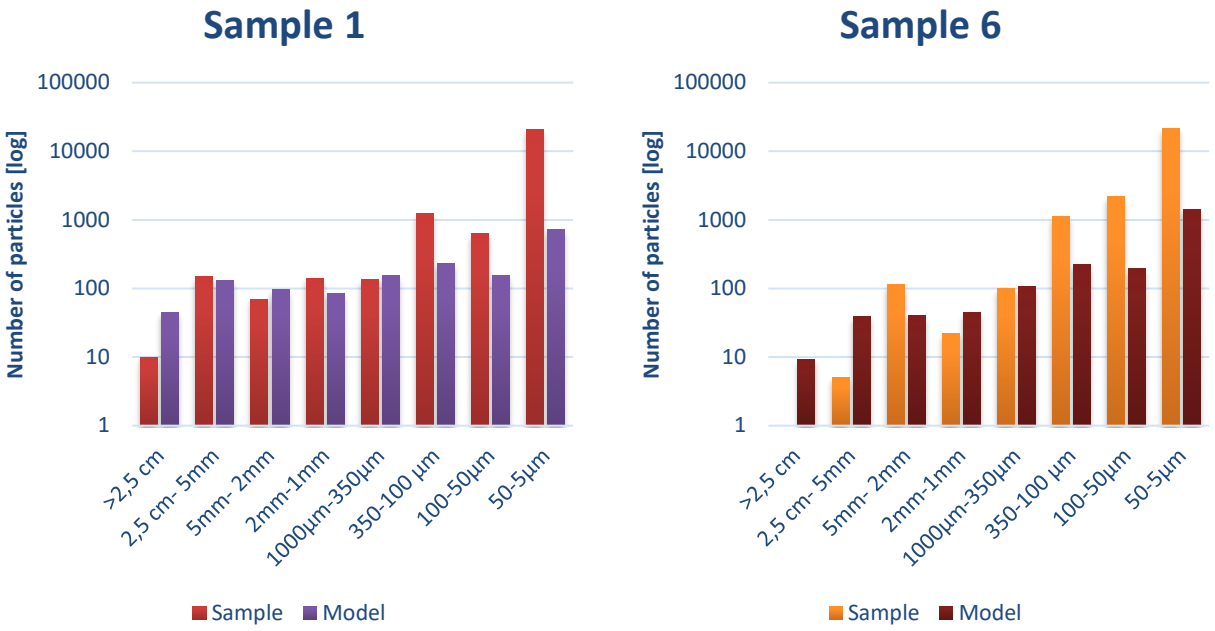


**Figure 48:** Counted and modelled particle size distributions including particle sizes <350 µm identified by µRaman for the two investigated samples. Values on the y-axes are log-scaled.

To check the validity of this finding, the model fit was repeated including particle counts from the µ-Raman analysis. Due to the large range of particle counts the logarithmic transformation of equation P2 was used (P5.2). For both samples, α-values increased (S1 from 0.2 to 0.72; S6 from 0.49 to 1.14) which was in agreement with the fact that the particle numbers detected in the lower size ranges were higher than predicted by the fit of the pure fragment data. Figure 49 shows the size distributions for both samples.

While for sample 1 the total number of modelled fragments (14055) still lower than the counted particles (about 22000), which suggests that small particles were created by abrasion, the modelled fragment number for sample 6 (33500) was higher than that of the counted one (about 25200). Visually, the fragmentation of sample 6 did not follow the classical fragmentation pattern, as perforation occurred at individual spots, but the entire surface showed increased surface haze. Thus, the power law cannot show good fittings for PET bottles.

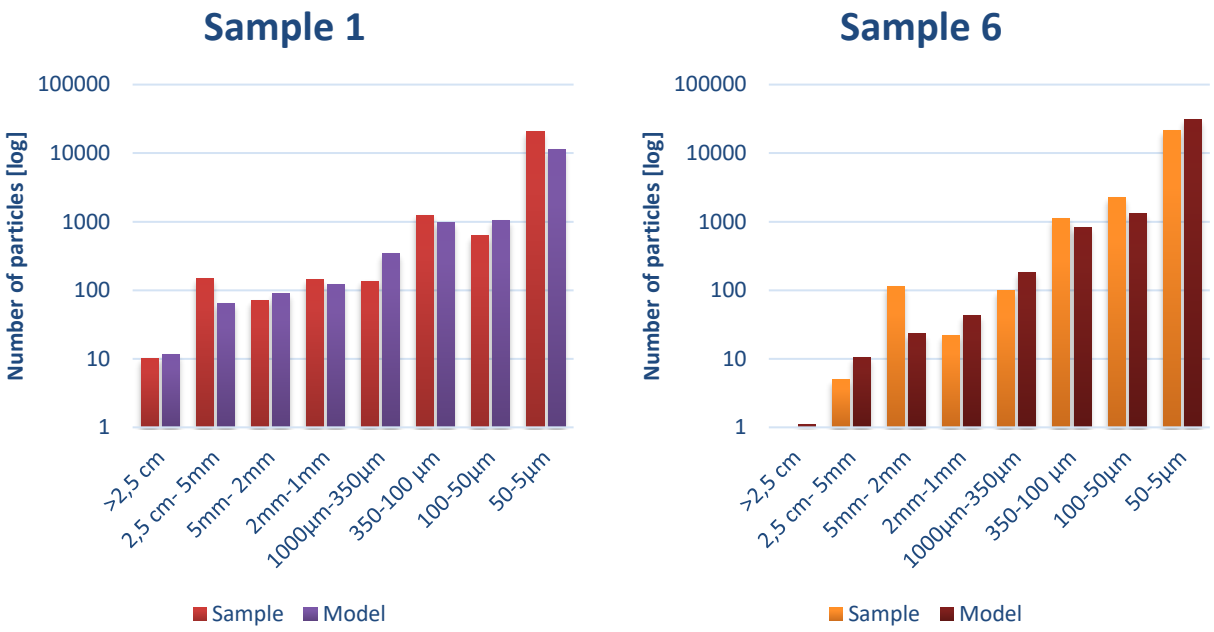


**Figure 49:** Counted and modelled particle size distributions including particle sizes <350 µm identified by µRaman for the two investigated samples using the new alpha and K values. Values on the y-axes are log-scaled.

The application of the power law to experimental data analysing the fragmentation of plastic objects under controlled conditions has shown that the number of small particles cannot result from fragmentation into smaller pieces alone. Fragmentation and abrasion of object surfaces must occur simultaneously.

## 6.6 Hypothesis

### 6.6.1 Hypothesis I - Applicability of the Power Law to the MP Fragmentation Process

Since the volume or mass of the plastic waste remains constant in a closed system, it is assumed that the experimental description of a fragmentation process is possible. The power law suggests exponential increase of particles with decreasing size as is known for a classical fragmentation pattern.

Hypothesis I

Particle size distributions from fragmentation can be described by a power law relationship, especially in closed experimental systems.

Figure 50 shows the theoretical development of a fragmentation process of a plastic object over the time represented by different sum functions of particle numbers over their sizes. At the starting point t0, considered object was fragmented into ten 50 mm

fragments (red line). After a period of time (t1>t0) the number of bigger particles decreased while the number of small particles resulting from the fragmentation processes (<5 mm) increased (purple line). If time progresses even further (t2≫t1), the 5 mm fragments will be completely fragmented, while the number of small fragments will increase exponentially (yellow line).

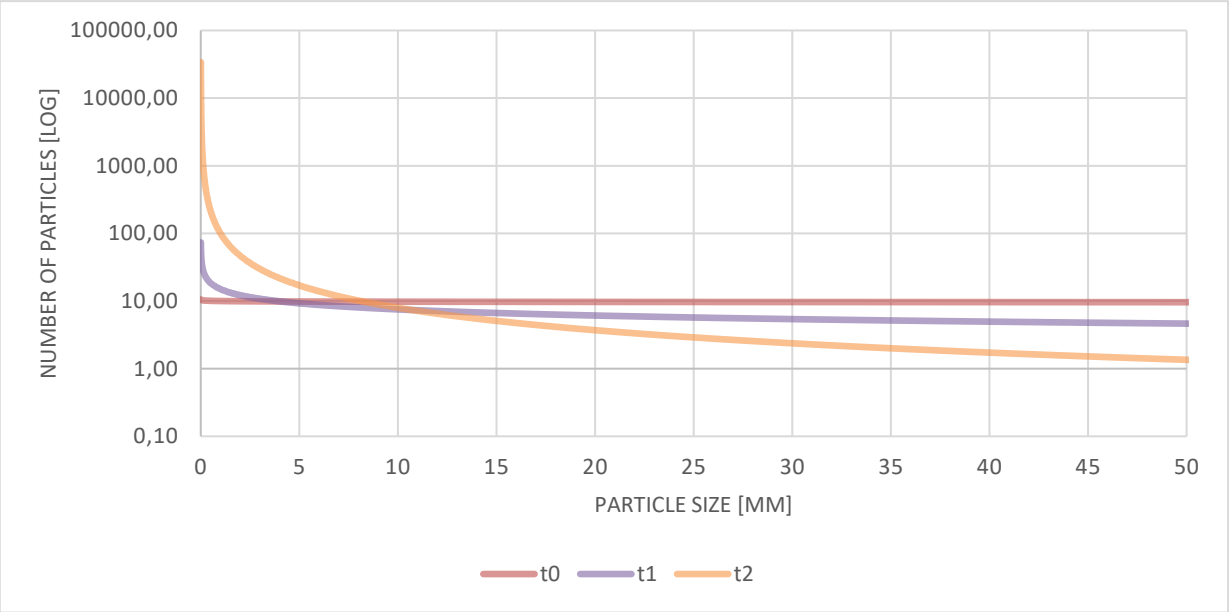


**Figure 50:** Theoretical development of plastic particle formation over the time (t0 <t1<<t2) illustrated by the sum function of the particle number over the particle size. The y-axis is log-scaled.

As mentioned earlier, data sets which are uniformly distributed over particle sizes cannot be fitted well by the power law. For illustrating a fragmentation process of plastic debris with the power law, the process must have formed enough small fragments. Further analysis is needed to find the tipping point of the process but it is assumed that it depends on the median of the total number of fragments formed during the process and the defined particle size categories. To be able to compare data sets with different size categories, application of the continuous model representation is necessary.

Mechanical stress (degradation) causes plastic debris not only to fragment but also to be abraded. Abrasion leads to the emergence of small particles, so that the particle number is massively increased, especially in the small particle size classes. In these controlled experiments, all samples had at least an increase in surface haze. This leads to the conclusion that fragmentation and abrasion take place simultaneously and cannot be separated from each other. Thus, the model does not fit because it only represents one of the two processes involved.

For environmental samples, the power law can be used to compare data sets with different particle size categories, as a continuous representation of particle numbers over time can be achieved regardless of size classes. An estimate of the number of particles in

smaller size ranges that are not detectable by analytical techniques can be achieved by extrapolation. For this a good model fit is important, which is expressed here by the NSE value. Data sets with low or negative NSE values cannot be represented by the power law as well as data sets with low particle counts. This excludes data sets with a uniform distribution of particles over the particle size or a distribution with the majority of particles in the larger size range. However, a redesign of the size classes by reducing the size of the class ranges may help.

In addition, it is very important to consider a lower particle size boundary. It is assumed that the particles change their fragmentation behaviour after reaching a certain size and break no longer following a classical fragmentation pattern. However, further research is needed to investigate fragmentation behaviour of small MPP (<100 µm) and nanoparticles.

All in all, the power law is useful to analyse the controlled fragmentation process of plastic waste when this process is far enough advanced, which means that many particles in small size classes have been already formed. The Power law can be used to represent the actual size distribution.

### 6.6.2 Hypothesis II – Emergence of meso- and microplastics

Fragmentation is considered to be the major breakdown process of large plastic items into smaller pieces in the environment. A classical fragmentation pattern of plastic debris leads to the stepwise emergence of smaller fragments. The longer a fragmentation process continues, the more and smaller fragments are formed. The size distribution of the fragments will be more or less exponential but will change with time.

> Hypothesis II
>
> Fragmentation of plastic material in the environment occurs under mechanical stress and produces plastic fragments of all size classes including meso- and microplastics.

The results of meso- and microplastic analysis (x>350 µm) support this hypothesis. Particles in the size range from 350 µm to 25 mm were formed. The number of particles produced within the exposure time varies depending on the experimental boundary conditions and the individual sample properties (see chapter 6.1). Especially the design of the experiment and the correlated potential of the samples to collide with the walls of the test vessels have a strong influence on the formation of fragments. More collisions took place in BE, which was why (higher) fragmentation was observed. In addition, prior UV irradiation led to a higher fragmentation at least for PS cups and LDPE bag samples. PET bottles and HDPE caps were more fragmented when exposed under breakwater conditions.

If sufficient particles have been formed by fragmentation, the data sets can be approximated by the power law. The conditions during the experiments - just like in the environment - cannot be standardised, i.e. randomness plays a role and causes deviations from the classical fragmentation pattern. Thus, not all particle size distributions of samples obey to the power law. Experiments showed that plastic litter follows a classical fragmentation pattern in the environment is not probable since even in experiments, which took place under controlled conditions (as possible), plastic objects showed various fragmentation pattern. Environmental influences, which lead on the one hand to a weakening of the plastic structure (weathering of plastics) and on the other hand to independent forces affecting plastics (e.g., increasing wind speeds on the beach), complicates a prediction of plastic fragmentation.

In conclusion, fragmentation occurred when plastics were exposed to mechanical forces leading to a formation of fragments in all sizes dependent on experimental conditions and sample properties.

### 6.6.3 Hypothesis III – Sample characteristics

Stiff, but hollow plastic objects, for example bottles and cups, are likely to be more susceptible to fragmentation when they are exposed to a momentum (e.g. by collision with other objects) stronger than the molecular binding forces. Compact objects such as bottle caps are more resistant against breaking. Flexible objects, e.g. bags and foils, also behave differently.

Hypothesis III

Object form (shape, compactness, stiffness) of plastic litter has an influence on the fragmentation behaviour leading to individual destruction patterns.

Compact formed plastic litter was more stable against collisions since the object stability itself was higher. Only four HDPE caps fragmented at all (BE, breakwater conditions) (Figure 51). The destruction of hollowed plastics was in the medium range but was strongly dependent on the plastic sample type. LDPE bag samples showed a different fragmentation pattern than all other samples. Collisions did not have a big impact, but they were still the most destroyed sample type in BE. Due to the harsh shaking conditions in combination with the flexibility of the samples, they were buried in the sediment. This led to shear stress caused by the movement of the sediment particles and resulted in tearing of the samples into fragments (Figure 52b) which was supported by their low thickness.

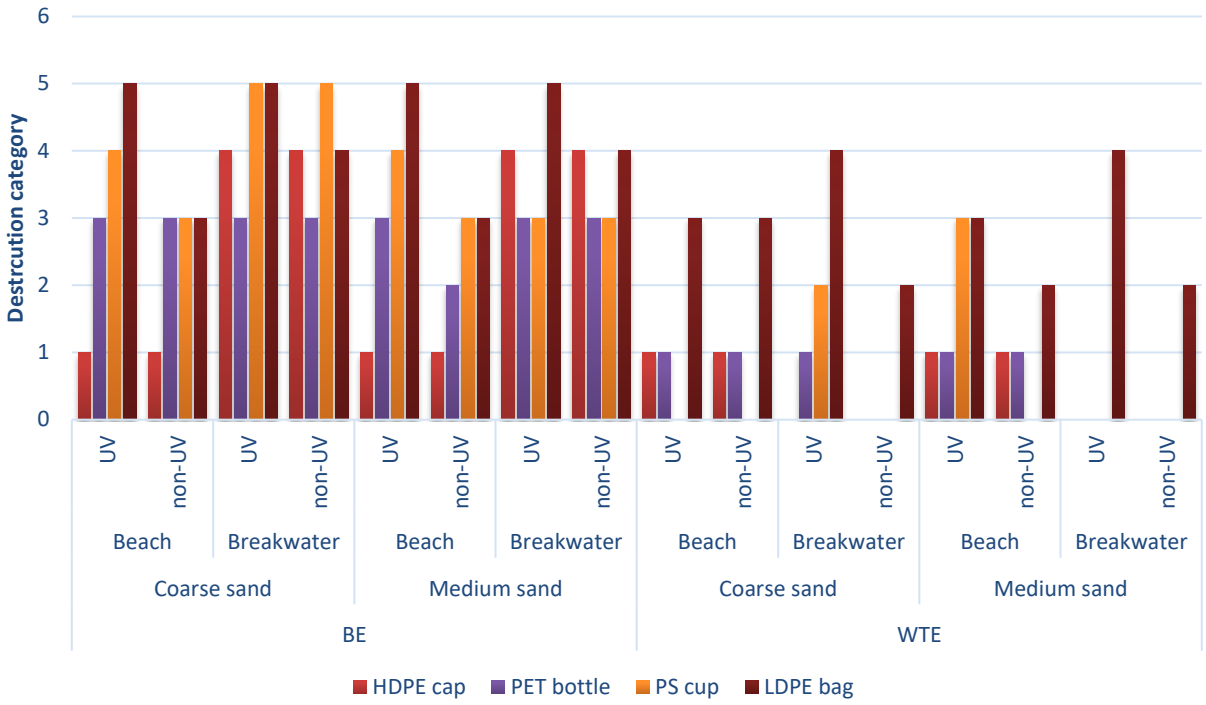


**Figure 51:** Destruction categories for each sample and experiment in comparison.

The breaking behaviour of PET bottles and PS cups also exhibited differences (Figure 52a, c). Both sample types were manufactured by moulding but while bottles were blow moulded (the shape is formed by injected air into liquid raw plastic), cups were formed by injection moulding (the melted plastic is injected directly into a custom mould). Due to this production process, cups have a weak point around the perimeter of the bottom part. This makes cups more vulnerable against collisions breaking more easily into pieces (Figure 52c). Since PET bottles do not have such weak points, none of the PET samples lost their shape during the mechanical stress exposure.

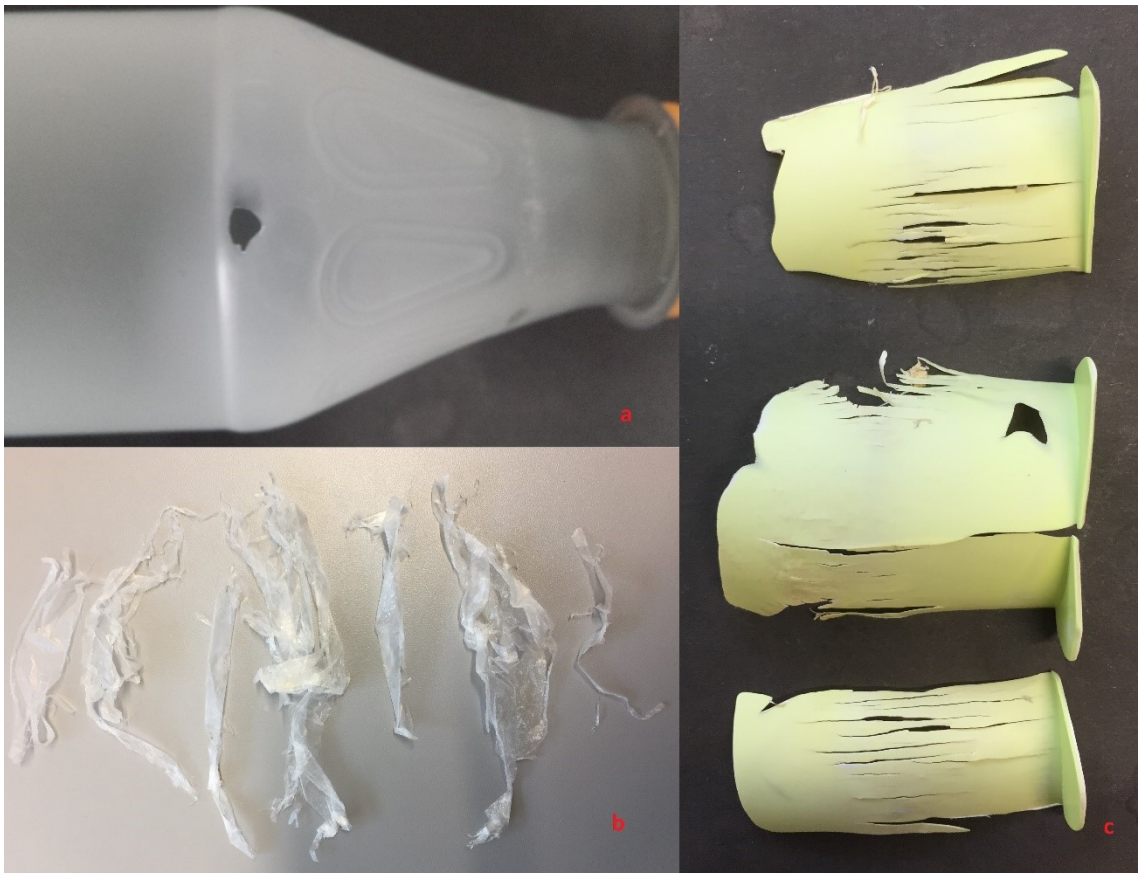


**Figure 52:** Selected samples to illustrate the influence of stiffness, compactness and flexibility on fragmentation and abrasion pattern.

In addition to the visible signs of fragmentation expressed by the destruction categories, the number of visible microplastic particles (>350 µm) is a clear indicator of the vulnerability of the samples to fragmentation (Figure 53). Mostly all LDPE bags had been completely fragmented into a huge number of particles, which could not be manually counted due to their large quantity.

In almost all corresponding experiments, the number of PS cup particles was higher than particles from PET bottles and HDPE caps. Only in breakwater experiments with medium sand, PS cups exhibited less meso- and microplastics than the other two sample types. Results consequently leads to a gradation of the degree of fragmentation of the sample types from LDPE bags over PS cups to PET bottles and HDPE caps. Samples with thick walls in combination with a stable and stiff shape (HDPE caps and PET bottles) potentially require higher impact forces and/or more time to break than thinner samples (PS cups, LDPE bags).

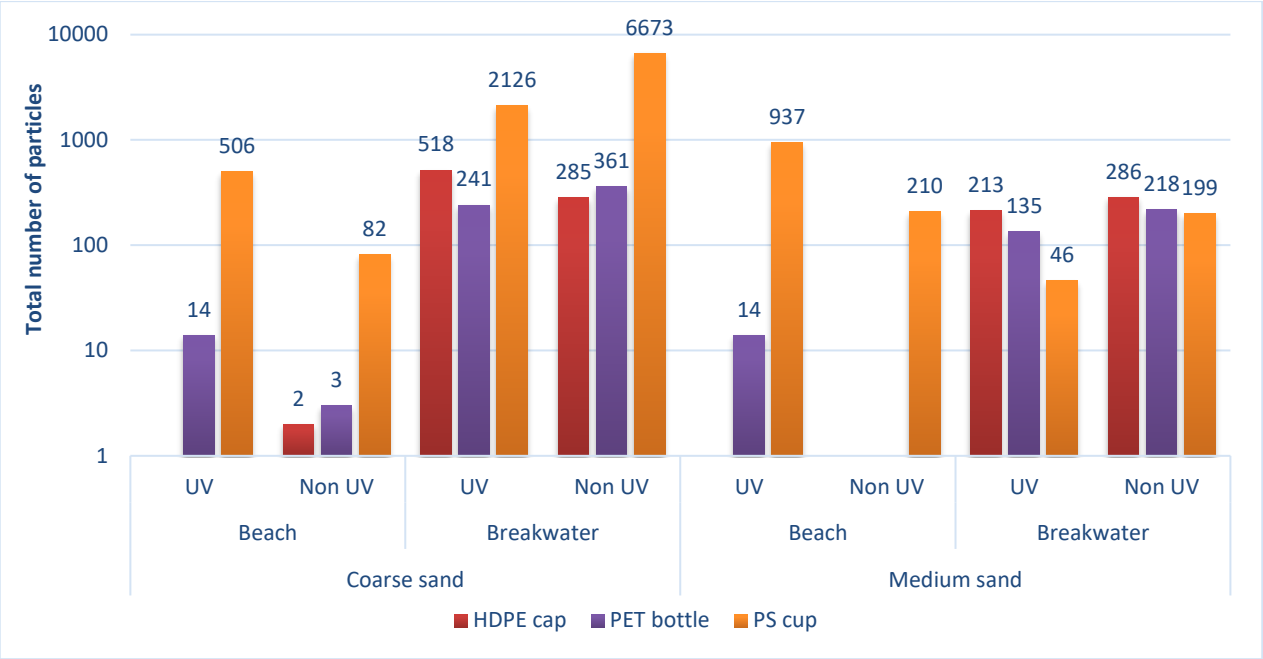


**Figure 53:** Total numbers of particles for HDPE caps, PET bottles and PS cups for each experiment.

All these characteristics can be influenced by functional additives. The addition of stabilisers, antistatic agents, flame retardants, plasticizers, lubricants, slip agents, curing agents, foaming agents, etc. to enhance the materials stability towards stress/degradation factors is a common plastic treatment. This leads to the conclusion that the more additives were added to a plastic debris the longer it can resist degradation (photodegradation as well as mechanical degradation depending on additive type). Degradation rate is thus most likely reduced. The samples were not tested for additives in this work, but as they were conventional plastic items mainly from food packaging, it can be assumed that non-toxic additives were contained.

All in all, different fragmentation behaviour of the four sample types can be observed. According to the individual sample form, different signs of destruction and fragmentation pattern occurred.

### 6.6.4 Hypothesis IV – Collisions trigger fragmentation

The process of fragmentation of an object is classically observed during milling. This includes that physical forces are exerted onto the objects by the grinder leading to breaking of the material into smaller pieces (fragments). It is thus assumed that fragmentation of plastic objects is also related to external physical forces acting upon the plastics. In the environment, this may happen by collisions with pebbles, stones, rocks on cliffs/reefs or weir structures.

Hypothesis IV

Fragmentation of plastic objects is triggered by collisions with environmental structures (stones, rocks, weirs).

In the fragmentation experiments, such situations were represented by the conditions of the bottle experiments, where the objects experience collisions with the inner wall of the glass bottle throughout the shaking process. External forces in the WT experiment were most likely too small to initiate fragmentation, because the setup did not induce wall collisions even though the frequency of the shaker was set to the maximum practical value. Here, fragmentation may only happen when the objects become (partly) buried under the sand or the sand-water matrix during the course of the experiment.

In this respect, the size of the samples in relation to the volume of the shaking vessel is an important experimental parameter. In BE, the size of the selected samples was only little less than that of the 3.5 L glass bottle, so that the inner walls of the vessel limited the freedom of movement of the samples. Thus, bumping against the walls during shaking was enabled and the resulting collision forces supported fragmentation.

Figure 54 shows the destruction category distribution of all samples separated for BE and WTE experimental setup.

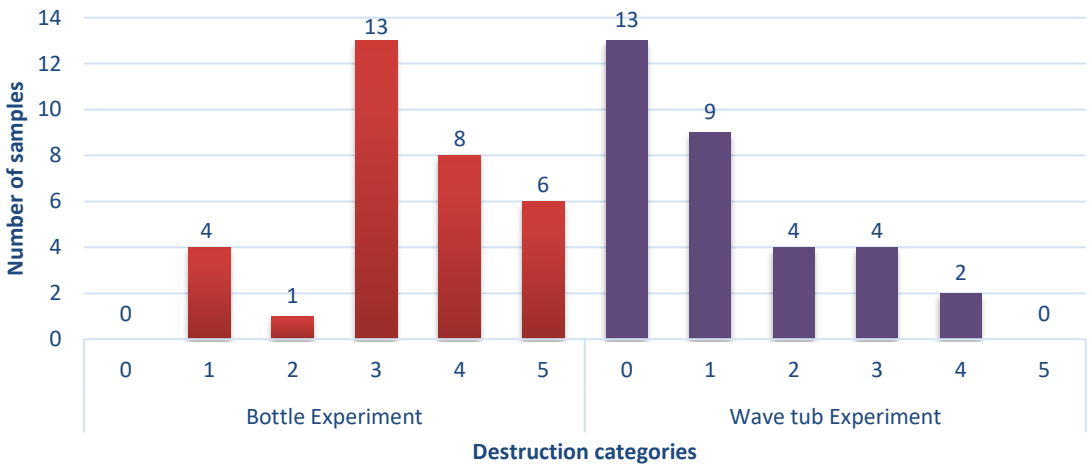


**Figure 54:** Classification of samples into destruction categories regarding the experimental design.

In BE, all samples except four had been fragmented (category ≥2). As described in the result, the collision force on HDPE caps was not sufficient enough to led to fragmentation under beach conditions. Due to the much lower collision potential in WTE, only 10 of 32 samples fragmented, nine samples showed only signs of abrasion (category 1) and 13 samples were not affected at all (category 0). The number of meso- and microplastic particles (>350 µm) for PET bottle, HDPE caps and PS cup confirms these observations. Almost no particles for the three sample types were found in WTE (44 particles in total), while a high number of particles were counted in BE (Table 35, appendix).

Plastic items obviously will break more easily when they are surrounded by natural counterparts like stones or other hard materials. In the marine environment, physical boundaries limiting the freedom of movement of plastic debris may exist at rocky sea-

shores, where the objects are waving between rocks and cliffs due to tidal movements. Especially in areas where natural bottlenecks occur, fragmentation processes (through impacts and collisions) may be accelerated. The results are consistent with the experiments of Chubarenko et al. (2020), who compared rocky shores with "grinding mills" where MP are generated and exported to the sea.

**Box 2**
**Influence of the shaker frequency in BE on the fragmentation intensity**

The BE was developed to simulate environmental conditions with collisions between plastic litter and hard surfaces. Shaking frequency was adjusted at 275 rpm since then movement of the samples relative to the matrix started and collisions between the samples and the inner wall of the bottle regularly occurred. Reducing the shaking frequency to 150 rpm (as used for WTE), reduced the number of collisions and lead to lower fragmentation probability.

One beach experiment and one breakwater setup were investigated applying both frequencies, 150 rpm and 275 rpm. Non-UV irradiated samples and medium sand were selected as representative conditions for the comparison. Observations during the shaking process confirmed that at the lower shaking frequency no collisions with the walls occurred.

Seven of the eight samples were not affected at all under these experimental conditions (category 0). Only the LDPE sample exposed under breakwater conditions showed signs of abrasion and one single crack (category 2). Since LDPE bags were generally affected stronger under breakwater conditions, this observation is not surprising.

Shaking frequency is an important experimental factor determining the number of collisions per time and increasing the level of fragmentation.

### 6.6.5 Hypothesis V – UV Irradiation

UV irradiance is known to weaken the structure of plastics by oxidative processes of the material itself or by reactive loss of additives (especially UV stabilisers). Plastics become brittle and are thus more prone to breaking and fragmentation.

Hypothesis V

UV exposure leads to material weakening and subsequently an increasing of the fragmentation probability. UV irradiated plastic samples show higher levels of fragmentation under identical conditions than virgin items.

This hypothesis was checked by experiments with samples that had previously been irradiated for 10/15 days (depending on the sample type) under artificial UV-light in comparison to the results for non-irradiated samples.

10/15 days UV irradiation had different effects on the fragmentation of the different sample types (Figure 55). HDPE caps were not influenced at all by previous irradiation exhibiting the same degradation behaviour as before. PET bottles also tend to stay unaffected with only two samples reacting by stronger abrasion or enhanced fragmentation, respectively (chapter 6.1.1).

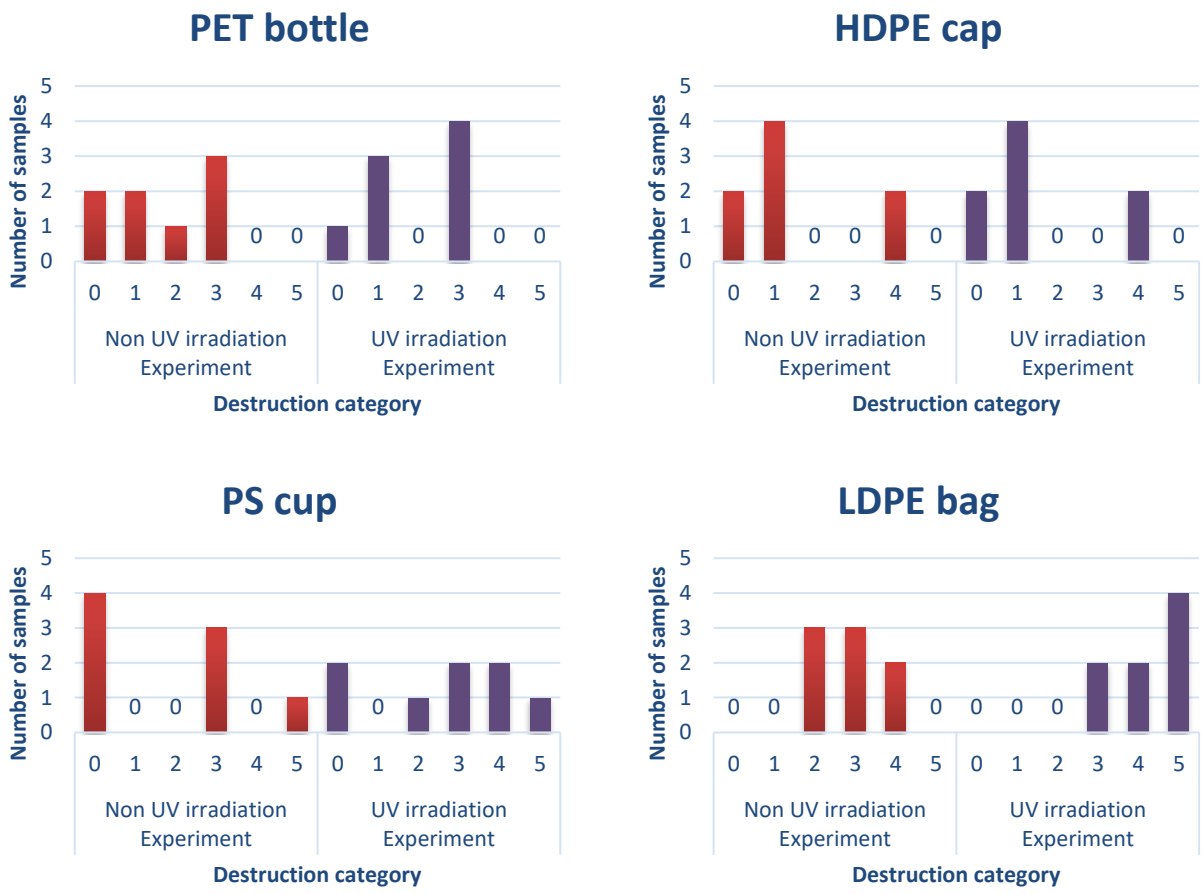


**Figure 55:** Classification of samples into destruction categories regarding UV irradiation.

For the HDPE caps and PET bottles, 15 days of UV irradiation in the irradiation chamber was obviously not strong enough to weaken these samples in a way that mechanical degradation was enhanced. Environmental exposure over 3 months may thus not yet

contribute to enhanced generation of MPP from such plastic objects. However, it may be that sample thickness plays an additional role since UV rays mainly affect the sample surface. The thicker an item the less material (volume) can be damaged.

In contrast, PS cups and LDPE bags changed their behaviour in the experiments after UV irradiation (Figure 55), mainly in the BE (collision experiments), but also partly in WTE. PE bags exhibited higher degrees of destruction after UV irradiation. Non-irradiated PS cups that did not fragment under all experimental conditions were sufficiently weakened by the irradiation to initiate this process.

It is known that certain materials are more vulnerable to UV radiation, so UV stabilisers (additives to inhibit-photoinitiation) are added to the polymer matrices (Yousif & Haddad, 2013). However, differences in the UV vulnerability of the different polymer types could not be investigated by this experimental setup.

The results provide experimental evidence that UV irradiation of plastic objects increases the probability for fragmentation of many plastic objects. It is likely that material thickness, light intensity, polymer type or additive composition are important parameters in this respect. Especially thin materials (LDPE carrier bags) become brittle, which increases the probability for fragmentation. Kalogerakis et al. (2017) and Song et al. (2017) also suggested that UV irradiation weakens the plastic structures and increases fragmentation depending on the irradiation time and the sensitivity of the plastic to UV light.

### 6.6.6 Hypothesis VI – Mechanical stress in the low tide surf- and swash zone

In addition to sandy beach zones, marine litter is also present in the surf- and swash zone of beaches. Plastic objects washed ashore from the open ocean are often trapped there for a certain time by wave action, where they experience mechanical stress (during breaking of waves) as well as friction stress when washed ashore with ripples.

Hypothesis VI

In the swash zone, friction stress may cause abrasion. In the low tide surf zone, shear stress by wave action will cause fragmentation of plastic objects into pieces.

To test the first part of the hypothesis, solely the results from WTE under breakwater conditions were considered since this setup simulates a gentle wave runup on the beach. Most of the samples were less affected in the experiments than expected; ten samples were even completely unaffected showing neither fragmentation nor signs of abrasion. Two UV irradiated samples showed signs of abrasion (PET bottle) or beginning fragmentation (cracking, PS cup) corroborating the intensifying effect on mechanical degradation.

LDPE bags again were the exception exhibiting tears (non-UV irradiated) or fragmenting (UV irradiated) with additional signs of surface abrasion (abrasion category 2). Contact pressure through the sand-water matrix was probably high enough for initiating the process of abrasion and subsequent fragmentation of those objects that were weakened by prior UV irradiation.

This was corroborated by µ-Raman analysis (µ-Raman sample number 4: WTE; medium sand, breakwater, UV) showing that the irradiated PE samples generated a large number (7900 particles; dilution factor 112) of microplastic particles smaller than 350 µm in the experiment (see chapter 6.2).

Nevertheless, the first part of the hypothesis is not fully confirmed by the experimental results. During the 30 days experimental exposure relatively little abrasion was observed. Either friction stress for plastics in the swash zone was not adequately represented by the experimental conditions here or it was less than expected.

Wave action and collisions with sediment particles lead to shear stress in the low tide surf zone. In the experimental setups, waves could not be generated so that conditions were not fully representative for the surf zone. However, forces exerted onto the objects in breakwater conditions in BE could be close to what they experience in the surf zone. Although an ultimate proof of this part of the hypothesis was not possible, the stronger fragmentation of objects in the BE breakwater experiments does at least not contradict it.

The results indicates that gentle wave movements in the swash zone indicates that only gentle abrasion processes occurs while almost no fragmentation of the object can be observed. Experimental setups did not simulate the turbulent wave movements in the surf zone, so the second part of the hypothesis cannot be confirmed.

### 6.6.7 Hypothesis VII – Friction stress on the beach

Plastic litter pollute beaches all over the world. Once the objects have been emitted, they can be moved along the sand surface, e.g. by wind, causing friction between plastics and the (hard) sand particles

> Hypothesis VII
>
> On the beach, friction stress from wind-induced movement along the sand surface will mainly induce abrasion. Abrasion will lead to an increasing number of small microplastics, while the plastic object is not necessarily fragmented.

For testing this hypothesis, solely the results from experiments simulating open beach conditions (wave tub with pure sand) were considered.

Figure 56 shows the distribution of all 16 samples in their abrasion categories for each sample type. All PET bottles, PE caps and LDPE bags showed clearly visible signs of

abrasion through friction stress on the surface (abrasion category 2). One PS cup was even cracked (UV irradiated) with the glossy coating being faded, while three PS cups were not visibly affected. As already mentioned, PS cups were coated with a shiny layer assumed to be at least 20 µm thick. This layer protected the cups from abrasion. However, UV irradiation seems to affect this coating, which explains in connection with a random experimental factor the cracking of one cup.

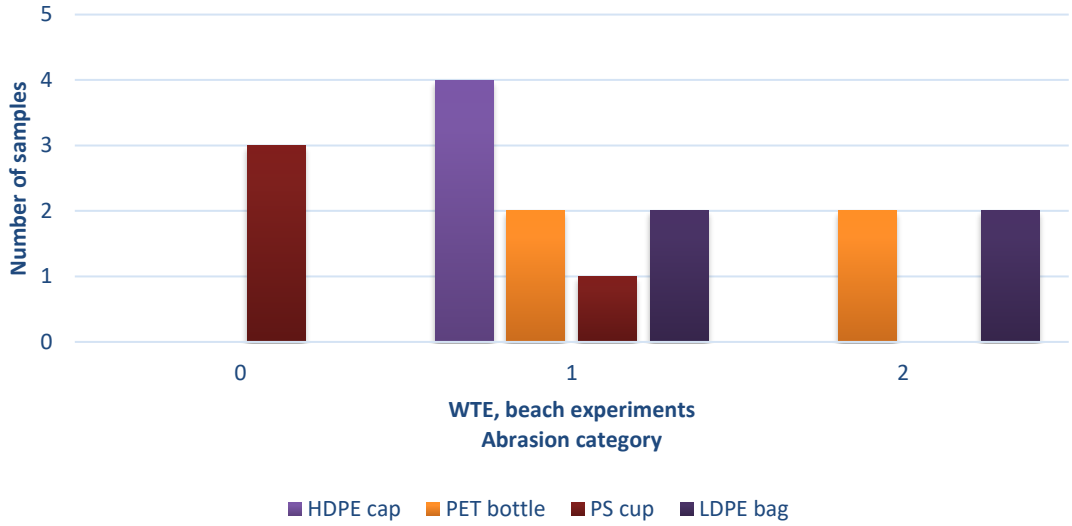


**Figure 56:** Overview over the abrasion categories of samples exposed in WTE under beach conditions divided by sample type.

Figure 57 exemplary shows surface asperities observed for a UV irradiated PS cup and a PET bottle. Both pictures give reason to the assumption that friction stress exerted by the sand particles led to the emergence of very small particles in the size range below 20 µm. Though originally planned, confirmation by µ-Raman analysis could not be delivered by the cooperation partner.

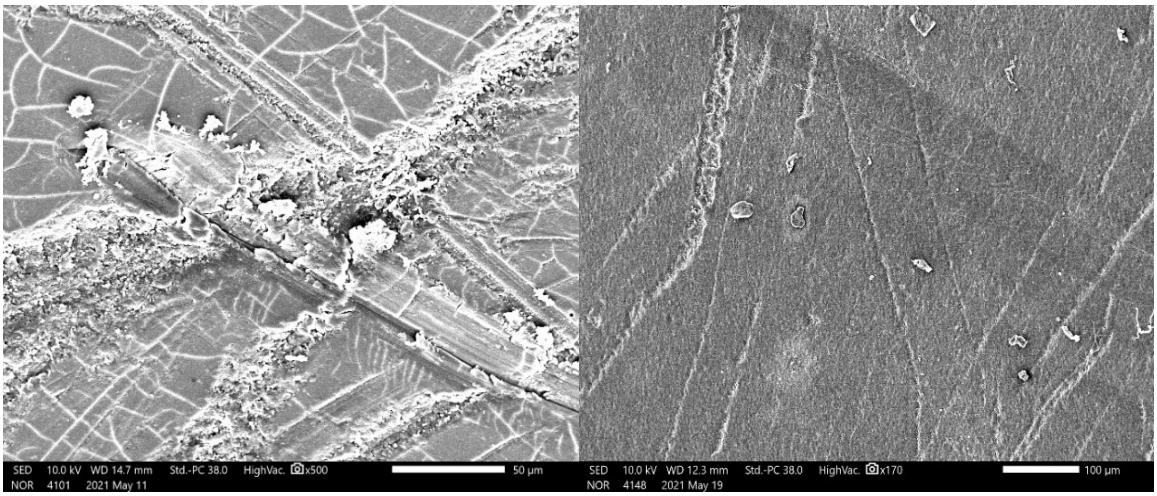


**Figure 57:** SEM images of samples exposed in WTE under beach conditions. On the left side: PS cup surface (destruction category 3) with a magnification of x500.
On the right side: PET bottle surface (destruction category 1) with a magnification of x170.

Since the number of visible meso- and microplastic particles (>350 µm) was negligible for PE, PET and PS samples, the minor role of fragmentation in this surrounding is confirmed by the results. Although visual analysis hints at abrasion being the main degradation process for plastic litter on beaches, the ultimate proof is thus still pending.

### 6.6.8 Hypothesis VIII – Influence of the sediment grain size

Abrasion through friction between sand and plastic surfaces produces small plastic particles. The grain size of the sediment particles is suspected to determine the size of the abraded particles. It could also be that the weakening effect of friction stress is stronger with larger sand particles (coarse sand), which then was responsible for higher fragmentation probability.

> Hypothesis VIII
>
> Grain size distribution of the sediment (sand) affects the size distribution of abraded particles. Fragmentation probability is affected by grain size.

The first part of the hypothesis could not be analysed because results from Raman analysis were not available for the samples. SEM pictures alone do not provide sufficient evidence to decide whether the size distribution of MP particles emerged from abrasion was different in the different setups.

25 of 32 samples were classified in the same destruction category in medium and coarse sand experiments. Table 31 shows the seven samples where the grain size could have affected the abrasion and fragmentation behaviour.

**Table 31:** Samples that with their destruction categories that were affected by the grain size distribution of the sediment changing their abrasion and fragmentation behaviour.

| Experimental design | Matrix | UV-Exposure | Sample Type | Destruction Category | |
|---|---|---|---|---|---|
| | | | | Medium | Coarse |
| **BE** | Beach | Non-UV | PET | 2 | 3 |
| **WTE** | Breakwater | UV | PET | 0 | 1 |
| **BE** | Breakwater | UV | PS | 3 | 5 |
| **BE** | Breakwater | Non-UV | PS | 3 | 5 |
| **WTE** | Beach | UV | PS | **3** | **0** |
| **WTE** | Breakwater | UV | PS | 0 | 2 |
| **WTE** | Beach | Non-UV | LDPE | 2 | 3 |

Experiments with coarse sand caused stronger destruction for six samples, while one PS sample was more affected in medium sand experiments (Figure 58, left side). Here, prior UV irradiation affected the protective coating (cf. chapter 6.1.3). This resulted in

cracking of the samples exposed in medium sand experiments while the sample exposed in coarse sand was not as much affected due to prior UV irradiation. Experimental design and parameters as well as sample type seemed not to play a role. Only the compact HPDE cup was unaffected while for example PS cups - both irradiated and non-irradiated - in the breakwater bottle experiment were clearly affected: In the coarse sand setup fragmentation had occurred leading to a large number of microplastic particles, while with medium sand the cups had only formed a few large fragments (Figure 58, right side).

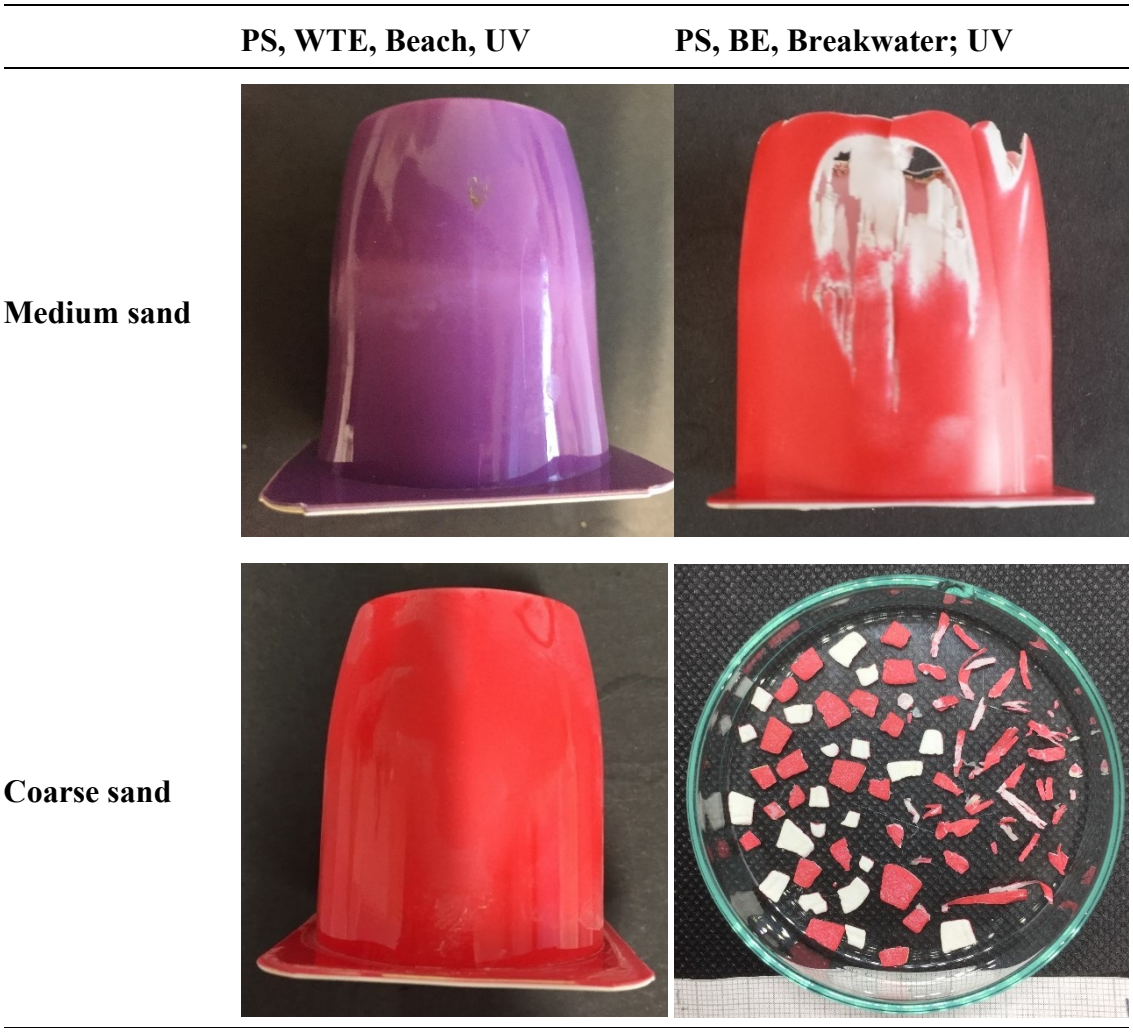


**Figure 58:** PS samples which were exposed in corresponding experiments with medium and coarse sand.

The sum of visible microplastic particles (>350 µm) formed during the experiments may serve as a proxy for the level of fragmentation. Almost no fragmentation (no particles) was observed in WTE, so that only BE results are discussed further. A clear tendency towards stronger fragmentation when samples were exposed with coarse sand occurred in the breakwater setup (Figure 59); especially PS cups were much more fragmented than exposed with medium sand. Unsurprisingly, such a trend could not be observed in the beach setup, where abrasion has already been identified as the major pro-

cess. Differences in numbers of visible particles were most likely the result of random variance in the experiments.

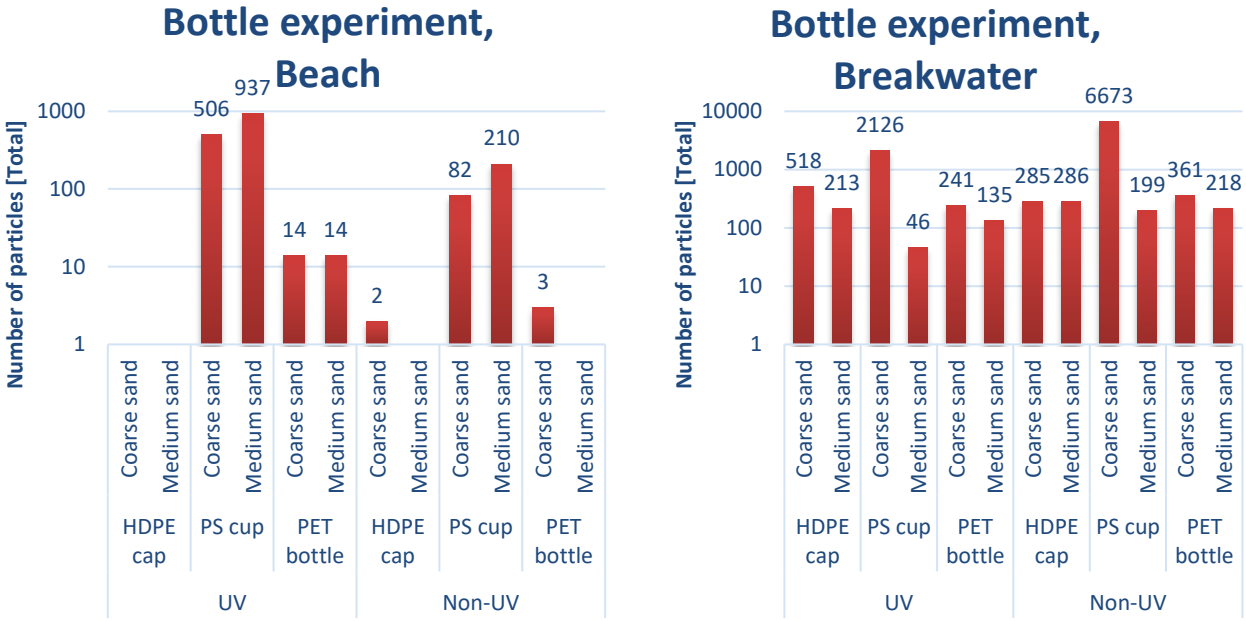


**Figure 59:** Number of meso- and microplastic particles for corresponding coarse and medium sand bottle experiments for HDPE caps, PS cups and PET bottle samples, divided by matrix conditions. The y-axis is logarithmically scaled.

The results corroborate the second part of the hypothesis. In the breakwater setup, coarse sand seems to increase fragmentation efficiency possibly due to the larger collision energy exerted by the larger particles in the BE. Chubarenko et al. (2020) also observed such an effect for size classes ranging from coarse sand (1-1.5 mm) to pebbles (4-6.4 cm). Therefore, it can be assumed that the observed effects of grain size on fragmentation would have been more prominent, if the grain size differences had been larger.

To conclude, experiments showed that a dependence of the fragmentation probability on the sediment grain size in the environment especially for larger sediment particles is to be expected, while influences on abrasion processes could not be analysed in this study.

## 6.7 Environmental relevance

The fate of plastic debris and the formation of secondary microplastic in the aquatic and, in particular, the marine environment has not been investigated in detail to date and literature is rare. Knowledge of the effect of environmental boundary conditions on mechanical degradation are important to understand the environmental exposure and can help to control plastic pollution. Experiments should give a first insight into the abrasion and fragmentation behaviour of plastic debris under selected boundary conditions. In this respect, it must be notified that the boundary conditions in the (marine) environ-

ment are much more variable and complex as in the laboratory experiments. However, even in the "controlled" experiments it was impossible to install reproducible conditions with regard to the mechanical forces exerted onto the plastic objects. In this chapter, the results are interpreted in terms of their environmental relevance.

One objective of this work was to get an idea of the time horizon for the destruction of plastic in the environment by mechanical stress. In this respect, it was interesting to relate the experimental conditions to what happens in the environment.

**Box 3**
**A first approach for the projection of experimental conditions to corresponding time intervals at natural conditions:**
**Shaking Frequency**

The shaking frequency expressed in revolutions per minute (rpm) describes the number of movements of the vessel per minute. One revolution of the shaker motor causes the vessel to be moved one time back and forth. One such movement could be interpreted as one wave in breakwater experiments or one movement of plastic on the beach caused by a gust of wind (in beach experiments). This simplifying assumption can be used for comparison with environmental conditions:

The wave frequency of gravity waves is usually in the range of 3 $min^{-1}$ to 60 $min^{-1}$ (Toffoli & Bitner-Gregersen, 2017) with a geometric mean of 13.4 $min^{-1}$. Assuming 10 $min^{-1}$ as representative for the Baltic Sea (Efimova et al., 2018), this simplified calculation results in a total number of gravity waves of 432000 waves within 30 days. In breakwater experiments, a shaking frequency of 275 rpm (BE) and 150 rpm (WTE) were applied, which is 27.5 and 15 times more than the estimated wave frequencies. This means that 30 days exposure in the breakwater experiment roughly corresponds to exposure in coastal areas of 4.5 years (BE) or swash zone exposure of 2.5 years (WTE).

Results of this simple calculation suggests that 2.5 years in the swash zone would lead to abrasion on the surface of plastic debris but not necessarily induce fragmentation. This would lead to numerous microplastic particles, which accumulate in the sediment or in the drift line or migrate into the open ocean. The only exceptions are thin, possibly pre-damaged objects such as bags, which will fragment earlier due to friction-induced weakening by abrasion. Such objects would fragment in macro-, meso- and microplastics after only a few months.

For beach experiments, similar estimations could be made under the assumption that each shaker movement represents movement of a plastic object triggered by a gust of wind. However, it was necessary to estimate the number of gust of winds per day that

are strong enough to move a certain plastic on the beach, which is virtually impossible. Another important point to mention is that wave or wind speed are not the influence factors, although they are strongly affecting the friction force for abrasion or the collision energy for fragmentation. Other factors are the angle of inclination of the beach surface, the percolation of the beach sediment, the wave period or the grain size of the beach (Efimova et al., 2018). Here, results showed, that grain size of particles on sandy beaches will most likely affect the fragmentation probability only little. However, pebbles and stone may exert larger forces on the plastic and thus increase fragmentation probability.

In the breakwater bottle experiments, at least the HDPE caps and the PET bottles collide with the inner walls of the shaking vessel during any movement of the shaker (see chapter 6.6.4). The impact force depending on the wave energy plays a major role for the fragmentation probability. It needs to be above a certain threshold to induce fragmentation, which is dependent on the characteristics of the plastic object such as the form or thickness. These factors make an interpretation of the experiments regarding the time horizon for fragmentation of plastics in such environmental areas complex. However, the high levels of destruction observed in these experiments may be looked at as representative for high tide surf zones, where collision forces arise from the breaking of waves forcing objects to collide with the sediment. The results indicate that the fragmentation probability of plastic waste will probably be higher in such environmental areas than on beaches with "flatter" inclination. Cliffs and areas along steep coastlines are other environments, where the fate of plastics could be similar to what occurred in the breakwater bottle experiments. Collisions can also play a role for plastics in rivers, namely when the objects pass rapids or transverse structures such as weirs. Thus, the potential for the formation of secondary MPP is high there. These particles subsequently follow the waterway systems and entering the oceans.

Besides the collision energy, the number of collisions an object experiences also has an influence on the fragmentation probability. During the WTE experiments, the pulse for movement of the objects was not strong enough to enable collisions with the wave tub walls. The extent of fragmentation and the time scale depend on many, often highly variable influences (e.g. mechanical forces) and are difficult to generalise.

UV irradiation weakens the structure of plastic objects leading to surface damage and brittleness. This leads to a higher fragmentation probability; especially thin objects are affected. The LDPE bags became after 15 days in the *Suntest* chamber brittle enough to break without mechanical force. The weakening reduced the threshold of the impact force for a breakup into fragments. Thus, plastics may fragment more quickly in environments with higher sunlight intensity. Direct UV exposure can be reduced by attached organic matter and/or burying the plastics in sand (Song et al., 2017). However, open beach areas are predestined locations with high UV exposure. High temperatures of the upper sand layer induced by sunlight additionally support chemical degradation pro-

cesses. UV vulnerable plastic debris (like thin PE bags) can become brittle easily and generate MPP only by the slight touch of wind.

**Box 4**
**A first approach for the projection of experimental conditions to corresponding time intervals at natural conditions:**
**UV Irradiation**

UV irradiation was simulated using a *Suntest* test chamber for accelerated weathering by setting the irradiation energy to 700 $Wm^{-2}$, which results in a total power of 16.8 $kWhm^{-2}$ over one day of continuous irradiation. The total annual solar irradiation at a city located close to the North Sea in the period 1981-2010 was around 1000 $kWhm^{-2}$ (DWD, 2010). From this, the average daily irradiation power calculates to 114 $Wm^{-2}$. The total irradiation power of the *Suntest* is thus approximately six times higher than under outdoor conditions close to the North Sea. PE carrier bags were irradiated for 10 days and PET bottles, PE caps and PS yoghurt cups for a total of 15 days. This is equivalent to outdoor light-induced weathering times of 60 days (2 months) or 90 days (3 months) respectively.

The experimental results allow for identifying environmental conditions that favor abrasion as well as those that favor fragmentation. Also, they show that abrasion starts immediately under certain conditions and releases small MPP (and eventually nanoplastics), whereas fragmentation often starts temporally delayed after pre-damage by abrasion, photo-oxidation or other influences. However, surface abrasion were observed in all experiments where fragmentaion took place. This indicates that abrasion and fragmentation processes occur simultaneously under environmental circumstances especially under breakwater conditions. Abrasion and other weathering factors potentially weaken the plastics structures increasing the fragmentation probability. It is expected that the number of particles and the size distribution will increase to some extent according to the Power Law, but exact predictions are impossible due to the additional abrasion.

Further ideas for calculating a time horizon for the mechanical degradation of plastic debris to microplastics from experiments are discussed now. Analysing the formation of small sand particles and comparing it with sand formation rates from geological data could give an indication of the time horizons for the formation of MPP. The formation time in experiments divided by real formation rates could be a calculation factor and thus indicate the time ratio between experiments and environment (depending on environmental conditions). Analysis of the small sand particles produced could not be performed with the available laboratory equipment.

Experimental results were not meaningful enough to enable estimation of the time horizon of fragmentation behaviour (or mechanical degradation rate) in the natural marine

environment, but they show the influence of the tested parameters on different plastic debris and their influence on the mechanical degradation rate in general. Different fragmentation patterns can be seen for different tested sample types. The results allowed a first assessment of the importance of secondary microplastics formation from fragmentation and abrasion as MPP source.

Fragmentation has been shown to be dependent on the number and strength of collisions with the walls of the vessels or matrix components (sand). On the other hand, areas on the beach with high collision potential for plastic objects in the marine environment are rare. On the beach as well as in the swash zone with only gentle wave action (wave runup) and low collision potential (WTE), plastic debris fragmentation is expected to be negligible, whereas abrasion by friction and thus the formation of small MP particles is most likely an important process. Main sources of secondary MP fragments could be rocky coastal sections with high wave action. However, UV irradiation on the beaches increase the fragmentation probability by weakening the material. Overall, the complex interaction of environmental conditions and weathering factors make predictions of the fragmentation behaviour of plastic waste in the marine environment very difficult, but the strong potential for formation of secondary MPP in all environmental areas has been proven in this thesis.

# 7 Conclusion and Outlook

The results of this thesis clearly show that the generation of secondary MPP in the marine environment due to fragmentation as well as abrasion processes induced by wave and wind action is undeniable. Abrasion was identified as the main process under conditions, where friction stress is the dominant influence factor. On sandy beaches, this happens through wind-induced movement of plastic litter objects. Advancing abrasion on the one hand leads to the preferable emergence of small microplastic particles and on the other hand contributes to weakening of the material measurable through reduced thickness.

Fragmentation is a more gradual process, where the plastic objects break into smaller pieces forming macroplastic and mesoplastics fragments in the first place. These pieces can undergo further fragmentation causing more and more little fragments to emerge with longer exposure times. The probability of "breaking" into pieces is dependent from environmental boundary conditions and material properties. For example, hollow stiff objects such as yoghurt cups are more susceptible than flexible polyethylene bags and turbulent conditions. Typical environments offering conditions that favour fragmentation are areas with high collision potential (cliffs, coasts).

It was furthermore demonstrated that UV irradiation of plastic objects has the potential to weaken the material leading to brittleness and decomposition. The effect is depending on the material and the objects thickness as well as time and intensity of irradiation. It was estimated that UV irradiation of plastic objects over a few months contributes to the weakening of the material increasing the probability for fragmentation.

Fragmentation and abrasion behaviour are dependent on environmental factors and site conditions. The samples follow different destruction patterns, which is conditioned by their individual properties such as shape/form and thickness of the object. The results lead to the conclusion that mechanical degradation is a major source of secondary MPP in the marine environment.

However, experimental conditions were not controllable or replicable in a way that the results could be generalized. Neither the expected number of secondary MPP generated under certain conditions nor the time frame of fragmentation can be clearly defined to date. Abrasion, however, will form small MPP on the short-term if plastic objects are exposed to respective friction stress on sandy beaches or in high tide surf zone.

Further research should focus on the analysis of the variability of experimental parameters to get further insight into the environmental relevance of the processes. Abrasion of particles from the plastic surface should be quantified by application of advanced analytical methods for small microplastics to samples exposed under realistic conditions.

More insight into the effect of turbulent wave action was possible by direct comparison of parallel experiments on an overhead shaker and a horizontal shaker.

Experimental setups to better represent conditions in the swash zone of beaches are needed to investigate mechanical degradation of plastics in this highly relevant environmental compartment. Furthermore, the mechanical degradation of MPP <1 mm and the resulting fragmentation/abrasion behaviour is of interest. It is conceivable that very small particles change their break behaviour by changing the "item form". The smaller the particles, the smaller the length/height/width ratio, and the rounder they become. The breakage of particles with a round shape is less likely, but abrasion still occurs.

The largest obstacle for detailed investigations of abrasion and fragmentation of plastics, however, is the lack of a standardised method for extraction of microplastics from sediment samples that is suitable for all sample volumes. Analytical methods require extracts that are almost free of matrix components, because they interfere with the detection and quantification process. In this study, first progress was achieved in improving the MP extraction from large sample volumes. As a compromise, interfering particles smaller than 63 µm were excluded by pre-sieving, whereby the information on particle numbers in this size class was lost.

Modelling the fragmentation process can be helpful to compare observations of MPP numbers between different sites, time points or experimental setups. Particle size distributions of classical fragmentation processes can be approximated by the power law. In the experiments, the power law often failed to describe the observed size class distribution due to under-predicting numbers in the small size classes (< 350 µm). This led to the conclusion that fragmentation rarely occurs without abrasion taking place at the same time. While the larger size classes are formed by fragmentation, abrasion preferably generates small microplastics explain the observed bias. The original idea that the form of the power law representation of MPP datasets could shed light on the state of the fragmentation process proved unworkably, because the size class distribution of an individual sample is dependent on too many variable and uncontrollable factors.

The results of this study strongly suggest that to stop the emission and/or intentional littering of plastic objects in the environment is a necessary step to prevent ongoing pollution by secondary MPP. However, it also became clear that generation of MPP through mechanical degradation of plastic litter already present in the marine environment will further proceed. In this respect, the actual accumulation of plastic litter on open beaches, in the swash- and surf zone and in other coastal areas is problematic, since a steady increase in meso- and microplastics will occur. Cleaning activities reducing the amount of large plastic objects - although only second-best choice - are thus still essential to reduce potential precursors for secondary MPP. To date, efficient cleaning of the marine environment from microplastics is not feasible and the respective pollution of the environment is thus irreversible. The analysis of the impact on marine flora

and fauna is therefore a top priority, followed by the identification of accumulation hotspots and further transport pathways that could pose a potential hazard.

# 8 References

Ali, S. S., Elsamahy, T., Koutra, E., Kornaros, M., El-Sheekh, M., Abdelkarim, E. A., Zhu, D., & Sun, J. (2021). Degradation of conventional plastic wastes in the environment: A review on current status of knowledge and future perspectives of disposal. *Science of the Total Environment*, *771*, 144719. https://doi.org/10.1016/j.scitotenv.2020.144719

Andrady, A. L. (2011). Microplastics in the marine environment. *Marine Pollution Bulletin*, *62*(8), 1596–1605. https://doi.org/10.1016/j.marpolbul.2011.05.030

Andrady, A. L. (2015). *Plastics and environmental sustainability* (1st ed.). John Wiley & Sons, Inc. https://doi.org/10.1002/9781119009405

Arthur, C., Baker, J., & Bamford, H. (2009). *Proceedings of the International Research Workshop on the Occurrence, Effects, and Fate of Microplastic Marine Debris*. *January*, 530.

Backhaus, K., Erichson, B., Plinke, W., & Weiber, R. (2016). *Multivariante Analysemethoden- Eine anwendungsorientierte Einführung* (14th ed.). Springer Gabler © Springer-Verlag. https://doi.org/10.1007/978-3-662-46076-4

Bader, H. (1970). The Hyperbolic Distribution of Particle Sizes. *Journal of geophysical research*, *75*(15), 2822–2830.

Baensch-Baltruschat, B., Kocher, B., Stock, F., & Reifferscheid, G. (2020). Tyre and road wear particles (TRWP) - A review of generation, properties, emissions, human health risk, ecotoxicity, and fate in the environment. *Science of the Total Environment*, *733*, 137823. https://doi.org/10.1016/j.scitotenv.2020.137823

Barge, M., Rech, J., Hamdi, H., & Bergheau, J. M. (2007). Experimental study of abrasive process. *Wear*, *264*(5–6), 382–388. https://doi.org/10.1016/j.wear.2006.08.046

Barnes, D. K. A., Galgani, F., Thompson, R. C., & Barlaz, M. (2009). Accumulation and fragmentation of plastic debris in global environments. *Philosophical Transactions of the Royal Society; B: Biological Sciences*, *364*(1526), 1985–1998. https://doi.org/10.1098/rstb.2008.0205

Bergmann, M., Klages, M., Bergmann, M., & Klages, M. (2015). *Marine Anthropogenic Litter* (Number June). https://doi.org/10.1007/978-3-319-16510-3

Bergmann, M., Wirzberger, V., Krumpen, T., Lorenz, C., Primpke, S., Tekman, M. B., & Gerdts, G. (2017). High Quantities of Microplastic in Arctic Deep-Sea Sediments from the HAUSGARTEN Observatory. *Environmental Science and Technology*, *51*(19), 11000–11010. https://doi.org/10.1021/acs.est.7b03331

Bertoldo, M., Bronco, S., Cappelli, C., Gragnoli, T., & Andreotti, L. (2003). Combining theory and experiment to study the photooxidation of polyethylene and polypropylene. *The Journal of Physical Chemistry B*, *107*(43), 11880–11888. https://doi.org/10.1021/jp035427h

Browne, M. A., Galloway, T., & Thompson, R. (2007). Microplastic - an emerging contaminant of potential concern? *Integrated Environmental Assessment and Management*, *3*(4), 559−561. https://doi.org/10.1002/ieam.5630030412

Buchanan, J. B. (1971). Pollution by synthetic fibres. *Marine Pollution Bulletin*, *2*, 23.

Cai, L., Wang, J., Peng, J., Wu, Z., & Tan, X. (2018). Observation of the degradation of three types of plastic pellets exposed to UV irradiation in three different environments. *Science of the Total Environment*, *628–629*(February), 740–747. https://doi.org/10.1016/j.scitotenv.2018.02.079

Cashman, M. A., Ho, K. T., Boving, T. B., Russo, S., Robinson, S., & Burgess, R. M. (2020). Comparison of microplastic isolation and extraction procedures from marine sediments. *Marine Pollution Bulletin*, *159*(May), 111507. https://doi.org/10.1016/j.marpolbul.2020.111507

Ceccarini, A., Corti, A., Erba, F., Modugno, F., la Nasa, J., Bianchi, S., & Castelvetro, V. (2018). The Hidden Microplastics: New Insights and Figures from the Thorough Separation and Characterization of Microplastics and of Their Degradation Byproducts in Coastal Sediments. *Environmental Science and Technology*, *52*(10), 5634–5643. https://doi.org/10.1021/acs.est.8b01487

Chen, Q., Wang, Q., Zhang, C., Zhang, J., Dong, Z., & Xu, Q. (2021). Aging simulation of thin-film plastics in different environments to examine the formation of microplastic. *Water Research*, *202*(July), 117462. https://doi.org/10.1016/j.watres.2021.117462

Chubarenko, I., Efimova, I., Bagaeva, M., Bagaev, A., & Isachenko, I. (2020). On mechanical fragmentation of single-use plastics in the sea swash zone with different types of bottom sediments: Insights from laboratory experiments. *Marine Pollution Bulletin*, *150*(November 2019). https://doi.org/10.1016/j.marpolbul.2019.110726

Claessens, M., Meester, S. de, Landuyt, L. van, Clerck, K. de, & Janssen, C. R. (2011). Occurrence and distribution of microplastics in marine sediments along the Belgian coast. *Marine Pollution Bulletin*, *62*(10), 2199–2204. https://doi.org/10.1016/j.marpolbul.2011.06.030

Claessens, M., van Cauwenberghe, L., Vandegehuchte, M. B., & Janssen, C. R. (2013). New techniques for the detection of microplastics in sediments and field collected organisms. *Marine Pollution Bulletin*, *70*(1–2), 227–233. https://doi.org/10.1016/j.marpolbul.2013.03.009

Cole, M., Lindeque, P., Halsband, C., & Galloway, T. S. (2011). Microplastics as contaminants in the marine environment: A review. *Marine Pollution Bulletin*, *62*(12), 2588–2597. https://doi.org/10.1016/j.marpolbul.2011.09.025

Cole, M., Webb, H., Lindeque, P. K., Fileman, E. S., Halsband, C., & Galloway, T. S. (2014). Isolation of microplastics in biota-rich seawater samples and marine organisms. *Scientific Reports*, *4*, 1–8. https://doi.org/10.1038/srep04528

Colton, J. B., Knapp, F. D., & Burns, B. R. (1974). Plastic Particles in Surface Waters of the Northwestern Atlantic. *Science*, *185*(4150), 491–497. https://www.jstor.org/stable/1738284

Cooper, D. A. (2012). *Effects of chemical and mechanical weathering processes on the degradation of plastic debris on marine beaches*.

Corcoran, P. L., Biesinger, M. C., & Grifi, M. (2009). Plastics and beaches: A degrading relationship. *Marine Pollution Bulletin*, *58*(1), 80–84. https://doi.org/10.1016/j.marpolbul.2008.08.022

Crichton, E. M., Noël, M., Gies, E. A., & Ross, P. S. (2017). A novel, density-independent and FTIR-compatible approach for the rapid extraction of microplastics from aquatic sediments. *Analytical Methods*, *9*(9), 1419–1428. https://doi.org/10.1039/c6ay02733d

de Falco, F., Gullo, M. P., Gentile, G., di Pace, E., Cocca, M., Gelabert, L., Brouta-Agnésa, M., Rovira, A., Escudero, R., Villalba, R., Mossotti, R., Montarsolo, A., Gavignano, S., Tonin, C., & Avella, M. (2018). Evaluation of microplastic release caused by textile washing processes of synthetic fabrics. *Environmental Pollution*, *236*, 916–925. https://doi.org/10.1016/j.envpol.2017.10.057

Dietrich, W. E. (1982). Settling velocity of natural particles. *Water Resources Research*, *18*(6), 1615–1626. https://doi.org/10.1029/WR018i006p01615

Duis, K., & Coors, A. (2016). Microplastics in the aquatic and terrestrial environment: sources (with a specific focus on personal care products), fate and effects. *Environmental Sciences Europe*, *28*(1), 2. https://doi.org/10.1186/s12302-015-0069-y

DWD, D. W. (2010). *Globalstrahlung in der Bundesrepublik Deutschland Mittlere Jahressummen , Zeitraum : 1981 - 2010*. www.dwd.de

Edo, C., González-Pleiter, M., Leganés, F., Fernández-Piñas, F., & Rosal, R. (2020). Fate of microplastics in wastewater treatment plants and their environmental dispersion with effluent and sludge. *Environmental Pollution*, *259*. https://doi.org/10.1016/j.envpol.2019.113837

Efimova, I., Bagaeva, M., Bagaev, A., Kileso, A., & Chubarenko, I. P. (2018). Secondary microplastics generation in the sea swash zone with coarse bottom sediments:

Laboratory experiments. *Frontiers in Marine Science*, *5*(SEP). https://doi.org/10.3389/fmars.2018.00313

Enders, K., Lenz, R., Stedmon, C. A., & Nielsen, T. G. (2015). Abundance, size and polymer composition of marine microplastics ≥10 μm in the Atlantic Ocean and their modelled vertical distribution. *Marine Pollution Bulletin*, *100*(1), 70–81. https://doi.org/10.1016/j.marpolbul.2015.09.027

Eriksen, M., Mason, S., Wilson, S., Box, C., Zellers, A., Edwards, W., Farley, H., & Amato, S. (2013). Microplastic pollution in the surface waters of the Laurentian Great Lakes. *Marine Pollution Bulletin*, *77*(1–2), 177–182. https://doi.org/10.1016/j.marpolbul.2013.10.007

Feldman, D. (2002). Polymer Weathering: Photo-Oxidation. *Journal of Polymers and the Environment*, *10*(4). https://doi.org/https://doi.org/10.1023/A:1021148205366

Felsing, S., Kochleus, C., Buchinger, S., Brennholt, N., Stock, F., & Reifferscheid, G. (2018). A new approach in separating microplastics from environmental samples based on their electrostatic behavior. *Environmental Pollution*, *234*, 20–28. https://doi.org/10.1016/j.envpol.2017.11.013

Fernández-González, V., Andrade-Garda, J. M., López-Mahía, P., & Muniategui-Lorenzo, S. (2021). Impact of weathering on the chemical identification of micro-plastics from usual packaging polymers in the marine environment. *Analytica Chimica Acta*, *1142*, 179–188. https://doi.org/10.1016/j.aca.2020.11.002

Finch, H. (2021). Comparison of Distance Measures in Cluster Analysis with Dichoto-mous Data. *Journal of Data Science*, *3*(1), 85–100. https://doi.org/10.6339/jds.2005.03(1).192

Fischer, M., & Scholz-Böttcher, B. M. (2017). Simultaneous Trace Identification and Quantification of Common Types of Microplastics in Environmental Samples by Pyrolysis-Gas Chromatography-Mass Spectrometry. *Environmental Science and Technology*, *51*(9), 5052–5060. https://doi.org/10.1021/acs.est.6b06362

Fok, L., Cheung, P. K., Tang, G., & Li, W. C. (2017). Size distribution of stranded small plastic debris on the coast of Guangdong, South China. *Environmental Pollu-tion*, *220*, 407–412. https://doi.org/10.1016/j.envpol.2016.09.079

Frias, J., Pagter, E., Nash, R., O'Connor, I., Carretero, O., Filgueiras, A., Viñas, L., Gago, J., Antunes, J., Bessa, F., Sobral, P., Goruppi, A., Tirelli, V., Pedrotti, M. L., Suaria, G., Aliani, S., Lopes, C., Raimundo, J., Caetano, M., … Gerdts, G. (2018). Standardised protocol for monitoring microplastics in sediments. *JPI-Oceans BASEMAN project*, *May*, 33. https://doi.org/10.13140/RG.2.2.36256.89601/1

Fries, E., Dekiff, J. H., Willmeyer, J., Nuelle, M.-T., Ebert, M., & Remy, D. (2013). Identification of polymer types and additives in marine microplastic particles using

pyrolysis-GC/MS and scanning electron microscopy. *Environmental Science: Processes & Impacts*, *15*(10), 1949. https://doi.org/10.1039/c3em00214d

Fuller, S., & Gautam, A. (2016). A Procedure for Measuring Microplastics using Pressurized Fluid Extraction. *Environmental Science and Technology*, *50*(11), 5774–5780. https://doi.org/10.1021/acs.est.6b00816

Gatidou, G., Arvaniti, O. S., & Stasinakis, A. S. (2019). Review on the occurrence and fate of microplastics in Sewage Treatment Plants. *Journal of Hazardous Materials*, *367*(December 2018), 504–512. https://doi.org/10.1016/j.jhazmat.2018.12.081

GESAMP Joint Group of Experts on the Scientific Aspects of Marine Environmental Protection. (2015). Sources, fate and effects of microplastics in the marine environment: a global assessment". *Reports and Studies GESAMP*, *90*, 96. https://doi.org/10.13140/RG.2.1.3803.7925

Gewert, B., Ogonowski, M., Barth, A., & MacLeod, M. (2017). Abundance and composition of near surface microplastics and plastic debris in the Stockholm Archipelago, Baltic Sea. *Marine Pollution Bulletin*, *120*(1–2), 292–302. https://doi.org/10.1016/j.marpolbul.2017.04.062

Gewert, B., Plassmann, M. M., & MacLeod, M. (2015). Pathways for degradation of plastic polymers floating in the marine environment. *Environmental Science: Processes Impacts*, *17*(9), 1513–1521. https://doi.org/10.1039/C5EM00207A

Gulmine, J. v., Janissek, P. R., Heise, H. M., & Akcelrud, L. (2003). Degradation profile of polyethylene after artificial accelerated weathering. *Polymer Degradation and Stability*, *79*(3), 385–397. https://doi.org/10.1016/S0141-3910(02)00338-5

Hammer, J., Kraak, M. H. S., & Parsons, J. R. (2012). *Reviews of Environmental Contamination and Toxicology* (Vol. 220). https://doi.org/10.1007/978-1-4614-3414-6

Hartmann, N. B., Hüffer, T., Thompson, R. C., Hassellöv, M., Verschoor, A., Daugaard, A. E., Rist, S., Karlsson, T., Brennholt, N., Cole, M., Herrling, M. P., Hess, M. C., Ivleva, N. P., Lusher, A. L., & Wagner, M. (2019). Are We Speaking the Same Language? Recommendations for a Definition and Categorization Framework for Plastic Debris. *Environmental Science and Technology*, *53*(3), 1039–1047. https://doi.org/10.1021/acs.est.8b05297

Hengstmann, E., Tamminga, M., vom Bruch, C., & Fischer, E. K. (2018). Microplastic in beach sediments of the Isle of Rügen (Baltic Sea) - Implementing a novel glass elutriation column. *Marine Pollution Bulletin*, *126*(August 2017), 263–274. https://doi.org/10.1016/j.marpolbul.2017.11.010

Hidalgo-Ruz, V., Gutow, L., Thompson, R. C., & Thiel, M. (2012). Microplastics in the Marine Environment: A Review of the Methods Used for Identification and Quantification. *Environmental Science & Technology*, *46*(6), 3060–3075. https://doi.org/10.1021/es2031505

Imhof, H. K., Schmid, J., Niessner, R., Ivleva, N. P., & Laforsch, C. (2012). A novel, highly efficient method for the separation and quantification of plastic particles in sediments of aquatic environments. *Limnology and Oceanography: Methods*, *10*(7), 524–537. https://doi.org/10.4319/lom.2012.10.524

Joint Research Centre, I. for E. and S. (2014). *MSDF Guidance on Monitoring Marine Litter in European Seas*. Publications Office. https://doi.org/10.2788/99475

Kalogerakis, N., Karkanorachaki, K., Kalogerakis, G. C., Triantafyllidi, E. I., Gotsis, A. D., Partsinevelos, P., & Fava, F. (2017). Microplastics generation: Onset of fragmentation of polyethylene films in marine environment mesocosms. *Frontiers in Marine Science*, *4*(MAR), 1–15. https://doi.org/10.3389/fmars.2017.00084

Kedzierski, M., le Tilly, V., Bourseau, P., Bellegou, H., César, G., Sire, O., & Bruzaud, S. (2016). Microplastics elutriation from sandy sediments: A granulometric approach. *Marine Pollution Bulletin*, *107*(1), 315–323. https://doi.org/10.1016/j.marpolbul.2016.03.041

Kershaw, P., Katsuhiko, S., Lee, S., Samseth, J., Woodring, D., & Smith, J. (2011). Plastic Debris in the Ocean. *UNEP Year book 2011: Emerging Issues in Our Global Environment*, 20–33. https://doi.org/10.1073/pnas.1314705111

Klein, S., Dimzon, I. K., Eubeler, J., & Knepper, T. P. (2018). Freshwater Microplastics - Analysis, Occurrence, and Degradation of Microplastics in the Aqueous Environment. In: M. Wagner & S. Lambert (Eds.), *The Handbook of Environmental Chemistry 58* (p. 302). https://doi.org/10.1007/978-3-319-61615-5

Koelmans, A. A., Kooi, M., Law, K. L., & van Sebille, E. (2017). All is not lost: Deriving a top-down mass budget of plastic at sea. *Environmental Research Letters*, *12*(11). https://doi.org/10.1088/1748-9326/aa9500

Kooi, M., & Koelmans, A. A. (2019). Simplifying Microplastic via Continuous Probability Distributions for Size, Shape, and Density. *Environmental Science & Technology Letters*, *6*(9), 551–557. https://doi.org/10.1021/acs.estlett.9b00379

Lancaster, J. K. (1969). Abrasive wear of polymers. *Wear*, *14*(4), 223–239. https://doi.org/https://doi.org/10.1016/0043-1648(69)90047-7

Li, J., Liu, H., & Paul Chen, J. (2018). Microplastics in freshwater systems: A review on occurrence, environmental effects, and methods for microplastics detection. *Water Research*, *137*(December 2017), 362–374. https://doi.org/10.1016/j.watres.2017.12.056

Li, W. C., Tse, H. F., & Fok, L. (2016). Plastic waste in the marine environment: A review of sources, occurrence and effects. *Science of the Total Environment*, *566–567*, 333–349. https://doi.org/10.1016/j.scitotenv.2016.05.084

Löder, M., & Gerdts, G. (2015). Marine anthropogenic litter. In: *Marine Anthropogenic Litter* (pp. 1–447). https://doi.org/10.1007/978-3-319-16510-3

Mai, L., Bao, L.-J., Shi, L., Wong, C. S., & Zeng, E. Y. (2018). A review of methods for measuring microplastics in aquatic environments. *Environmental Science and Pollution Research*, 11319–11332. https://doi.org/10.1007/s11356-018-1692-0

Moore, C. J. (2008). Synthetic polymers in the marine environment: A rapidly increasing, long-term threat. *Environmental Research*, *108*(2), 131–139. https://doi.org/10.1016/j.envres.2008.07.025

Naji, A., Esmaili, Z., & Khan, F. R. (2017). Plastic debris and microplastics along the beaches of the Strait of Hormuz, Persian Gulf. *Marine Pollution Bulletin*, *114*(2), 1057–1062. https://doi.org/10.1016/j.marpolbul.2016.11.032

Nash, E., & Sutcliffe, V. (1970). River flow forecasting through conceptual models Part I - A discussion of principles. *Journal of Hydrology*, *10*, 282–290.

Nuelle, M.-T., Dekiff, J. H., Remy, D., & Fries, E. (2014). A new analytical approach for monitoring microplastics in marine sediments. *Environmental Pollution*, *184*, 161–169. https://doi.org/10.1016/j.envpol.2013.07.027

Patterson, R. N., Watts, K. C., & Timmons, M. B. (1999). The power law in particle size analysis for aquacultural facilities. *Aquacultural Engineering*, *19*(4), 259–273. https://doi.org/10.1016/S0144-8609(98)00054-5

PlascticEurope. (2020). Plastics – the Facts 2020. *PlasticEurope*, 1–64. https://www.plasticseurope.org/en/resources/publications/4312-plastics-facts-2020

PlasticEurope. (2019). *Plastics - the Facts 2019*. https://www.plasticseurope.org/en/resources/market-data

PlastikNet. (2020). *Statuspapier Mikroplastik-Analytik Probenahme, Probenaufbereitung und Detektionsverfahren*.

Reuwer, A.-K. (2015). *Fragmentierung von Kunststoffpartikeln unter Umwelteinflüssen und Optimierung der Analyse verwitterter Kunststoffpartikel*.

Rezania, S., Park, J., Md Din, M. F., Mat Taib, S., Talaiekhozani, A., Kumar Yadav, K., & Kamyab, H. (2018). Microplastics pollution in different aquatic environments and biota: A review of recent studies. *Marine Pollution Bulletin*, *133*(March), 191–208. https://doi.org/10.1016/j.marpolbul.2018.05.022

Ritter, A., & Muñoz-Carpena, R. (2013). Performance evaluation of hydrological models: Statistical significance for reducing subjectivity in goodness-of-fit assessments. *Journal of Hydrology*, *480*, 33–45. https://doi.org/10.1016/j.jhydrol.2012.12.004

Rummel, C. D., Jahnke, A., Gorokhova, E., Kühnel, D., & Schmitt-Jansen, M. (2017). Impacts of biofilm formation on the fate and potential effects of microplastic in the

aquatic environment. *Environmental Science and Technology Letters*, *4*(7), 258–267. https://doi.org/10.1021/acs.estlett.7b00164

Ryan, P. G., Moore, C. J., van Franeker, J. A., & Moloney, C. L. (2009). Monitoring the abundance of plastic debris in the marine environment. *Philosophical Transactions of the Royal Society B: Biological Sciences*, *364*(1526), 1999–2012. https://doi.org/10.1098/rstb.2008.0207

Schulz, M., van Loon, W., Fleet, D. M., Baggelaar, P., & van der Meulen, E. (2017). OSPAR standard method and software for statistical analysis of beach litter data. *Marine Pollution Bulletin*, *122*(1–2), 166–175. https://doi.org/10.1016/j.marpolbul.2017.06.045

Schwaferts, C., Niessner, R., Elsner, M., & Ivleva, N. P. (2019). Trends in Analytical Chemistry Methods for the analysis of submicrometer- and nanoplastic particles in the environment. *Trends in Analytical Chemistry*, *112*, 52–65. https://doi.org/10.1016/j.trac.2018.12.014

Schymanski, D., Oßmann, B. E., Benismail, N., Boukerma, K., Dallmann, G., von der Esch, E., Fischer, D., Fischer, F., Gilliland, D., Glas, K., Hofmann, T., Käppler, A., Lacorte, S., Marco, J., Rakwe, M. el, Weisser, J., Witzig, C., Zumbülte, N., & Ivleva, N. P. (2021). Analysis of microplastics in drinking water and other clean water samples with micro-Raman and micro-infrared spectroscopy: minimum requirements and best practice guidelines. *Analytical and Bioanalytical Chemistry*. https://doi.org/10.1007/s00216-021-03498-y

Shah, A. A., Hasan, F., Hameed, A., & Ahmed, S. (2008). Biological degradation of plastics: A comprehensive review. *Biotechnology Advances*, *26*(3), 246–265. https://doi.org/10.1016/j.biotechadv.2007.12.005

Shaikh, T. N., & Agrawal, S. A. (2014). Qualitative and Quantitative Characterization of Textile Material by Fourier Transform. *International Journal of Innovative Research in Science, Engineering and Technology, Vol. 3, Issue 1, January 2014, pp 8496- 8502*, *3*(1), 8496–8502.

Sighicelli, M., Pietrelli, L., Lecce, F., Iannilli, V., Falconieri, M., Coscia, L., di Vito, S., Nuglio, S., & Zampetti, G. (2018). Microplastic pollution in the surface waters of Italian Subalpine Lakes. *Environmental Pollution*, *236*, 645–651. https://doi.org/10.1016/j.envpol.2018.02.008

Singh, B., & Sharma, N. (2008). Mechanistic implications of plastic degradation. *Polymer Degradation and Stability*, *93*(3), 561–584. https://doi.org/10.1016/j.polymdegradstab.2007.11.008

Song, Y. K., Hong, S. H., Jang, M., Han, G. M., Jung, S. W., & Shim, W. J. (2017). Combined Effects of UV Exposure Duration and Mechanical Abrasion on Micro-

plastic Fragmentation by Polymer Type. *Environmental Science and Technology*, *51*(8), 4368–4376. https://doi.org/10.1021/acs.est.6b06155

Sun, J., Dai, X., Wang, Q., van Loosdrecht, M. C. M., & Ni, B. J. (2019). Microplastics in wastewater treatment plants: Detection, occurrence and removal. *Water Research*, *152*, 21–37. https://doi.org/10.1016/j.watres.2018.12.050

Thompson, R. C., Swan, S. H., Moore, C. J., & vom Saal, F. S. (2009). Our plastic age. *Philosophical Transactions of the Royal Society B: Biological Sciences*, *364*(1526), 1973–1976. https://doi.org/10.1098/rstb.2009.0054

Thompson, Richard C., Olson, Y., Mitchell, R. P., Davis, A., Rowland, S. J., John, A. W. G., McGonigle, D., & Russell, A. E. (2004). Lost at Sea: Where Is All the Plastic? *Science*, *304*(5672), 838. https://doi.org/10.1126/science.1094559

Toffoli, A., & Bitner-Gregersen, E. M. (2017). Types of Ocean Surface Waves, Wave Classification. *Encyclopedia of Maritime and Offshore Engineering*, 1–8. https://doi.org/10.1002/9781118476406.emoe077

Tzeng, S. L., Wu, H. M., & Chen, C. H. (2009). Selection of proximity measures for matrix visualization of binary data. *Proceedings of the 2009 2nd International Conference on Biomedical Engineering and Informatics, BMEI 2009*. https://doi.org/10.1109/BMEI.2009.5305137

Valadez-Gonzalez, A., Cervantes-Uc, J. M., & Veleva, L. (1999). Mineral filler influence on the photo-oxidation of high density polyethylene: I. Accelerated UV chamber exposure test. *Polymer Degradation and Stability*, *63*(2), 253–260. https://doi.org/10.1016/S0141-3910(98)00102-5

van Cauwenberghe, L., Vanreusel, A., Mees, J., & Janssen, C. R. (2013). Microplastic pollution in deep-sea sediments. *Environmental Pollution*, *182*, 495–499. https://doi.org/10.1016/j.envpol.2013.08.013

Veiga, J. M., Fleet, D., Kinsey, S., Nilsson, P., Vlachogianni, T., Werner, S., Galgani, F., Thompson, R. C., Dagevos, J., Gago, J., Sobral, P., & Cronin, R. (2016). Identifying sources of marine litter. In: *JRC Technical Report* (Number January 2017). https://doi.org/10.2788/018068

Wagner, M., Scherer, C., Alvarez-Muñoz, D., Brennholt, N., Bourrain, X., Buchinger, S., Fries, E., Grosbois, C., Klasmeier, J., Marti, T., Rodriguez-Mozaz, S., Urbatzka, R., Vethaak, A. D., Winther-Nielsen, M., & Reifferscheid, G. (2014). Microplastics in freshwater ecosystems: what we know and what we need to know. *Environmental Sciences Europe*, *26*(1), 12. https://doi.org/10.1186/s12302-014-0012-7

Wang, J., Tan, Z., Peng, J., Qiu, Q., & Li, M. (2016). The behaviors of microplastics in the marine environment. *Marine Environmental Research*, *113*, 7–17. https://doi.org/10.1016/j.marenvres.2015.10.014

Wessel, C. C., Lockridge, G. R., Battiste, D., & Cebrian, J. (2016). Abundance and characteristics of microplastics in beach sediments: Insights into microplastic accumulation in northern Gulf of Mexico estuaries. *Marine Pollution Bulletin*, *109*(1), 178–183. https://doi.org/10.1016/j.marpolbul.2016.06.002

Wiedenbeck, M. (2010). Handbuch der sozialwissenschaftlichen Datenanalyse. In: *Handbuch der sozialwissenschaftlichen Datenanalyse* (pp. 525–552). © VS Verlag für Sozialwissenschaften | Springer Fachmedien Wiesbaden. https://doi.org/10.1007/978-3-531-92038-2

Witzig, C. S., Földi, C., Wörle, K., Habermehl, P., Pittroff, M., Müller, Y. K., Lauschke, T., Fiener, P., Dierkes, G., Freier, K. P., & Zumbülte, N. (2020). When Good Intentions Go Bad - False Positive Microplastic Detection Caused by Disposable Gloves. *Evironmental Science and Technology*, *54*(19), 12164–12172. https://doi.org/https://doi.org/10.1021/acs.est.0c03742

Woodall, L. C., Sanchez-Vidal, A., Canals, M., Paterson, G. L. J., Coppock, R., Sleight, V., Calafat, A., Rogers, A. D., Narayanaswamy, B. E., & Thompson, R. C. (2014). The deep sea is a major sink for microplastic debris. *Royal Society Open Science*, *1*(4). https://doi.org/10.1098/rsos.140317

Woyzichovski, T. (2020). *Sekundäres Mikroplastik in der Umwelt: Modellansätze zur Fragmentierung und Diskussion neuartiger Detektionsmethoden -Bachelorarbeit*.

Yang, H., Chen, G., & Wang, J. (2021). Microplastics in the marine environment: Sources, fates, impacts and microbial degradation. *Toxics*, *9*(2), 1–19. https://doi.org/10.3390/toxics9020041

Yousif, E., & Haddad, R. (2013). Photodegradation and photostabilization of polymers, especially polystyrene: Review. *SpringerPlus*, *2*(1), 1–32. https://doi.org/10.1186/2193-1801-2-398

Yuan, J., Ma, J., Sun, Y., Zhou, T., Zhao, Y., & Yu, F. (2020). Microbial degradation and other environmental aspects of microplastics/plastics. *Science of the Total Environment*, *715*, 136968. https://doi.org/10.1016/j.scitotenv.2020.136968

Zaroogian, G. E., Pesch, G., & Morrison, G. (1969). Formulation of an artificial sea water media suitable for oyster larvae development. *Am. Zool*, *9*, 1144.

Zhang, K., Hamidian, A. H., Tubić, A., Zhang, Y., Fang, J. K. H., Wu, C., & Lam, P. K. S. (2021). Understanding plastic degradation and microplastic formation in the environment: A review. *Environmental Pollution*, *274*. https://doi.org/10.1016/j.envpol.2021.116554

Zhao, S., Danley, M., Ward, J. E., Li, D., & Mincer, T. J. (2017). An approach for extraction, characterization and quantitation of microplastic in natural marine snow using Raman microscopy. *Analytical Methods*, *9*(9), 1470–1478. https://doi.org/10.1039/C6AY02302A

Zhou, Q., Zhang, H., Fu, C., Zhou, Y., Dai, Z., Li, Y., Tu, C., & Luo, Y. (2018). The distribution and morphology of microplastics in coastal soils adjacent to the Bohai Sea and the Yellow Sea. *Geoderma*, *322*(March), 201–208. https://doi.org/10.1016/j.geoderma.2018.02.015

Zweifel, H. (1998). *Stabilization of Polymeric Materials* (U. W. Suter, Ed.; 1st ed.). Springer Berlin Heidelberg. https://doi.org/10.1007/978-3-642-80305-5

# 9 Appendix

## A Materials and Methods

**Table 32:** Overview of the experimental procedure for the analysis of plastic particles for all samples in bottle experiments.

| | | | | Sample type | Macro-meso-and MPP | Meso-and MPP count-ing | Sam-ple Clean up | Thermogravimet-ric Analysis (LDPE fragmentation pattern) | µ-Raman | Microscop-ic Analysis: Counting | Estima-tion over weight | Thick-ness | SEM |
|---|---|---|---|---|---|---|---|---|---|---|---|---|---|
| **BE** | Coarse Sand | Beach | UV | LDPE bag | - | No | Yes | Yes (2c) | Yes | Yes | no | No | No |
| | | | | HDPE cap | removed | Yes | | - | | | no | No | Yes |
| | | | | PS cup | removed | Yes | | - | | | no | No | No |
| | | | | PET bottle | removed | Yes | | - | | | no | No | No |
| | | | Non-UV | LDPE bag | removed | No | no | Yes (1) | No | Yes | no | No | No |
| | | | | HDPE cap | removed | Yes | | - | | | no | No | No |
| | | | | PS cup | removed | Yes | | - | | | no | Yes | No |
| | | | | PET bottle | removed | Yes | | - | | | no | No | No |
| | | Breakwater | UV | LDPE bag | - | No | Yes | Yes (2c) | Yes | Yes | no | No | No |
| | | | | HDPE cap | removed | Yes | | - | | | yes | No | No |
| | | | | PS cup | removed | Yes | | - | | | yes | No | No |
| | | | | PET bottle | removed | Yes | | - | | | yes | No | No |
| | | | Non- | LDPE bag | - | No | Yes | Yes (2b) | No | Yes | no | No | No |

| | | | Sample type | Macro-meso- and MPP | Meso- and MPP count-ing | Sam-ple Clean up | Thermogravimet-ric Analysis (LDPE fragmentation pattern) | µ-Raman | Microscop-ic Analysis: Counting | Estima-tion over weight | Thick-ness | SEM |
|---|---|---|---|---|---|---|---|---|---|---|---|---|
| | | UV | HDPE cap | removed | Yes | | - | | | yes | No | No |
| | | | PS cup | removed | Yes | | - | | | yes | No | No |
| | | | PET bottle | removed | Yes | | - | | | yes | Yes | Yes |
| | Beach | UV | LDPE bag | - | No | Yes | Yes (2c) | No | Yes | no | No | No |
| | | | HDPE cap | removed | Yes | | - | | | no | No | No |
| | | | PS cup | removed | Yes | | - | | | yes | No | No |
| | | | PET bottle | removed | Yes | | - | | | no | Yes | Yes |
| | | Non-UV | LDPE bag | removed | No | no | Yes (1) | Yes | Yes | no | No | No |
| | | | HDPE cap | removed | Yes | | - | | | no | No | No |
| | | | PS cup | removed | Yes | | - | | | no | No | No |
| | | | PET bottle | removed | Yes | | - | | | no | No | No |
| Medi-um Sand | Breakwater | UV | LDPE bag | - | No | no | Yes (2c) | No | Yes | no | No | No |
| | | | HDPE cap | removed | Yes | | - | | | no | No | No |
| | | | PS cup | removed | Yes | | - | | | no | Yes | Yes |
| | | | PET bottle | removed | Yes | | - | | | no | No | No |
| | | Non-UV | LDPE bag | - | No | Yes | Yes (2b) | No | Yes | no | No | No |
| | | | HDPE cap | removed | Yes | | - | | | no | No | No |
| | | | PS cup | removed | Yes | | - | | | no | No | No |
| | | | PET bottle | removed | Yes | | - | | | no | No | No |

**Table 33**: Overview of the experimental procedure for the analysis of plastic particles for all samples in wave tub experiments.

| | | | | Sample type | Macro-meso- and MPP | Meso- and MPP count-ing | Sam-ple Clean up | Thermogravimet-ric Analysis (LDPE fragmentation pattern) | µ-Raman | Microscop-ic Analysis: Counting | Estima-tion over weight | Thick-ness | SEM |
|---|---|---|---|---|---|---|---|---|---|---|---|---|---|
| **WTE** | Coarse Sand | Beach | UV | LDPE bag | removed | Yes | No | Yes (1) | Yes | Yes | No | No | No |
| | | | | HDPE cap | removed | Yes | | - | | | no | No | No |
| | | | | PS cup | removed | Yes | | - | | | no | No | No |
| | | | | PET bottle | removed | Yes | | - | | | no | No | No |
| | | | Non-UV | LDPE bag | To less sample | Yes | No | No (1) | No | Yes | No | No | No |
| | | | | HDPE cap | removed | Yes | | - | | | no | No | No |
| | | | | PS cup | removed | Yes | | - | | | no | No | No |
| | | | | PET bottle | removed | Yes | | - | | | no | No | No |
| | | Breakwater | UV | LDPE bag | removed | Yes | No | Yes (2a) | No | Yes | No | No | No |
| | | | | HDPE cap | removed | Yes | | - | | | yes | No | No |
| | | | | PS cup | removed | Yes | | - | | | yes | No | No |
| | | | | PET bottle | removed | Yes | | - | | | yes | No | No |
| | | | Non-UV | LDPE bag | To less sample | Yes | No | No (1) | No | Yes | No | No | No |
| | | | | HDPE cap | removed | Yes | | - | | | yes | No | No |
| | | | | PS cup | removed | Yes | | - | | | yes | No | No |
| | | | | PET bottle | removed | Yes | | - | | | yes | No | Yes |

| | | | Sample type | Macro-meso- and MPP | Meso- and MPP counting | Sample Clean up | Thermogravimetric Analysis (LDPE fragmentation pattern) | µ-Raman | Microscopic Analysis: Counting | Estimation over weight | Thickness | SEM |
|---|---|---|---|---|---|---|---|---|---|---|---|---|
| Medium Sand | Beach | UV | LDPE bag | removed | Yes | No | Yes (1) | No | Yes | No | No | No |
| | | | HDPE cap | removed | Yes | | - | | | no | No | Yes |
| | | | PS cup | removed | Yes | | - | | | yes | Yes | Yes |
| | | | PET bottle | removed | Yes | | - | | | no | Yes | Yes |
| | | Non-UV | LDPE bag | To less sample | Yes | No | No (1) | No | Yes | No | No | No |
| | | | HDPE cap | removed | Yes | | - | | | no | No | No |
| | | | PS cup | removed | Yes | | - | | | no | No | No |
| | | | PET bottle | removed | Yes | | - | | | no | No | No |
| | Breakwater | UV | LDPE bag | removed | Yes | No | Yes (2a) | Yes | Yes | No | No | No |
| | | | HDPE cap | removed | Yes | | - | | | no | No | No |
| | | | PS cup | removed | Yes | | - | | | no | No | No |
| | | | PET bottle | removed | Yes | | - | | | no | No | No |
| | | Non-UV | LDPE bag | To less sample | Yes | No | No (1) | No | Yes | No | No | No |
| | | | HDPE cap | removed | Yes | | - | | | no | No | No |
| | | | PS cup | removed | Yes | | - | | | no | No | No |
| | | | PET bottle | removed | Yes | | - | | | no | No | No |

# B Results

**Table 34:** Meso- and microplastic particle counts (>350 µm) for all samples in BE.

| | | | | Sample type | >2,5 cm | 2,5 cm-5mm | 5mm-2mm | 2mm-1mm | 1000µm-350µm | Total |
|---|---|---|---|---|---|---|---|---|---|---|
| BE | Coarse Sand | Beach | UV | LDPE bag | Bag was completely fragmented into MPP | | | | | |
| | | | | HDPE cap | 0 | 0 | 0 | 0 | 0 | 0 |
| | | | | PS cup | 10 | 148 | 70 | 142 | 136 | 506 |
| | | | | PET bottle | 0 | 1 | 4 | 6 | 3 | 14 |
| | | | Non-UV | LDPE bag | 4 | 140 | 120 | 74 | 40 | 378 |
| | | | | HDPE cap | 0 | 0 | 1 | 1 | 0 | 2 |
| | | | | PS cup | 0 | 7 | 36 | 29 | 10 | 82 |
| | | | | PET bottle | 0 | 0 | 2 | 1 | 0 | 3 |
| | | Breakwater | UV | LDPE bag | Bag was completely fragmented into MPP | | | | | |
| | | | | HDPE cap | 0 | 13 | 83 | 72 | 350 | 518 |
| | | | | PS cup | 0 | 10 | 10 | 206 | 1900 | 2126 |
| | | | | PET bottle | 0 | 5 | 114 | 22 | 100 | 241 |
| | | | Non-UV | LDPE bag | Bag was completely fragmented into MPP | | | | | |
| | | | | HDPE cap | 0 | 20 | 53 | 12 | 200 | 285 |
| | | | | PS cup | 0 | 47 | 26 | 700 | 5900 | 6673 |
| | | | | PET bottle | 0 | 9 | 142 | 10 | 200 | 361 |
| | Medium Sand | Beach | UV | LDPE bag | Bag was completely fragmented into MPP | | | | | |
| | | | | HDPE cap | 0 | 0 | 0 | 0 | 0 | 0 |
| | | | | PS cup | 8 | 180 | 204 | 245 | 300 | 937 |
| | | | | PET bottle | 0 | 1 | 4 | 3 | 6 | 14 |
| | | | Non-UV | LDPE bag | 0 | 5 | 5 | 5 | 0 | 15 |
| | | | | HDPE cap | 0 | 0 | 0 | 0 | 0 | 0 |
| | | | | PS cup | 0 | 6 | 40 | 68 | 96 | 210 |
| | | | | PET bottle | 0 | 0 | 0 | 0 | 0 | 0 |
| | | Breakwater | UV | LDPE bag | Bag was completely fragmented into MPP | | | | | |
| | | | | HDPE cap | 0 | 8 | 112 | 81 | 12 | 213 |
| | | | | PS cup | 0 | 2 | 29 | 14 | 1 | 46 |
| | | | | PET bottle | 0 | 25 | 78 | 31 | 1 | 135 |
| | | | Non-UV | LDPE bag | Bag was completely fragmented into MPP | | | | | |
| | | | | HDPE cap | 0 | 17 | 99 | 132 | 38 | 286 |
| | | | | PS cup | 0 | 0 | 48 | 109 | 42 | 199 |
| | | | | PET bottle | 0 | 4 | 37 | 119 | 58 | 218 |

**Table 35:** Meso- and microplastic particle counts (>350 µm) for all samples in WTE.

| | | | | Sample type | >2,5 cm | 2,5 cm-5mm | 5mm-2mm | 2mm-1mm | 1000µm-350µm | Total |
|---|---|---|---|---|---|---|---|---|---|---|
| WTE | Coarse Sand | Beach | UV | LDPE bag | 0 | 0 | 8 | 21 | 24 | 53 |
| | | | | HDPE cap | 0 | 0 | 0 | 0 | 0 | 0 |
| | | | | PS cup | 0 | 0 | 3 | 4 | 5 | 12 |
| | | | | PET bottle | 0 | 0 | 0 | 0 | 0 | 0 |
| | | | | not identi-fied | 0 | 0 | 1 | 6 | 8 | 15 |
| | | | Non-UV | LDPE bag | 0 | 0 | 5 | 7 | 2 | 14 |
| | | | | HDPE cap | 0 | 0 | 0 | 0 | 0 | 0 |
| | | | | PS cup | 0 | 0 | 0 | 0 | 0 | 0 |
| | | | | PET bottle | 0 | 0 | 0 | 0 | 0 | 0 |
| | | Breakwater | UV | LDPE bag | Bag was completely fragmented into MPP | | | | | |
| | | | | HDPE cap | 0 | 0 | 0 | 0 | 0 | 0 |
| | | | | PS cup | 0 | 0 | 0 | 0 | 0 | 0 |
| | | | | PET bottle | 0 | 0 | 0 | 0 | 0 | 0 |
| | | | Non-UV | LDPE bag | 0 | 0 | 0 | 0 | 0 | 0 |
| | | | | HDPE cap | 0 | 0 | 0 | 0 | 0 | 0 |
| | | | | PS cup | 0 | 0 | 0 | 0 | 0 | 0 |
| | | | | PET bottle | 0 | 0 | 0 | 0 | 0 | 0 |
| | Medium Sand | Beach | UV | LDPE bag | 0 | 17 | 55 | 28 | 4 | 104 |
| | | | | HDPE cap | 0 | 0 | 0 | 0 | 0 | 0 |
| | | | | PS cup | 0 | 0 | 3 | 3 | 0 | 6 |
| | | | | PET bottle | 0 | 0 | 0 | 6 | 0 | 6 |
| | | | Non-UV | LDPE bag | 0 | 0 | 0 | 0 | 0 | 0 |
| | | | | HDPE cap | 0 | 0 | 0 | 0 | 0 | 0 |
| | | | | PS cup | 0 | 0 | 0 | 0 | 0 | 0 |
| | | | | PET bottle | 0 | 0 | 0 | 0 | 0 | 0 |
| | | Breakwater | UV | LDPE bag | Bag was completely fragmented into MPP | | | | | |
| | | | | HDPE cap | 0 | 0 | 1 | 0 | 0 | 1 |
| | | | | PS cup | 0 | 0 | 0 | 0 | 4 | 4 |
| | | | | PET bottle | 0 | 0 | 0 | 0 | 0 | 0 |
| | | | Non-UV | LDPE bag | 0 | 0 | 0 | 0 | 0 | 0 |
| | | | | HDPE cap | 0 | 0 | 0 | 0 | 0 | 0 |
| | | | | PS cup | 0 | 0 | 0 | 0 | 0 | 0 |
| | | | | PET bottle | 0 | 0 | 0 | 0 | 0 | 0 |

**Table 36:** Results from µ-Raman analysis (Bottle experiment; Coarse sand; Breakwater; UV).

| Experiment | BE | Coarse sand | Breakwater | UV | | |
|---|---|---|---|---|---|---|
| | | | (Particle/Filter) | | | |
| Material | 350-100 µm | 100-50 µm | 50-20 µm | 20-10 µm | 10-5 µm | Total |
| PE | 0 | 0 | 3 | 0 | 7 | 10 |
| PS | 0 | 0 | 0 | 0 | 0 | 0 |
| PET | 7 | 14 | 21 | 28 | 86 | 156 |
| PP | 17 | 0 | 0 | 7 | 0 | 24 |
| Extrapolation | Factor | 160 | | | | |
| | | | (Particle/Filter) | | | |
| Material | 350-100 µm | 100-50 µm | 50-20 µm | 20-10 µm | 10-5 µm | Total |
| PE | 0 | 0 | 555 | 0 | 1109 | 1664 |
| PS | 0 | 0 | 0 | 0 | 0 | 0 |
| PET | 1109 | 2219 | 3328 | 4438 | 13868 | 24963 |
| PP | 0 | 1109 | 0 | 1109 | 555 | 2774 |

**Table 37**: Results from µ-Raman analysis (Bottle experiment; Medium sand; Beach; Non-UV).

| Experiment | BE | Medium sand | Beach | non-UV | | |
|---|---|---|---|---|---|---|
| | | | (Particle/Filter) | | | |
| Material | 350-100 µm | 100-50 µm | 50-20 µm | 20-10 µm | 10-5 µm | Total |
| PE | 0 | 0 | 0 | 0 | 0 | 0 |
| PS | 0 | 0 | 0 | 0 | 0 | 0 |
| PET | 3 | 14 | 10 | 27 | 78 | 132 |
| PP | 0 | 0 | 0 | 0 | 0 | 0 |
| Extrapolation | Factor | 26 | | | | |
| | | | (Particle/Filter) | | | |
| Material | 350-100 µm | 100-50 µm | 50-20 µm | 20-10 µm | 10-5 µm | Total |
| PE | 0 | 0 | 0 | 0 | 0 | 0 |
| PS | 0 | 0 | 0 | 0 | 0 | 0 |
| PET | 89 | 358 | 268 | 715 | 2056 | 3487 |
| PP | 0 | 0 | 0 | 0 | 0 | 0 |

**Table 38:** Results from µ-Raman analysis (Wave tub experiment; Medium sand; Breakwater; UV).

| Experiment | WTE | Medium sand | Breakwater | UV | | |
|---|---|---|---|---|---|---|
| | | | (Particle/Filter) | | | |
| **Material** | 350-100 µm | 100-50 µm | 50-20 µm | 20-10 µm | 10-5 µm | Total |
| **PE** | 3 | 13 | 10 | 10 | 35 | 71 |
| **PS** | 0 | 0 | 0 | 0 | 0 | 0 |
| **PET** | 0 | 0 | 0 | 0 | 0 | 0 |
| **PP** | 0 | 0 | 0 | 0 | 0 | 0 |
| **Extrapolation** | **Factor** | **112** | | | | |
| | | | (Particle/Filter) | | | |
| **Material** | 350-100 µm | 100-50 µm | 50-20 µm | 20-10 µm | 10-5 µm | Total |
| **PE** | 359 | 1437 | 1078 | 1078 | 3953 | 7905 |
| **PS** | 0 | 0 | 0 | 0 | 0 | 0 |
| **PET** | 0 | 0 | 0 | 0 | 0 | 0 |
| **PP** | 0 | 0 | 0 | 0 | 0 | 0 |

**Table 39:** Results from µ-Raman analysis (Bottle experiment; Coarse sand; Beach; UV; Sub-sample 1).

| Experiment | BE | Coarse sand | Beach | UV | | |
|---|---|---|---|---|---|---|
| **Subsample 1** | | | (Particle/Filter) | | | |
| **Material** | 350-100 µm | 100-50 µm | 50-20 µm | 20-10 µm | 10-5 µm | Total |
| **PE** | 0 | 0 | 0 | 13 | 10 | 22 |
| **PS** | 0 | 0 | 3 | 19 | 54 | 77 |
| **PET** | 0 | 0 | 3 | 32 | 29 | 64 |
| **PP** | 0 | 0 | 0 | 0 | 3 | 3 |
| **Extrapolation** | **Factor** | **451** | | | | |
| | | | (Particle/Filter) | | | |
| **Material** | 350-100 µm | 100-50 µm | 50-20 µm | 20-10 µm | 10-5 µm | Total |
| **PE** | 0 | 0 | 0 | 5771 | 4329 | 10100 |
| **PS** | 0 | 0 | 1443 | 8657 | 24528 | 34628 |
| **PET** | 0 | 0 | 1443 | 14428 | 12986 | 28857 |
| **PP** | 0 | 0 | 0 | 0 | 1443 | 1443 |

**Table 40:** Results from µ-Raman analysis (Bottle experiment; Coarse sand; Beach; UV; Subsample 2).

| **Experiment** | **BE** | **Coarse sand** | **Beach** | **UV** | | |
|---|---|---|---|---|---|---|
| **Subsample 2** | | | **(Particle/Filter)** | | | |
| **Material** | 350-100 µm | 100-50 µm | 50-20 µm | 20-10 µm | 10-5 µm | Total |
| **PE** | 0 | 3 | 10 | 14 | 14 | 41 |
| **PS** | 0 | 0 | 0 | 3 | 10 | 14 |
| **PET** | 0 | 0 | 3 | 10 | 17 | 31 |
| **PP** | 0 | 0 | 0 | 0 | 0 | 0 |
| **Extrapolation** | **Factor** | **451** | | | | |
| | | | **(Particle/Filter)** | | | |
| **Material** | 350-100 µm | 100-50 µm | 50-20 µm | 20-10 µm | 10-5 µm | Total |
| **PE** | 0 | 1542 | 4625 | 6167 | 6167 | 18502 |
| **PS** | 0 | 0 | 0 | 1542 | 4625 | 6167 |
| **PET** | 0 | 0 | 1542 | 4625 | 7709 | 13876 |
| **PP** | 0 | 0 | 0 | 0 | 0 | 0 |

**Table 41:** Data of all 64 sample objects used for the cluster analysis (1=yes; 0=no).

| | | | | Sample type | Sample is visibly affected | Original sample shape is destroyed | Surface haze | Plastic object is perforated or cracked | Mesoplastic particles (5mm – 25mm) emerge | Large MPP (1mm – 5mm) emerge | Small MPP (<1mm) emerge |
|---|---|---|---|---|---|---|---|---|---|---|---|
| **Bottle Experiment** | Coarse Sand | Beach | UV | LDPE bag | 1 | 1 | 1 | 1 | 1 | 1 | 1 |
| | | | | HDPE cap | 1 | 0 | 1 | 0 | 0 | 0 | 0 |
| | | | | PS cup | 1 | 1 | 1 | 1 | 1 | 1 | 1 |
| | | | | PET bottle | 1 | 0 | 1 | 1 | 1 | 1 | 1 |
| | | | Non-UV | LDPE bag | 1 | 0 | 1 | 1 | 1 | 1 | 1 |
| | | | | HDPE cap | 1 | 0 | 1 | 0 | 0 | 1 | 0 |
| | | | | PS cup | 1 | 0 | 1 | 1 | 1 | 1 | 1 |
| | | | | PET bottle | 1 | 0 | 1 | 1 | 0 | 1 | 0 |
| | | Breakwater | UV | LDPE bag | 1 | 1 | 1 | 1 | 0 | 1 | 1 |
| | | | | HDPE cap | 1 | 1 | 1 | 1 | 1 | 1 | 1 |
| | | | | PS cup | 1 | 1 | 1 | 1 | 1 | 1 | 1 |
| | | | | PET bottle | 1 | 0 | 1 | 1 | 1 | 1 | 1 |
| | | | Non-UV | LDPE bag | 1 | 1 | 1 | 1 | 0 | 1 | 1 |
| | | | | HDPE cap | 1 | 1 | 1 | 1 | 1 | 1 | 1 |
| | | | | PS cup | 1 | 1 | 1 | 1 | 1 | 1 | 1 |
| | | | | PET bottle | 1 | 0 | 1 | 1 | 1 | 1 | 1 |
| | Medium Sand | Beach | UV | LDPE bag | 1 | 1 | 1 | 1 | 1 | 1 | 1 |
| | | | | HDPE cap | 1 | 0 | 1 | 0 | 0 | 0 | 0 |
| | | | | PS cup | 1 | 1 | 1 | 1 | 1 | 1 | 1 |
| | | | | PET bottle | 1 | 0 | 1 | 1 | 1 | 1 | 1 |
| | | | Non-UV | LDPE bag | 1 | 0 | 1 | 1 | 1 | 1 | 0 |
| | | | | HDPE cap | 1 | 0 | 1 | 0 | 0 | 0 | 0 |

| | | | | Sample type | Sample is visibly affected | Original sample shape is destroyed | Surface haze | Plastic object is perforated or cracked | Mesoplastic particles (5mm – 25mm) emerge | Large MPP (1mm – 5mm) emerge | Small MPP (<1mm) emerge |
|---|---|---|---|---|---|---|---|---|---|---|---|
| | | | | PS cup | 1 | 0 | 1 | 1 | 1 | 1 | 1 |
| | | | | PET bottle | 1 | 0 | 1 | 1 | 0 | 0 | 0 |
| | | Breakwater | UV | LDPE bag | 1 | 1 | 1 | 1 | 1 | 1 | 1 |
| | | | | HDPE cap | 1 | 1 | 1 | 1 | 1 | 1 | 1 |
| | | | | PS cup | 1 | 0 | 1 | 1 | 1 | 1 | 1 |
| | | | | PET bottle | 1 | 0 | 1 | 1 | 1 | 1 | 1 |
| | | | Non-UV | LDPE bag | 1 | 1 | 1 | 1 | 1 | 1 | 1 |
| | | | | HDPE cap | 1 | 1 | 1 | 1 | 1 | 1 | 1 |
| | | | | PS cup | 1 | 0 | 1 | 1 | 0 | 1 | 1 |
| | | | | PET bottle | 1 | 0 | 1 | 1 | 1 | 1 | 1 |
| **Wave tub Experiment** | Coarse Sand | Beach | UV | LDPE bag | 1 | 0 | 1 | 1 | 0 | 1 | 1 |
| | | | | HDPE cap | 1 | 0 | 1 | 0 | 0 | 0 | 0 |
| | | | | PS cup | 0 | 0 | 0 | 0 | 0 | 1 | 1 |
| | | | | PET bottle | 1 | 0 | 1 | 0 | 0 | 0 | 0 |
| | | | Non-UV | LDPE bag | 1 | 0 | 1 | 1 | 0 | 1 | 1 |
| | | | | HDPE cap | 1 | 0 | 1 | 0 | 0 | 0 | 0 |
| | | | | PS cup | 0 | 0 | 0 | 0 | 0 | 0 | 0 |
| | | | | PET bottle | 1 | 0 | 1 | 0 | 0 | 0 | 0 |
| | | Breakwater | UV | LDPE bag | 1 | 1 | 1 | 1 | 1 | 1 | 1 |
| | | | | HDPE cap | 0 | 0 | 0 | 0 | 0 | 0 | 0 |
| | | | | PS cup | 1 | 0 | 1 | 1 | 0 | 0 | 0 |
| | | | | PET bottle | 1 | 0 | 1 | 0 | 0 | 0 | 0 |
| | | | Non-UV | LDPE bag | 1 | 0 | 1 | 1 | 0 | 0 | 0 |

| | | | | Sample type | Sample is visibly affected | Original sample shape is destroyed | Surface haze | Plastic object is perforated or cracked | Mesoplastic particles (5mm – 25mm) emerge | Large MPP (1mm – 5mm) emerge | Small MPP (<1mm) emerge |
|---|---|---|---|---|---|---|---|---|---|---|---|
| | | | | HDPE cap | 0 | 0 | 0 | 0 | 0 | 0 | 0 |
| | | | | PS cup | 0 | 0 | 0 | 0 | 0 | 0 | 0 |
| | | | | PET bottle | 1 | 0 | 1 | 0 | 0 | 0 | 0 |
| | Medium Sand | Beach | UV | LDPE bag | 1 | 0 | 1 | 1 | 1 | 1 | 1 |
| | | | | HDPE cap | 1 | 0 | 1 | 0 | 0 | 0 | 0 |
| | | | | PS cup | 1 | 0 | 1 | 1 | 0 | 1 | 0 |
| | | | | PET bottle | 1 | 0 | 1 | 0 | 0 | 1 | 0 |
| | | | Non-UV | LDPE bag | 1 | 0 | 1 | 1 | 0 | 0 | 0 |
| | | | | HDPE cap | 1 | 0 | 1 | 0 | 0 | 0 | 0 |
| | | | | PS cup | 0 | 0 | 0 | 0 | 0 | 0 | 0 |
| | | | | PET bottle | 1 | 0 | 1 | 0 | 0 | 0 | 0 |
| | | Breakwater | UV | LDPE bag | 1 | 1 | 1 | 1 | 1 | 1 | 1 |
| | | | | HDPE cap | 0 | 0 | 0 | 0 | 0 | 1 | 0 |
| | | | | PS cup | 0 | 0 | 0 | 0 | 0 | 0 | 1 |
| | | | | PET bottle | 0 | 0 | 0 | 0 | 0 | 0 | 0 |
| | | | Non-UV | LDPE bag | 1 | 0 | 1 | 1 | 0 | 0 | 0 |
| | | | | HDPE cap | 0 | 0 | 0 | 0 | 0 | 0 | 0 |
| | | | | PS cup | 0 | 0 | 0 | 0 | 0 | 0 | 0 |
| | | | | PET bottle | 0 | 0 | 0 | 0 | 0 | 0 | 0 |

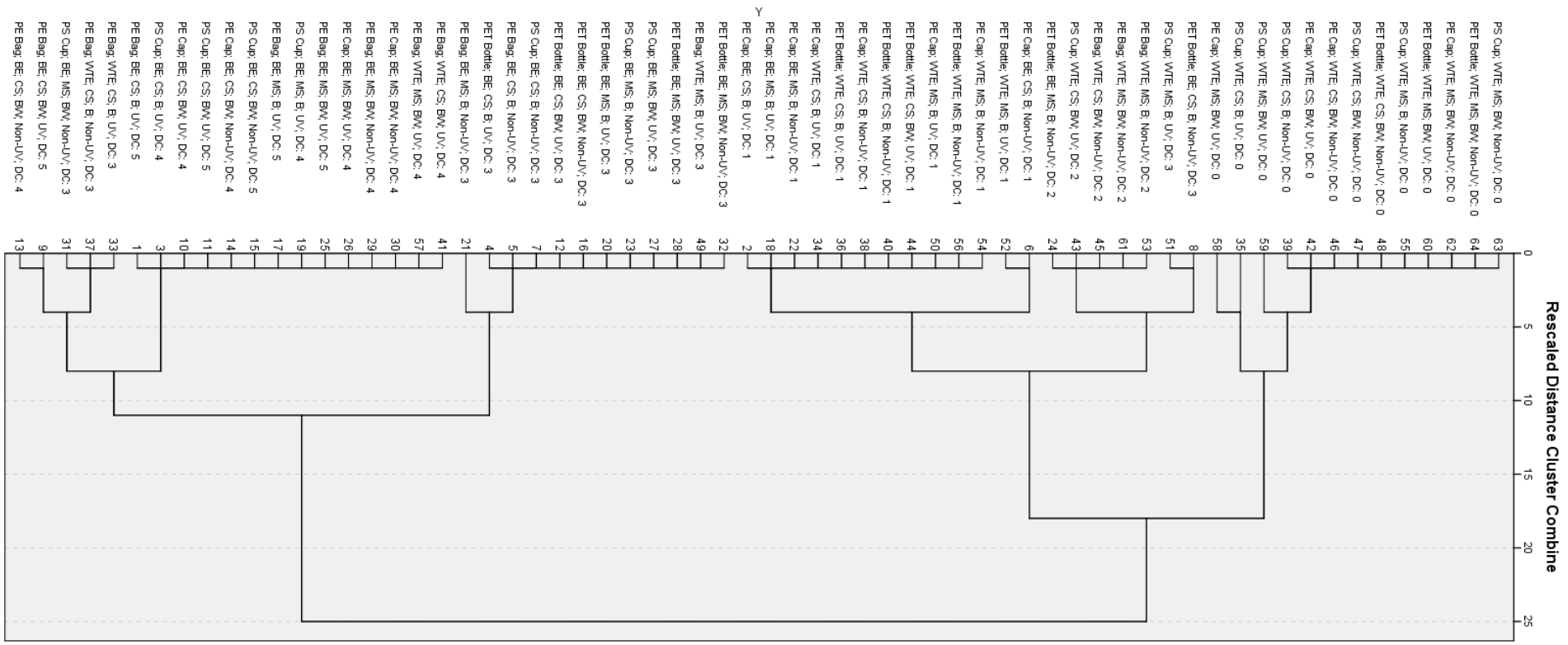


**Figure 60:** Dendrogram from hierarchical cluster analysis.

# 10 Acknowledgments – Danksagung

Nun ist es an der Zeit meinen Dank gegenüber den nachstehenden Personen auszudrücken, ohne deren Unterstützung und Mithilfe diese Doktorarbeit nicht zustande gekommen wäre:

Als Erstes möchte ich meinem Doktorvater Dr. Jörg Klasmeier für die Betreuung dieser Arbeit und seine hilfreiche Unterstützung, seine Zeit und seine guten Ideen danken. Mit seiner Hilfe, sein Feedback und mit konstruktiven Gesprächen habe ich es geschafft, diese Arbeit und die damit verbundenen Untersuchungen relativ stressfrei zu bewältigen.

Auch möchte ich Priv.-Doz. Dr. Marcus Schulz und Prof. Dr. Peter Fiener dafür danken, dass Sie sich als meine Zweit- und Drittprüfer zur Verfügung stellen.

Des Weiteren möchte ich mich bei meinen Laborkolleginnen Katrin Ellerbrake und Antje Möhlmeyer für ihre ständige Unterstützung im Labor danken. Sie haben mir mit Rat und Tat beiseite gestanden. Ebenso Sarah Falk, mit der ich immer über alles reden konnte und mich immer wieder aufgeheitert hat.

Ebenfalls gilt mein Dank Dipl.-Ing. (FH) Bröker aus dem Labor für Kunststoffprüfung der Hochschule Osnabrück, der mir bei der Dickenmessung meiner Proben geholfen hat genauso wie Dr. Katherina Psathaki aus dem „Center of Cellular Nanoanalytics (CellNanOs)“ der Universität Osnabrück, die mir eine große Hilfe bei der Nutzung des Rasterelektronenmikroskopes war. Außerdem danke an Anja Schuster aus dem Fachbereich Biologie/Chemie der Universität Osnabrück, mit deren Hilfe ich die Thermogravimetrischen Untersuchungen durchführen konnte. Auch möchte ich Kerstin Rücker aus der Arbeitsgruppe anorganische Chemie I / Funktionale Nanomaterialien dafür danken, dass ich mehr oder weniger selbständig ihr FT-IR Messgerät nutzen durfte.

Meinen besonderen Dank gelten Dr. Nicole Zumbülte, Cordula Witzig und deren Team vom TZW: DVGW-Technologiezentrum Wasser in Karlsruhe, die meine Proben Mithilfe ihres µ-Raman analysiert und ausgewertet haben.

Für die Finanzierung meiner Zeit als wissenschaftliche Mitarbeiterin gilt mein Dank dem BMBF-Forschungsprojekt „MicBin“ (Projekt im Rahmen des Forschungsschwerpunkts "Plastik in der Umwelt). Für die Zeit der Fertigstellung meiner Arbeit wurde ich vom Pool zur Frauenförderung des Gleichstellungbüros der Universität Osnabrück mit einem Stipendium unterstützt.

Gerade während der stressigen Homeoffice Zeit war mein Freund Timo Kikillus eine große Unterstützung ebenso wie meine Familie, insbesondere meine Mutter Veronika, meine Schwester Carina und mein Neffe Jonathan, mit denen ich sehr oft nach einem langen Tag am Computer im Freien spazieren gehen konnte, um auf andere Gedanken zu kommen. Außerdem möchte ich noch Delia, Rebecca und Bernd erwähnen, die (hoffentlich) dafür gesorgt haben, dass auch Menschen, die nicht im Thema sind, etwas mit der Arbeit anfangen können. Vielen Dank.

# 11 Affidavit

I declare that I wrote this dissertation independently and on my own. I clearly marked any language or ideas borrowed from other sources as not my own and documented their sources. The thesis does not contain any work that I have handed in or have had graded as an examination earlier on.

_____ _____

Place, date Signature